Uniwersytet Jagielloński
Collegium Medicum

Agnieszka Karaś

The role of mitochondrial bioenergetic metabolism in maintaining the endothelial function of blood vessels: effects of ageing and inflammation

Rola mitochondrialnego metabolizmu bioenergetycznego w utrzymaniu czynności śródbłonka naczyń krwionośnych: wpływ starzenia i stanu zapalnego

PhD Thesis

Supervisor: prof. dr hab. Stefan Chłopicki, MD, PhD
Auxiliary supervisor: dr hab. Patrycja Kaczara, PhD

Jagiellonian Centre for Experimental Therapeutics (JCET)
JCET Director: prof. dr hab. Stefan Chłopicki, MD, PhD

Kraków, 2025

Table of contents

The research presented in this PhD thesis was funded by:

PRELUDIUM 20 grant no. 2021/41/N/NZ5/03396

National Science Centre, Poland (PI: Agnieszka Karaś)

TEAM-TECH Core Facility grant (application 0016)

Foundation of Polish Science (FNP) (PI: prof. dr hab. Stefan Chłopicki)

MAESTRO 13 grant no. 2021/42/A/NZ4/00273

National Science Centre, Poland (PI: prof. dr hab. Stefan Chłopicki)

ACKNOWLEDGEMENTS

First and foremost, I would like to express my profound gratitude to my supervisor,
***prof. dr hab. Stefan Chłopicki**, for his mentorship and patience.*
His expertise and valuable insights were essential for shaping this research,
and also for my professional growth.

*I am also deeply grateful to my auxiliary supervisor **dr hab. Patrycja Kaczara**,*
for her thoughtful advice and assistance,
both scientifically and in the face of unexpected challenges.

*I would like to thank also the **JCET team** for all the advice and inspiring work environment,*
*and all the collaborators, especially from **Medical University of Gdańsk***
*and **Helsinki Metabolomics Center,** whose contributions were vital for this research.*

*Finally, my warmest thanks go to **my loved ones, especially my Parents,** whose faith in me*
and unconditional support made this accomplishment possible.

LIST OF ABBREVIATIONS

AA – Antimycin A
AEC – Adenylate energy charge
DHEA – Dehydroepiandrosterone
E4P – Erythrose 4-phosphate
ECAR – Extracellular acidification rate
eNOS – Endothelial nitric oxide synthase
EPR – Electron paramagnetic resonance
ETC – Electron transport chain
FBS – Foetal bovine serum
FMD – Flow-mediated dilation
G6PD – Glucose 6-phosphate dehydrogenase
GAPDH – Glyceraldehyde 3-phosphate dehydrogenase
GST – Glycolysis stress test
HPLC – High-performance liquid chromatography
IAA – Iodoacetate
IL-1β – Interleukin 1β
KH – Krebs-Henselheit (buffer)
MEM – Minimum essenstial medium
MID – Mass isotopomer distibution
MRI – Magnetic resonance imaging
MST – Mitochondrial stress test
MTX – Methotrexate
NAD – Nicotinamide adenine dinucleotide
NO – Nitric oxide
NOS – Nitric oxide synthase
NOX – NADPH oxidase
OCR – Oxygen consumption rate
PC – Pyruvate carboxylase
PDH – Pyruvate dehydrogenase
PDK – Pyruvate dehydrogenase kinase
PPP – Pentose phosphate pathway
PWV – Pulse wave velocity
R5P – Ribose 5-phosphate
Ru5P – Ribulose 5-phosphate
S7P – Sedoheptulose 5-phosphate
SILAC – Stable isotope labelling with amino acids in cell culture
TAN – Total adenine nucleotides
TCA – Tricarboxylic acid cycle
UPLC – Ultra-performance liquid chromatography
VSMCs – Vascular smooth muscle cells
Xu5P – Xylulose 5-phosphate

ABSTRACT

Ageing and inflammation, key contributors to vascular dysfunction, are also associated with the impairment of mitochondrial function. Multiple known mitochondria-related mechanisms could affect vascular function. However, the functional consequences of metabolic pathways alterations in the regulation of NO-dependent function in basal conditions, ageing, and vascular inflammation remain unclear.

Therefore, the aims of this PhD thesis were the following:

1) To investigate the link between various metabolic pathways and NO-dependent endothelial function in the isolated murine aorta,
2) To characterise the functional and metabolic phenotype of the murine aorta in young and old mice,
3) To compare the metabolic and functional responses to vascular inflammation in the isolated aorta of young and old mice.

The results of this study demonstrated that vascular mitochondrial oxidative metabolism was required to maintain NO production and endothelium-dependent vasodilation in the isolated murine aorta. This process was linked to the production of intracellular ATP but not to extracellular ATP signalling. In contrast, inhibition of glycolysis had a minor effect on NO production and ATP levels in the vessel wall.

Furthermore, comparative studies in young and old C57BL/6 mice revealed that vascular ageing was associated with impaired NO-dependent endothelial function and structural remodelling of the vessel wall, fibrosis and hypertrophy, accompanied by increased aortic stiffness. The age-related deterioration of vascular phenotype and function was associated with decreased NAD pool and impaired mitochondrial and glycolytic capacity, as measured in aortic rings *ex vivo* using a Seahorse XFe96 Analyzer. Metabolic vascular reprogramming was confirmed by fluxomic analysis using fully labelled ^{13}C glucose.

The important set of results of this PhD thesis revealed that IL-1β-induced vascular inflammation led to endothelial dysfunction and functional activation of mitochondrial respiration in the aorta isolated from young C57BL/6 mice. However, in the aorta of old mice, proinflammatory stimulation resulted in endothelial dysfunction without concomitant functional metabolic response. Targeted fluxomic analysis showed that IL-1β-induced vascular inflammation resulted in the activation of the pentose phosphate pathway (PPP) and purine metabolism in both young and old mice. However, in young mice, the PPP activity was less pronounced, and glycolysis and tricarboxylic acid (TCA) cycle were upregulated as well.

Interestingly, in the aorta of aged mice, displaying a shift towards PPP under basal conditions, IL-1β-induced a robust upregulation of PPP and purine metabolism without noticeable activation of glycolysis and TCA. In the IL-1β-stimulated aorta of aged mice, the metabolic flux into TCA and pyruvate oxidation was impaired, but anaplerotic-derived carbon influx to TCA was detected and attributed to pyruvate carboxylase activation. In contrast to the PPP activation profile, a flux into serine, glycine and proline synthesis was observed in both young and old mice after stimulation with IL-1β. Furthermore, no substantial inflammation-related differences in ATP, ADP, or AMP levels were observed in the aorta of young mice. However, a trend towards ATP consumption was observed in the aorta of aged mice.

Notably, the inhibition of the PPP enzyme, glucose 6-phosphate dehydrogenase, by dehydroepiandrosterone significantly improved vascular phenylephrine-induced contractility and endothelium-dependent vasodilation in response to IL-1β in the aorta of aged mice. In contrast, no such effect was observed in the aorta of young mice, which was likely due to a preserved adaptive metabolic response to vascular inflammation in young aorta.

In summary, the results presented in this PhD thesis demonstrated the pivotal function of vascular mitochondrial metabolism in preserving endothelial function. The impaired vascular metabolic flexibility in response to acute proinflammatory stimuli was closely associated with metabolic reprogramming towards the increased activity of PPP and decreased pyruvate oxidation, which contributed to the exacerbation of vascular dysfunction in the setting of inflammation. This finding highlights the potential of bioenergetic enzymes linked to PPP or pyruvate oxidation as novel therapeutic targets for the prevention of age-related deterioration of vascular function, particularly in the presence of inflammation. Finally, the deterioration of mitochondrial respiration flexibility in response to acute proinflammatory stimuli could be an early hallmark of age-dependent vascular dysfunction.

STRESZCZENIE

Starzenie się i stan zapalny, dwa istotne czynniki przyczyniające się do dysfunkcji śródbłonka naczyń krwionośnych, są również związane z upośledzeniem funkcji mitochondriów. Wiele spośród znanych mechanizmów związanych z dysfunkcją mitochondriów może wpływać również na funkcjonowanie naczyń krwionośnych. Niemniej jednak, konsekwencje zmian szlaków metabolicznych w ścianie naczynia dla funkcji śródbłonka zależnej od NO pozostają niewyjaśnione zarówno w warunkach podstawowych jak i podczas starzenia i stanu zapalnego.

Dlatego też, cele niniejszej pracy doktorskiej były następujące:

1) Zbadanie związku między poszczególnymi szlakami metabolicznymi a funkcją śródbłonka zależną od NO w izolowanej aorcie mysiej,
2) Scharakteryzowanie fenotypu, profilu funkcjonalnego i metabolicznego ściany naczynia aorty mysiej podczas starzenia,
3) Porównanie metabolicznej i funkcjonalnej odpowiedzi na wywołany stan zapalny w izolowanej aorcie młodych i starych myszy.

Wyniki przeprowadzonych badań wykazały, że mitochondrialny metabolizm oksydacyjny w ścianie naczynia był niezbędny do utrzymania produkcji NO i rozkurczu aorty mysiej zależnego od śródbłonka. Z tym procesem związane było wyczerpanie wewnątrzkomórkowej puli ATP, ale nie zależał on od zewnątrzkomórkowej sygnalizacji ATP. W przeciwieństwie do tych obserwacji, zahamowanie glikolizy miało niewielki wpływ na produkcję NO i poziom ATP w ścianie naczynia.

Co więcej, badania porównawcze z wykorzystaniem młodych oraz starzejących się, zdrowych myszy C57BL/6 wykazały, że starzenie się naczyń krwionośnych związane było z upośledzoną funkcją śródbłonka oraz przebudową struktury ściany naczynia, zwłóknieniem i hipertrofią komórek mięśniówki gładkiej, której również towarzyszyła zwiększona sztywność aorty. Związane z wiekiem zaburzenie fenotypu i funkcji naczyń krwionośnych było związane ze zmniejszoną pulą NAD i upośledzoną rezerwą mitochondrialną i glikolityczną, mierzoną w izolowanych krążkach aorty *ex vivo* za pomocą analizatora Seahorse XFe96.

Metaboliczne przeprogramowanie naczyń krwionośnych związane ze starzeniem zostało potwierdzone przez analizę fluksomiczną z użyciem glukozy ze znakowanymi atomami węgla ^{13}C.

Co istotne, dowiedziono również, że zapalenie wywołane stymulacją IL-1β w izolowanej aorcie młodych myszy C57BL/6 prowadzi do dysfunkcji śródbłonka

i funkcjonalnej aktywacji oddychania mitochondrialnego i glikolizy. Natomiast w aorcie starych myszy stymulacja prozapalna spowodowała również dysfunkcję śródbłonka bez jednoczesnej odpowiedzi metabolicznej. Analiza fluksomiczna wykazała, że stan zapalny indukowany IL-1β wywołał aktywację szlaku pentozofosforanowego (PPP – ang. *pentose phosphate pathway*) i metabolizmu puryn zarówno w aorcie młodych jak i starych myszy. Jednak u młodych myszy aktywność PPP była mniej nasilona i towarzyszyła jej również aktywacja glikolizy i cyklu kwasów trójkarboksylowych (TCA – ang. *tricarboxylic acid cycle*). Co ciekawe, w aorcie starych myszy, wykazujących większą aktywność PPP w warunkach podstawowych, IL-1β wywołała silną stymulację PPP i metabolizmu puryn bez znaczącej aktywacji podstawowego metabolizmu bioenergetycznego, glikolizy i TCA. Ponadto, w odpowiedzi na stan zapalny utlenianie pirogronianu było osłabione, co wiązało się z anaplerotycznym włączaniem węgla pochodzącego z pirogronianu do cyklu TCA, przypisanym aktywności karboksylazy pirogronianowej. Po stymulacji prozapalnej stwierdzono również zwiększony przepływ węgla w kierunku syntezy seryny, proliny i glicyny zarówno u młodych, jak i starych myszy. W aorcie młodych myszy nie zaobserwowano istotnych różnic w poziomach ATP, ADP lub AMP związanych ze stanem zapalnym. Zaobserwowano jednak tendencję do zużycia ATP w aorcie starych myszy podczas zapalenia.

Dodatkowo wykazano, że zahamowanie enzymu szlaku pentozofosforanowego, dehydrogenazy glukozo-6-fosforanowej, przez dehydroepiandrosteron znacząco poprawia funkcję śródbłonka i skurcz naczynia w odpowiedzi na fenylefrynę w aorcie starych myszy podczas odpowiedzi na stymulację prozapalną. W aorcie młodych myszy nie zaobserwowano takiego wpływu dehydroepiandrosteronu, co najprawdopodobniej wynika z zachowanej adaptacyjnej odpowiedzi metabolicznej na bodziec zapalny.

Podsumowując, wyniki przedstawione w niniejszej pracy doktorskiej wskazują na kluczową funkcję metabolizmu mitochondrialnego w ścianie naczynia w zachowaniu prawidłowej funkcji śródbłonka. Upośledzenie rezerwy metabolicznej w ścianie naczynia wraz z wiekiem jest związane z przeprogramowaniem metabolicznym w kierunku dominującej aktywności szlaku pentozofosforanowego i upośledzonego utleniania pirogronianu, co dodatkowo przyczyniło się do pogorszenia funkcji naczyń w warunkach stanu zapalnego. Powyższe wnioski wskazują na potencjał enzymów bioenergetycznych związanych ze szlakiem pentozofosforanowym lub utlenianiem pirogronianu jako potencjalnych nowych celów terapeutycznych dla poprawy funkcji starzejących się naczyń krwionośnych, w szczególności podczas stanu zapalnego.

I. INTRODUCTION

1. Endothelial cell function

Endothelial cells are a single layer of cells coating the interior wall of the blood vessels. Except for playing the role of a barrier and intermediate between blood and the tissues, endothelial cells produce a number of mediators with endocrine, paracrine and autocrine properties. One of the best-studied functions of endothelium is the control of vascular tone and release of vasoactive factors, but endothelium is also implicated in the control of thrombosis, inflammation and several other processes. One of the most critical mediators released by endothelium is nitric oxide (NO), discovered as an endothelial-derived relaxing factor (EDRF) (Palmer et al., 1987). Released NO acts as a paracrine mediator, stimulating guanyl cyclase in vascular smooth muscle cells to produce cyclic GMP, which subsequently induces a signalling cascade leading to vasodilation (Murad, 1994).

Another important endothelium-derived factor is prostacyclin (PGI_2) (Gryglewski et al., 1976; Moncada et al., 1976), which belongs to eicosanoids and acts by activation of adenylate cyclase generating cAMP. Endothelial cells also release multiple other vasodilatory factors and vasoconstrictors, e.g., endothelin-1 or thromboxane A2 (Krüger-Genge et al., 2019). It was estimated that NO mediates about 25% of basal blood flow, about half of acetylcholine-mediated dilation and 100% of flow-mediated dilation (Joannides et al., 1995; Shiva and Gladwin, 2007). NO also mediates endothelial anti-thrombotic and anti-inflammatory responses (Shiva and Gladwin, 2007), making it a key factor in mediating endothelial function.

Endothelial dysfunction, defined as the impairment of endothelium-dependent vasodilation, is a hallmark and prognostic factor of multiple cardiovascular diseases (Daiber and Chlopicki, 2020). Furthermore, what has been established and is now generally accepted is that endothelial dysfunction is implicated in a variety of other human diseases, such as auto-inflammatory diseases, diabetes, viral infections, cancer or sepsis (Rajendran et al., 2013; Ray et al., 2023). In particular, endothelial dysfunction plays a vital role in ageing-related cardiovascular diseases.

2. Vascular ageing

Cardiovascular disease remains a leading cause of death and disability worldwide (Lakatta and Levy, 2003). Despite a variety of risk factors underlying cardiovascular morbidity, ageing remains the major risk factor not only for cardiovascular disease but also for cancer and dementia (Martin et al., 2024; Niccoli and Partridge, 2012). Ageing is associated with changes in the vasculature, systemic endothelial dysfunction and stiffening of large elastic arteries, and these two phenotypes were proposed to predict overall age-related cardiovascular risk (Toda, 2012; Ungvari et al., 2018).

Ageing has been demonstrated to be associated with endothelial dysfunction (Toda, 2012), which in turn contributes to the pathogenesis of cardiovascular diseases. Importantly, ageing was proved to be an independent risk factor for endothelial dysfunction as analysed in normotensive subjects compared with hypertensive (Taddei et al., 1995). Furthermore, additional conventional risk factors induce accelerated vascular ageing phenotype, further exacerbating the cardiovascular prevalence (Ungvari et al., 2020). The critical role of endothelium-derived NO in ageing was confirmed by Li et al., showing that endothelial nitric oxide synthase (eNOS)-deficient mice exhibit accelerated ageing phenotype resulting in premature death (Li et al., 2004). The mechanisms of ageing-dependent endothelial dysfunction are mainly linked to reduced NO bioavailability, which can result from impaired NOS activity and deactivation of NO by reacting with reactive oxygen species (ROS) and forming peroxynitrite (Kamper et al., 2004; Spier et al., 2004; Toda, 2012; Van Der Loo et al., 2000), rather than reduced eNOS expression (Donato et al., 2009). Endothelial dysfunction is also further aggravated by the presence of lifestyle-related risk factors, such as smoking, obesity, high salt and alcohol intake or lack of physical activity (Toda, 2012). Interestingly, aerobic exercise was proven to maintain preserved endothelial function in active aged subjects (Eskurza et al., 2004; Spier et al., 2004).

Arterial stiffening is primarily attributed to structural changes in the vessel wall, such as increased collagen deposition and elastin degradation, but also to functional changes in vascular smooth muscle cells (Lakatta and Levy, 2003). Furthermore, advanced glycation end-products (AGEs) were proven to accumulate in aged vessels and contribute to structural remodelling *via* cross-linking structural proteins (Fleenor, 2012). Apart from changes in the extracellular matrix, smooth muscle cells were demonstrated to display intrinsic stiffening with ageing due to the changes in the cytoskeleton (Qiu et al., 2010). Increased stiffness of large elastic arteries has multiple consequences for the health span, as it results in an increase

in central and peripheral blood pressure. In particular, it can promote the development of left ventricular hypertrophy (Chung et al., 2012), which leads to heart failure. Arterial stiffness was also demonstrated to contribute to organ damage due to changes in blood pressure pulsatility (Mitchell, 2008). Significantly, arterial stiffness in humans increases in aged humans independently from hypertension (Vaitkevicius et al., 1993) and is strongly correlated with the probability of cardiovascular events (Mitchell et al., 2010). However, physical activity displayed beneficial effects not only for endothelial function, as mentioned above, but also for reducing arterial stiffness (Vaitkevicius et al., 1993).

In summary, endothelial dysfunction and arterial stiffness represent two important vascular phenotypes associated with advanced age and which predict age-related cardiovascular risk. Consequently, this establishes ageing as a standalone and independent risk factor for cardiovascular disease, thereby underscoring the necessity to understand mechanisms of vascular ageing.

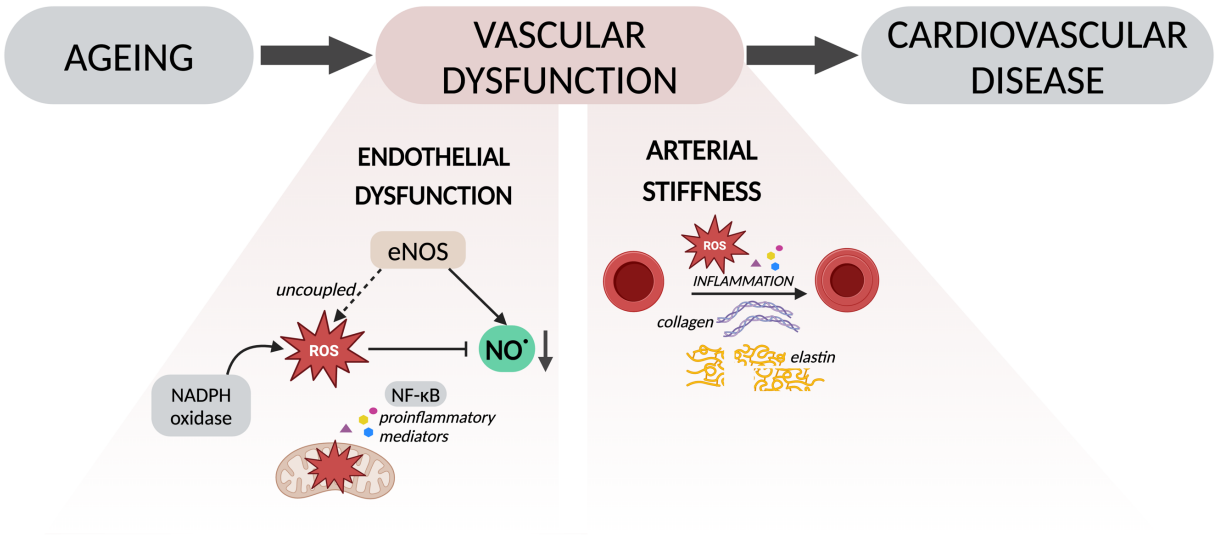

Figure 1. ***Schematic illustration of ageing-dependent mechanisms of two major phenotypes of aged vessels – endothelial dysfunction and arterial stiffness.*** *Endothelial dysfunction is linked to reduced NO bioavailability, which can result from ROS production due to eNOS uncoupling or NADPH oxidase activity, mitochondrial dysfunction and vascular inflammation. Arterial stiffness results from structural changes in the vascular wall including collagen deposition or elastin degradation driven by inflammation and oxidative stress (ROS). Figure adapted from Rossman et al., 2018.*

3. Inflammaging

Chronic low-grade inflammation is one of the hallmarks of ageing (López-Otín et al., 2023), also referred to as inflammaging (Fabbri et al., 2015; Franceschi et al., 2018).

Inflammation drives many age-related chronic diseases (Furman et al., 2019) and is strongly associated with endothelial dysfunction as an underlying factor and a consequence.

The underlying mechanisms of inflammaging are associated with immune dysregulation and the persistent presence of proinflammatory mediators in the circulation of older individuals (Fabbri et al., 2015). Proinflammatory markers were demonstrated to increase the risk of cardiovascular events (Ridker et al., 1997; Sprague and Khalil, 2009), and inflammaging is considered an emerging target in cardiovascular disease. Inflammaging is supposed to stem not only from enhanced inflammatory responses but also from impairment of the resolution of inflammation (Sendama, 2020). Resolution of inflammation is crucial for tissue repair and downregulation of inflammatory response. If the pro-resolving mechanisms are impaired, e.g., in ageing, proinflammatory signalling becomes chronic, and there is an increased risk of tissue remodelling susceptibility to secondary infections that can further promote proinflammatory state (Fullerton and Gilroy, 2016). Furthermore, chronic inflammation triggers the recruitment of inflammatory cells and activation of endothelial cells and vascular smooth muscle cells (VSMCs), promoting atherosclerotic plaque formation (Doran, 2022). Taken together, impairment of the inflammation resolution significantly contributes to cardiovascular risk.

Interestingly, inflammaging was linked to metabolic reprogramming of immune cells, with a shift towards accelerated glycolysis and diminished oxidative metabolism, which support the persistence of inflammation (Netea et al., 2020; Riksen and Netea, 2021). Mitochondrial dysfunction is considered as one of the underlying causes of inflammaging (Aranda et al., 2024). Noteworthy, similar metabolic patterns, to some extent, may exist in endothelial cells stimulated with proinflammatory factors, including accelerated glycolysis and diminished oxidative metabolism (Xiao et al., 2021). Furthermore, vascular ageing has been associated with mitochondrial dysfunction in the aorta linked to impaired OXPHOS and elevated levels of interleukin 6 (IL-6) proinflammatory cytokine (Tyrrell et al., 2020a), which can suggest that metabolic reprogramming resulting from ageing and chronic inflammation or inflammageing can also occur in the vasculature.

The prospect of vascular metabolic reprogramming as an additional mechanism of age-dependent endothelial dysfunction becomes a compelling area for further research.

4. Mitochondrial dysfunction in inflammation and ageing

Mitochondrial dysfunction and chronic inflammation both belong to the main hallmarks of ageing (López-Otín et al., 2023). Mitochondrial dysfunction can contribute

to the development of endothelial dysfunction (Gioscia-Ryan et al., 2014), atherosclerosis (Tyrrell et al., 2020b) or increased aortic stiffness (Fleenor et al., 2012; LaRocca et al., 2014a). Multiple studies reported on various aspects of the alterations in mitochondrial function in the context of mitochondrial signalling, ROS production, or mitophagy, but less is known about the role of bioenergetic pathways in the regulation of endothelial function. Excessive oxidative stress has been demonstrated in ageing (Donato et al., 2007); furthermore, ROS were considered a main driver of ageing (Harman, 1972, 1956). On the other hand, overexpression of antioxidative enzymes failed to increase lifespan (Pérez et al., 2009) or increased lifespan in a ROS-independent manner (Cabreiro et al., 2011). Oxidative stress increased with age and correlated with longevity in some models, but oxidative stress does not appear to be a primary driver of aging based on studies in mice (Pérez et al., 2009). Of note, mitochondrial bioenergetics was proven to play a role in vascular ageing; however, the main aspects of those studies were related to ROS production by dysfunctional electron transport chain. These findings raise the question of whether ROS is a primary event or could be rather a secondary effect of impaired mitochondrial bioenergetic function.

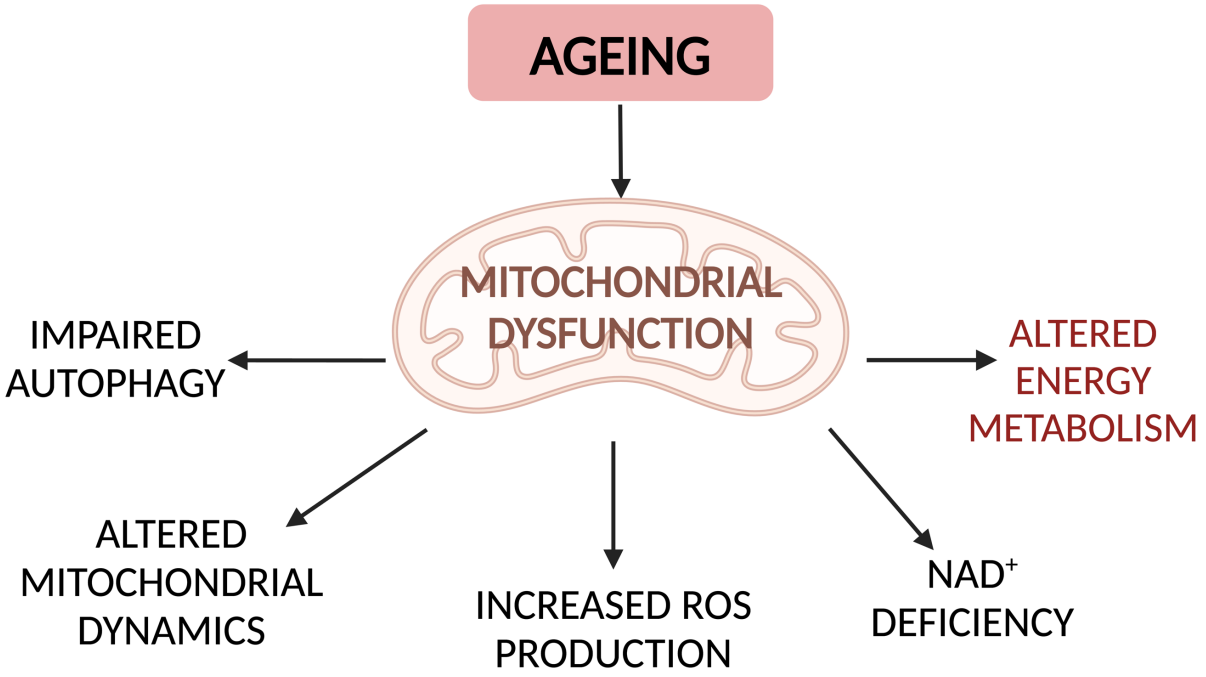

Figure 2. ***Schematic illustration of mitochondria-related dysfunctional mechanisms in ageing.***

To date, the most effective lifespan- and health span-increasing strategies were aerobic exercise and caloric restriction (Csiszar et al., 2009; Walford et al., 1987). Life-long caloric restriction prevented age-dependent arterial stiffening and endothelial dysfunction in mice (Rossman et al., 2018). Interestingly, the underlying mechanisms of a beneficial effect

of caloric restriction were attributed to key nutrient-sensing pathways depending on mTOR (mammalian target of rapamycin) signalling, AMPK (AMP-activated protein kinase) signalling or sirtuins (Rossman et al., 2018; Ungvari et al., 2018). Significantly, all of abovementioned pathways improved mitochondrial oxidative metabolism.

mTOR signalling is known to stimulate mitochondrial oxidative metabolism by modulating the transcription of mitochondrial genes (Morita et al., 2015). AMPK was proven to promote mitochondrial function *via* multiple mechanisms (Herzig and Shaw, 2018). For instance, activation of AMPK stimulated mitochondrial respiration in the murine aorta, and this effect was modulated by 12-HETE as shown in our recent publication (Olkowicz et al., 2024). Taken together, mitochondrial bioenergetic metabolism could also play a role in the mechanisms of vascular ageing.

Understanding the molecular basis of ageing and extending health span is considered a priority of modern geroscience (Campisi et al., 2019; Fontana et al., 2014) and there is an emerging need for novel therapies that focus on age-related phenotypes. Importantly, dysfunctional vasculature is the common factor for all the most common age-related pathologies, including not only cardiovascular disease but also cancer and cerebrovascular diseases. Thus, it is of particular interest to study the mechanisms of vascular ageing, as providing novel therapies targeting vascular ageing could simultaneously cover multiple diseases.

5. Vascular metabolism and its role in inflammation

Given the context of the importance of mitochondrial bioenergetic metabolism in the mechanisms of vascular ageing, it must be emphasized that the main energy source of endothelium is glycolysis rather than mitochondrial oxidative phosphorylation (OXPHOS) (Culic et al., 1997; De Bock et al., 2013; Dobrina and Rossi, 1983), even though endothelium is in the constant contact with blood and thus highly supplied with oxygen.

Glycolysis generates less ATP per unit of glucose, and the strong dependency on glycolytic ATP seems unfavourable; however, several hypotheses explain this adaptation of endothelial cells. Limiting OXPHOS-derived ATP production can protect endothelial cells from oxidative stress, as mitochondria are the main source of ROS (Slade et al., 2017). Notably, one of the main functions of endothelial cells is NO synthesis by endothelial nitric oxide synthase (eNOS). Excessive superoxide production can scavenge endothelial NO and consequently impair vasodilation. NO reacts with superoxide ($O_2^{\cdot-}$) forming peroxynitrite ($ONOO^-$), a strong oxidant, which could have detrimental effects on vascular function (Radi,

2013). Furthermore, limiting oxygen utilisation by endothelial cell metabolism allows more oxygen to diffuse into tissues. Endothelial cells also regulate the process of vessel sprouting *via* glycolysis-dependent mechanisms, and this metabolic adaptation is linked to their angiogenic function (De Bock et al., 2013).

Another advantage of the predominance of glycolytic metabolism of endothelial cells is the possibility to shunt glucose into alternative pathways, such as pentose phosphate pathway (PPP), hexosamine biosynthesis pathway (HBP) or polyol pathway (PP). The main purpose of PPP is to produce NADPH for antioxidant defence and biosynthetic purposes, as well as to produce precursors of nucleotides. The irreversible oxidative phase of PPP, regulated by the activity of glucose 6-phosphate dehydrogenase, the main rate-limiting enzyme, provides NADPH and ribose 5-phosphate. The non-oxidative part is reversible and shares intermediates with glycolysis; however, it can produce only ribose 5-phosphate. Under physiological conditions, around 1–3% of glucose in endothelial cells is utilised by PPP (De Bock et al., 2013). HBP is used to produce uridine diphosphate N-acetylglucosamine (UDP-GlcNAc). UDP-GlcNAc is used for protein glycation, in endothelial cells particularly for the formation of glycocalyx, which is essential for endothelial cell function (Zeng et al., 2018).

On the other hand, endothelial cell phenotype and bioenergetics may vary significantly depending on the specific organ in which they reside (Aird, 2012; Kalucka et al., 2020). For instance, liver sinusoidal endothelial cells have been shown to rely more on OXPHOS-related ATP production than glycolysis (Kaczara et al., 2024). Despite the established dependence of majority of endothelial cells on glycolysis, recent studies also demonstrated that mitochondrial ATP production is required for maintaining endothelium-dependent vasodilation (Wilson et al., 2023), which proves the key role of cell metabolism in maintaining vascular function.

In contrast to endothelial cells, quiescent vascular smooth muscle cells (VSMCs) rely more on OXPHOS-derived ATP. However, VSMCs possess an ability to switch the phenotype from a quiescent, contractile to synthetic proliferative state under stress conditions. Contractile VSMCs are a predominant form in healthy vessels (Pan et al., 2020) and play a crucial role in maintaining vascular tension. Phenotype switching of VSMCs is implicated in the pathogenesis of multiple cardiovascular diseases, such as atherosclerosis, aortic aneurysm or hypertension (Bkaily et al., 2021; Cao et al., 2022).

Changes in endothelial cell and vascular smooth muscle cell metabolism are implicated in multiple conditions, such as atherosclerosis, diabetes or hypertension (Li et al., 2019; Shi et al., 2020). It was demonstrated that proinflammatory stimulation of endothelial cells accelerates

glycolytic flux and downregulates OXPHOS, which promotes inflammation (Schnitzler et al., 2020; Xiao et al., 2021). Furthermore, enhancement of OXPHOS was proven to reduce vascular inflammation (Forteza et al., 2023; Xiao et al., 2021).

In VSMCs, the switch to synthetic phenotype is also driven by metabolic reprogramming towards accelerated glycolysis (Butler and Siegman, 1985; Zhang et al., 2022).

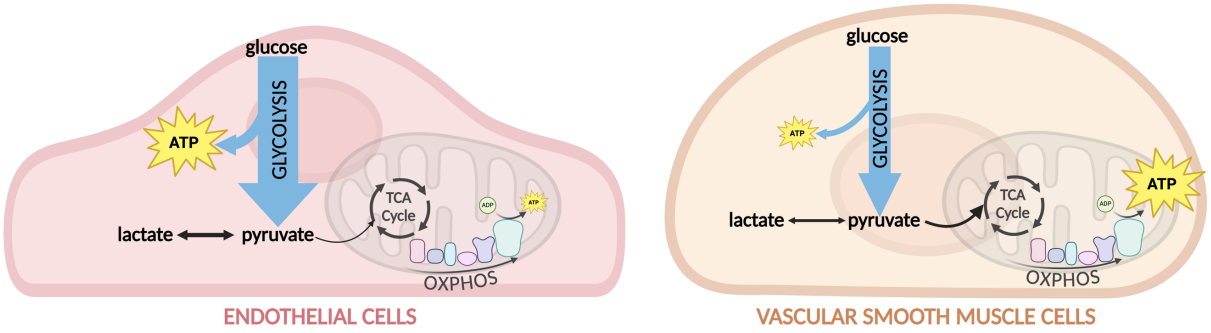

Figure 3. ***Schematic illustration of endothelial cell metabolism compared to metabolism of quiescent vascular smooth muscle cells****. Endothelial cells rely more on glycolytic ATP production than mitochondrial, quiescent vascular smooth muscle cells rely on OXPHOS-derived ATP. TCA – tricarboxylic acid cycle; OXPHOS – oxidative phosphorylation.*

Pharmacological modulation of metabolic pathways could downregulate inflammatory response and consequently improve endothelial function. However, the details of vascular metabolic mechanisms contributing to the maintenance of NO-dependent function and the development of endothelial dysfunction are still unclear.

Noteworthy, the knowledge about vascular metabolic reprogramming was mainly based on research performed on cell cultures and studying separately the metabolism of endothelial cells and vascular smooth muscle cells. The complexity of metabolic crosstalk and the release of multiple paracrine factors between cells in the vascular wall renders the metabolic reprogramming of one cell type as a potential causative agent of alterations in other cell types. Therefore, this type of investigation must take into account the interconnected nature of cells within the vascular wall, as metabolic reprogramming in endothelial cells or VSMCs will inevitably affect each other.

Taken together, existing literature emphasizes the role of metabolic reprogramming in vascular function. However, the question of how vascular inflammatory responses and aging processes contribute to the amplification of vascular metabolomic reprogramming and the deterioration of age-related vascular function remains largely unexplored.

II. AIM OF THE STUDY

Vascular ageing has been associated with chronic low-grade inflammation, a phenomenon termed "inflammaging". Ageing has also been demonstrated to be linked to mitochondrial dysfunction, while inflammatory conditions have been proven to modulate bioenergetic metabolism. However, the details of metabolic alterations in the vessel wall during inflammaging and their contribution to endothelial dysfunction are still not elucidated.

The primary objective of this PhD thesis was therefore to assess the role of vascular mitochondrial bioenergetic metabolism in maintaining endothelial function, with a focus on the contributions of ageing and vascular inflammation.

The specific aims of the present PhD thesis were as follows:

1) To investigate the link between various metabolic pathways and NO-dependent endothelial function in the isolated murine aorta,
2) To characterise the phenotype, functional and metabolic profile of the aged vessel wall of the murine aorta,
3) To compare the metabolic and functional response to induced inflammation in the isolated aorta of young and old mice.

The present PhD thesis in majority consists of original, unpublished results. Only a part of the results was published in:

Karaś, A., Bar, A., Pandian, K., Jasztal, A., Kuryłowicz, Z., Kutryb-Zając, B., Buczek, E., Rocchetti, S., Mohaissen, T., Jędrzejewska, A., Harms, A.C., Kaczara, P., Chłopicki, S., 2024. Functional deterioration of vascular mitochondrial and glycolytic capacity in the aortic rings of aged mice. GeroScience 46, 3831–3844.
Available at: https://doi.org/10.1007/s11357-024-01091-6.
5-year Journal Impact Factor = 6.2 (2023)

III. MATERIALS AND METHODS

1. Experimental models

The studies were carried out using healthy male C57BL/6 mice from the Mossakowski Medical Research Center, Polish Academy of Sciences, Warsaw, Poland. For age group comparisons, young (3–8 months old) and old (18–28 months old) male C57BL/6 mice from Warsaw Medical University, Warsaw, Poland were used. All experiments were carried out according to the Guide for the Care and Use of Laboratory Animals of the National Academy of Sciences (National Institutes of Health publication 85-23, revised 1996) and the Guidelines for the Care and Treatment of Animals of the European Community. The mice were housed under specific pathogen-free conditions (SPF) in a room with constant environmental conditions (22–25°C, 65%–75% humidity, and a 12-hour light/dark cycle) and fed with a standard chow diet and water ad libitum. The sizes of experimental groups and the exact age of mice are reported in the legends of the corresponding graphs.

2. Aorta isolation and preparation for *ex vivo* experiments

Mice were anaesthetised using ketamine/xylazine (100 and 10 mg/kg, respectively) by intraperitoneal administration. For aorta collection, the lungs, liver, pancreas, stomach, spleen, oesophagus, intestines, and kidneys were removed. Aorta was carefully isolated and placed in a dissection Petri dish in ice-cold Krebs-Henseleit (KH) buffer, composed of [mM]: NaCl 118; KCl 4.70; $CaCl_2$ 2.52; $MgSO_4$ 1.64; $NaHCO_3$ 24.88; KH_2PO_4 1.18; glucose 10,00; sodium pyruvate 2.00; EDTA 0.50. Then, using fine micro scissors and forceps (Fine Science Tools), the aorta was divided into thoracic and abdominal parts and was cleaned under a dissecting microscope. Next, the aorta for short incubations (15 min–6h) was placed in KH buffer, and for longer incubations (6h–24h) Minimum Essential Medium containing Gibco-MEM Vitamin Solution, 1% Gibco Antibiotic-Antimycotic, 1% Sigma Non-essential Amino Acid Solution and 0.1% Gibco One Shot Fetal Bovine Serum (FBS). Aortic samples designated for evaluation under basal conditions were cleaned in KH buffer at room temperature and placed in KH buffer heated to 37 °C.

For analysis of the effects of metabolic pathways inhibitors on vascular function, the aorta was preincubated for 15 min or 2h with oligomycin, rotenone, antimycin A or iodoacetate in KH buffer. For wire myography assessments, incubation was performed directly in the myograph organ chambers after aorta stretching and stabilisation.

To assess the effects of acute inflammation on vascular function and metabolism, the aorta was incubated with 1–10 ng/ml interleukin 1β (IL-1β, Sino Biological, China) for 2h or 24h in MEM with 0.1% FBS. In addition, the inhibitors of the PPP and purine synthesis were added for aorta incubation together with IL-1β, dehydroepiandrosterone (DHEA, 50 μM; Sigma-Aldrich, USA) and methotrexate (MTX, 10 μM; Sigma-Aldrich, USA).

Isolated aorta exposed to different factors was used to assess contractile and vasodilatory function, bioenergetics, NO production or metabolite content. For metabolomics and analysis of energetic nucleotides, the aortic segments were snap-frozen in liquid nitrogen directly after incubation. All KH buffer components, media and media supplements were purchased at Sigma-Aldrich (USA).

3. Optimisation of the approach of functional measurement of vascular energy metabolism in isolated aortic rings using the Seahorse XFe96 Analyzer

3.1. Microplate and cartridge preparation

The thoracic part of the aorta, freshly isolated or after incubation, was cut into ~1mm long, even rings and then placed on the Seahorse XFe96 Spheroid Microplate (Agilent, USA) in the assay medium in the middle of a well with vessel walls perpendicular to the bottom of the plate (Karaś et al., 2024). The MST assay was performed in assay medium: Seahorse XF Base Medium Minimal DMEM (Agilent, USA) supplemented with glucose (5.5 mM), pyruvate (1 mM), and glutamine (2 mM), pH 7.4. For the GST procedure, the medium was supplemented only with 2 mM glutamine. All air bubbles were removed from the assay medium immediately prior to placement of the rings, and the plate was kept constantly on a preheated pad to prevent bubble formation. The sensor cartridge was hydrated in Seahorse XF Calibrant (Agilent, USA) solution overnight at 37°C. Media and reagents were prepared freshly on the day of the experiment; the sensor cartridge was loaded with reagents before the measurement.

3.2. Assay performance

Changes in oxygen consumption rate (OCR) and extracellular acidification rate (ECAR) were measured over time, and the response for different reagents was assessed after sequential injections of reagents from built-in ports in sensor cartridges. The mitochondrial stress test (MST) was performed with the sequential addition of 10 μg/ml oligomycin (12.6 μM), 1 μM FCCP (carbonyl cyanide 4-[trifluoromethoxy]phenylhydrazone; 1 μM; Sigma-Aldrich, USA) and 5 μM rotenone with 5 μM antimycin A.

The glycolysis stress test (GST) was performed with the sequential addition of 10 mM glucose, 10 μg/ml oligomycin, and 50 mM 2-deoxyglucose (Sigma-Aldrich, USA).

3.3. Normalisation of the results

All measurements were normalised for protein content in the aortic rings. After the Seahorse assay, the media was removed, and all aortic rings were stored at -80°C. For tissue disruption, aortic rings were placed in homogenisation tubes with 1.4mm ceramic beads (Precellys Soft Tissue Homogenizing Kit CK14) with the addition of 40 μl of T-Per Tissue Protein Extraction Reagent (Thermofisher, USA). The aortic rings were homogenised mechanically using Precellys Evolution Tissue Homogenizer (Bertin, USA), 3 times at a speed of 7800 rpm. All samples were then incubated for 15 min in an ultrasound bath with ice. Homogenates were centrifuged (16602 *g*, 15 min, 4°C), and the supernatants were transferred into new tubes. Protein concentration was measured using Pierce™ BCA Protein Assay Kit (Thermofisher, USA). The protein content values in every aortic ring have been input into the analytic software prior to the calculation of the bioenergetic parameters.

3.4. Data analysis

Data from the Seahorse measurement were recorded and analysed with Wave software (Agilent, USA). Changes in ECAR rates were used in the GST assay to calculate glycolytic parameters, basal glycolysis, glycolytic capacity, glycolytic reserve, and nonglycolytic acidification. Based on OCR measurements in the MST assay, the following parameters of mitochondrial function were calculated: basal respiration (OCR), ATP-linked respiration, proton leak, maximal respiration, spare respiratory capacity, and nonmitochondrial respiration. In addition, basal glycolysis was analysed using MST measurements. All calculations were performed following Agilent MST and GST user guides.

4. Wire myography – analysis of vascular function *ex vivo*

The thoracic aorta was cut into 8 rings (2–3 mm long) and mounted between two pins in myograph organ bath chambers (620M, Danish Myo Technology) filled with 5 ml of KH buffer. Initially, the aortic rings were equilibrated for 30 min in KH buffer gassed with carbogen at 37°C. Then, the resting tensions of the rings were increased stepwise to reach 10 mN, and the rings were equilibrated in resting tension for 30 min. The viability of the aorta was assessed based on contractility at 30 mM and 60 mM KCl. The contractile function of the aorta was evaluated as a maximum contraction induced by 3 μM phenylephrine, or as a response to the cumulative concentrations of phenylephrine (Phe, 0.01–3 μM).

Next, the aortic rings were precontracted with increasing concentrations of phenylephrine (0.01–1 μM) to obtain 80–90% of the maximal contraction. Cumulative acetylcholine concentrations (Ach, 0.01–10 μM) were added to examine endothelium-dependent relaxation. Relaxation was expressed as a percentage of phenylephrine-induced contraction. As a control of vasodilation, which is independent of endothelial function, sodium nitroprusside (SNP) was added to precontracted rings in cumulative concentrations (0.001–1 μM) (Wojcik et al., 2015). All tissue responses were recorded using PowerLab software (LabChart, AD Instruments, Australia). Calculations were performed using custom Python scripts. All myography reagents were purchased from Sigma-Aldrich, USA.

5. Direct measurement of NO production using EPR spectroscopy

NO spin trapping was performed based on the protocol proposed by Dikalov and Fink (Dikalov and Fink, 2005) with modifications. The solutions of $FeSO_4 \cdot 7H2O$ (4.45 mg/10 mL) and DETC (7.2 mg/10 mL) were prepared fresh on the day of the experiment, dissolved in ice-cold 0.9% NaCl deoxygenated in argon flow. All solutions were then stored on ice under argon flow. The isolated aorta was opened longitudinally and placed on the 48-well plate in 600 μl of KH buffer containing metabolic inhibitors; then, all samples were preincubated for 15 min at 37°C. Colloidal solution of the $Fe^{2+}(DETC)_2$ complex was prepared by mixing in a 1:1 (vol/vol) ratio of DETC with $FeSO_4 \cdot 7H2O$ to obtain a 0.8 mM complex. To each well with aortic samples, 8 μl of calcium ionophore (A23187, Cayman Chemical, USA; in DMSO) was added, followed by 200 μl of spin trap complex to obtain a mixture containing 1 μM A23187 and 200 μM $Fe^{2+}(DETC)_2$. After the ionophore and spin trap were administered, the aortas were incubated again for 90 min. Immediately after incubation, each aorta was collected and frozen in the centre of the column with 600 μl of KHB buffer in 1 ml of syringes by immersion in liquid nitrogen. The samples were stored at –80°C. Frozen columns with aorta were placed directly into a quartz finger Dewar filled with liquid nitrogen. EPR spectra were measured using an EMX Plus EPR spectrometer (Bruker, Germany) equipped with a high-sensitivity resonance cavity ER 4119HS at liquid nitrogen temperature (77 K). The resulting spectra were converted to ASCII using the DNPLab package (http://dnplab.net/), then the noise was digitally removed, and the spectra were corrected for the averaged baseline. The NO-$Fe(DETC)_2$ signal amplitude was read out using Python scripts.

6. Indirect assessment of NOS activity by analysis of the arginine metabolism using tracer-based metabolomics

Analysis of the conversion of labelled L-arginine was employed to assess NOS and arginase activity in the isolated aorta according to previously described protocols (Karaś et al., 2024; Pandian et al., 2023). The aorta was incubated for 24 hours in RPMI SILAC medium containing 150 µM of labelled L-arginine ($^{13}C_6$,$^{15}N_4$ L-arginine-HCl, Sigma-Aldrich, USA) and 1% FBS. For the last 90 min, NOS activity was stimulated with calcium ionophore (1 µM A23187). After the incubation, the aorta was weighed, and the effluent was collected for analysis, frozen at –80°C, and then freeze-dried. Samples were analysed using the AccQ-TagAQC derivatisation strategy (Waters, Waters B.V. Art. No. 186003836, The Netherlands) and ultra-performance liquid chromatography (UPLC) coupled to QTRAP 6500 mass spectrometer (Pandian et al., 2023).

7. Analysis of the bio energetic nucleotide content in the aorta or aortic effluent with HPLC

For analysis of extracellular AMP accumulation, abdominal parts of the aorta were incubated in KH buffer containing inhibitors of AMP degradation: adenosine 5′-(α,β-methylene)diphosphate (AOPCP, 150 µM; Sigma-Aldrich, USA), 2′-Deoxycoformycin (DCF, 10 µM; Sigma-Aldrich, USA), *S*-(4-Nitrobenzyl)-6-thioinosine (NBTI, 10 µM; Sigma-Aldrich, USA); and stimulated with IL-1β (10 ng/ml). The effluents for the analysis of extracellular AMP were collected during 2 hours of incubation (0', 30', 60' and 120') and transferred directly on an HPLC plate placed on dry ice, freezing instantly.

After incubation with IL-1β or metabolic inhibitors, aortic segments were quickly snap-frozen in liquid nitrogen and then freeze-dried. The tissue samples were homogenised in 100 µl 0.4 M $HClO_4$ using a glass homogeniser. Homogenates were centrifuged (16602 *g*, 15 min, 4°C), and the supernatant was transferred to the new tubes. The pellet was dissolved in 2M NaOH and used for the protein measurement using Bradford assay. Each supernatant was neutralised with 2M KOH until pH ~6.5. Samples were then incubated on ice for 15 min and centrifuged (16602 *g*, 10 min, 4°C). Nucleotide concentrations were assessed in supernatants and aortic effluents using high-performance liquid chromatography (HPLC) (Smolenski et al., 1990). All results were normalised for protein content in aortic fragments.

8. Targeted LC/MS-based fluxomics

The entire thoracic part of the aorta was incubated for 22 hours in MEM + 0.1% FBS with IL-1β (10 ng/ml) or without IL-1β. Then, aortae were transferred to KH buffer without pyruvate containing 10 mM D-glucose-$^{13}C_6$ (Cambridge Isotope Laboratories, USA) and 2 mM glutamine, and samples were kept in control condition or in the presence of IL-1β accordingly to the first part of the incubation. The aortic samples were snap-frozen in liquid nitrogen after 2 hours of incubation with labelled glucose and stored at –80°C. LC/MS sample preparation and analysis were performed in cooperation with the Metabolomics Unit, Institute for Molecular Medicine Finland (University of Helsinki). The samples were prepared and analysed as described previously (Balboa et al., 2022; Panagaki et al., 2022) with minor modifications. Briefly, the stored samples were thawed on ice, weighed, and transferred to homogenisation tubes. Mechanical homogenisation was performed in 500 µl of extraction solvent (40:40:20; Acetonitrile:Methanol:Water). Samples were centrifuged, and supernatant (450 µl) was transferred to a phospholipid removal plate and subjected to 300 mbar suction for 5 minutes. 350 µl of sample from the collection plate was transferred to an evaporation tube and evaporated to dry under a nitrogen stream. The samples were reconstituted in 40 µl extraction buffer (40:40:20; Acetonitrile:Methanol:Water), transferred to LC-MS vials and analysed with Thermo Vanquish UHPLC coupled with Q-Exactive Orbitrap mass spectrometer. A SeQuant ZIC-pHILIC (2.1 × 100 mm, 5-µm particle) column (Merck) was used for chromatographic separation. Peak areas were normalised to Total Ion Count (TIC).

9. Histological analysis of the vascular wall phenotype

Histological evaluation of the aged vascular wall phenotype was conducted on 5-µm cross-sections taken from the thoracic part of the aorta below the aortic arch (Bar et al., 2019). Aortic sections were stained with haematoxylin and eosin (HE) to assess the morphology of the vessel wall and with picrosirius red (PSR) to stain collagen fibres. The sections were scanned using an Olympus BX51 microscope equipped with the dotSlide virtual microscopy system (Olympus, Tokyo, Japan). Image segmentation with Ilastik software was used for quantitative analysis of stained images. As previously described, media thickness was measured from the PSR-stained images (Stamm et al., 2021). Collagen fibre content within the aortic media was assessed by calculating the red pixel count using Ilastik software. Collagen content was expressed as a percentage of total red pixels in the media area.

10. Analysis of aortic stiffness *in vivo* with Doppler

Aortic stiffness was examined as pulse wave velocity (PWV) in the thoracic and abdominal aorta. PWV was measured with a Doppler flow velocity system. Mice were anaesthetised using isoflurane mixed with oxygen, and PWV was measured using 20–MHz Doppler probes. Velocity signals were recorded simultaneously at distinct locations along the thoracic and abdominal aorta, following established protocol (Bar et al., 2020).

11. Assessment of endothelial function *in vivo* with magnetic resonance imaging (MRI)

Endothelial function in old mice was also assessed *in vivo* with magnetic resonance imaging methodology according to previously published protocols (Bar et al., 2015, 2020). The imaging was performed using a 9.4 T scanner (BioSpec 94/20, USR; Bruker BioSpin GmbH; Germany). Mice were anaesthetised with isoflurane and imaged in a supine position, with physiological parameters monitored throughout. Vascular relaxant responses in the abdominal and thoracic aorta were analysed using time-resolved 3D imaging before and 25 minutes after intraperitoneal Ach injection. Flow-mediated dilation in response to active hyperaemia was assessed as relaxation after short-term (5 min) vessel occlusion described in detail elsewhere (Sternak et al., 2018). Data analysis was performed using ImageJ software 1.46r (National Institutes of Health), and vessel volume changes were calculated using custom MATLAB scripts.

12. Statistical analysis

Statistical analyses were performed using GraphPad Prism 10.1 (GraphPad Software). The normality of the distribution was assessed with the Shapiro-Wilk test, and the homogeneity of variance was evaluated using the Brown-Forsythe test. Comparisons between two groups were performed using the t-test or the U-Mann Whitney test for nonparametric data. One-way or two-way ANOVA was used to compare more groups or the Kruskal-Wallis test for nonparametric data. Details of the used statistical test are marked in figure legends. Significance was considered a value of $p \leq 0.05$.

IV. RESULTS

1. METABOLIC REGULATION OF ENDOTHELIAL NO PRODUCTION

1.1. The effect of inhibitors of mitochondrial electron transport chain (ETC) and glycolysis on NO production in the murine aorta

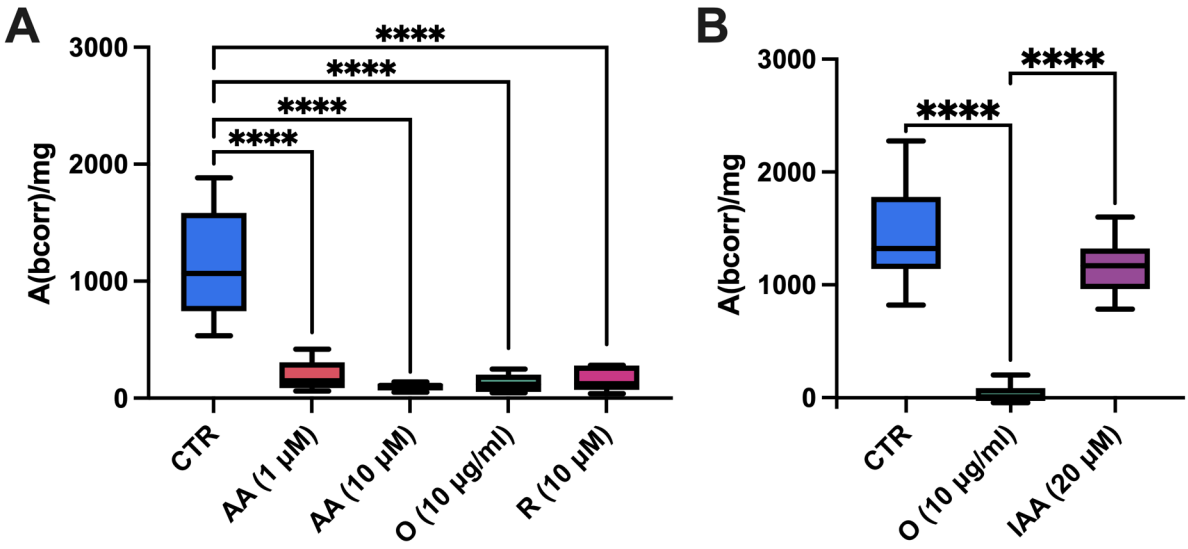

Figure 4. ***The influence of metabolic inhibitors on NO production in the murine aorta ex vivo evaluated with electron paramagnetic resonance spectroscopy (EPR).*** *The aorta isolated from young C57BL/6 mice was longitudinally opened and incubated in KH buffer with metabolic inhibitors: antimycin A (AA, 1 µM, 10 µM), rotenone (R, 10 µM) oligomycin (O, 10 µg/ml) (n=5–8) (**A**) or iodoacetate (IAA, 20 µM) (n=6–9) (**B**). NO was trapped with diethyldithiocarbamic acid sodium salt ($Fe^{2+}(DETC)_2$) and measured as NO-$Fe^{2+}(DETC)_2$ signal with electron paramagnetic resonance (EPR) spectroscopy. Results are presented as box plots (mean is indicated with line, box extends from 25th to 75th percentile, whiskers represent minimum/maximum), analysed with one-way ANOVA, post-hoc Tukey test, ****p ≤ 0.0001 (In cooperation with dr Janusz Pyka, JCET).*

To assess the effect of inhibition of mitochondrial respiration and glycolysis on NO-dependent endothelial function, the NO content in the aorta stimulated with ionophore was measured with EPR spectroscopy after incubation with various metabolic inhibitors. Inhibitors of the mitochondrial electron transport chain (ETC), rotenone (R), antimycin A (AA), and oligomycin (O) fully inhibited the detection of the NO-DETC signal in the aorta. Importantly, this effect was observed using antimycin A at relatively low concentrations (1 µM) (**Figure 4**).

On the contrary, iodoacetate (IAA), the inhibitor of the glycolytic enzyme glyceraldehyde 3-phosphate dehydrogenase (GAPDH), did not influence the NO production in the aorta (**Figure 4**).

1.2. The effects of inhibitors of mitochondrial ETC and glycolysis on endothelial function and vascular contractility assessed in the murine aorta *ex vivo* using wire myography

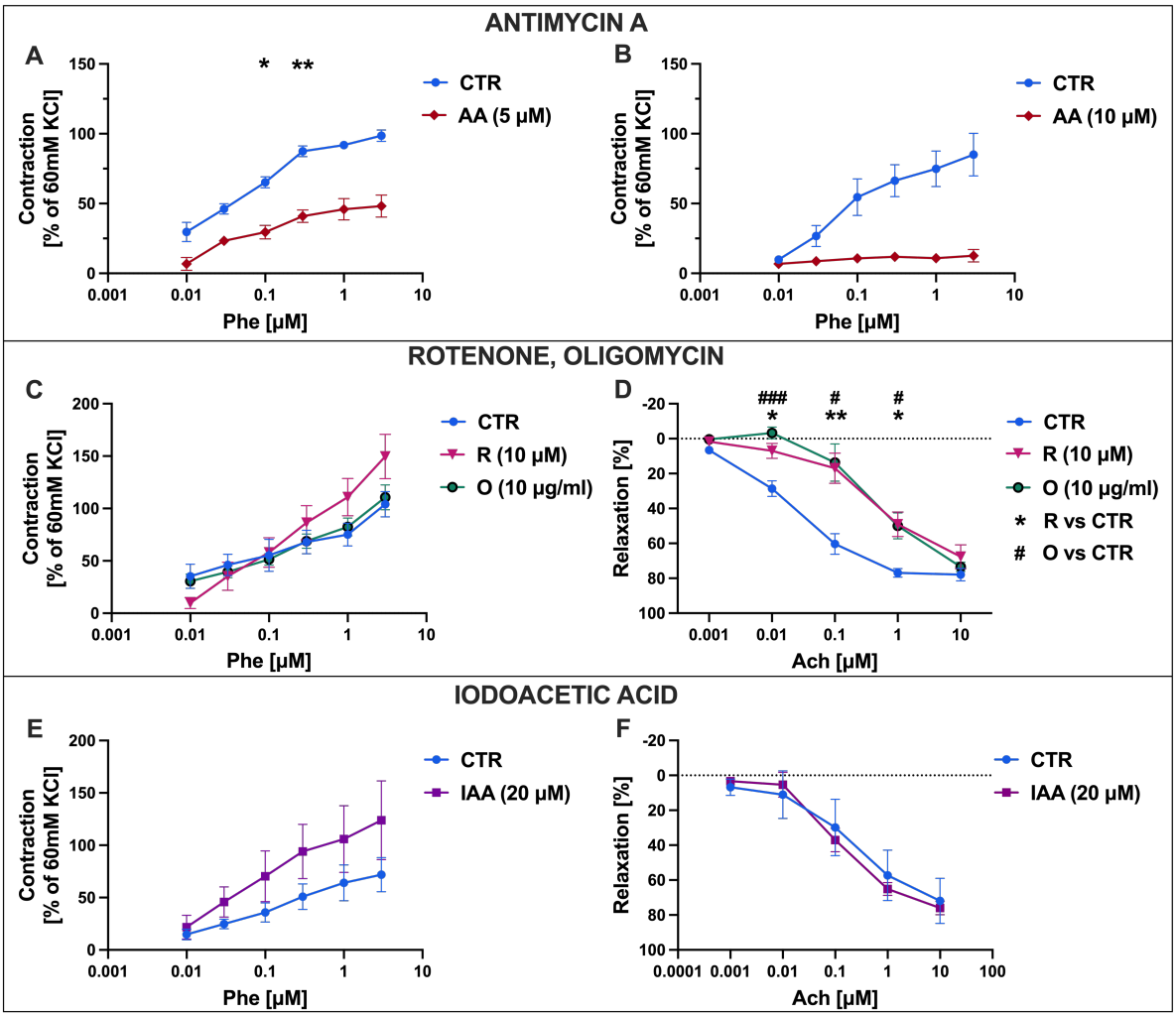

Figure 5. ***Effects of metabolic inhibitors on vascular function in the murine aorta ex vivo.*** *Aortic rings isolated from 3-month-old C57BL/6 mice were pre-incubated in myograph organ bath chambers for 15 min with metabolic inhibitors: antimycin A (AA), rotenone (R), oligomycin (O), or iodoacetic acid (IAA). Contraction (**A, B, C, E**) was assessed as the response to an increasing concentration of phenylephrine (Phe, 0.01 – 3 µM), endothelial function (**D, F**) was measured as relaxation of the aortic rings in response to an increasing concentration of acetylcholine (Ach, 0.001 – 10 µM). Relaxation is presented as a percentage of phenylephrine-induced contraction. Data represent means ± SEM (n=3–6), analysed with two-way ANOVA with post-hoc Šídák test, for CTR vs AA or R: *p ≤ 0.05, ** p ≤ 0.01; for CTR vs O: #p ≤ 0.05, ##p ≤ 0.01, ####p ≤ 0.0001.*

The role of vascular bioenergetics in endothelial regulation of vascular tone was assessed using wire myography on murine aortic rings exposed to ETC or glycolysis inhibitors in the organ bath. In addition to the standard assessment of acetylcholine-dependent vasodilation, vascular contractility in response to α_1-adrenergic stimuli was evaluated by

increasing concentrations of phenylephrine. Antimycin A (10 μM) fully inhibited vascular contraction induced by phenylephrine, and antimycin A at the lower concentration (5 μM) inhibited maximal contraction induced by 3 μM phenylephrine by ~49% (**Figure 5A, B**). On the contrary, rotenone (10 μM) and oligomycin (10 μg/ml) did not influence phenylephrine-induced vessel contractility (**Figure 5C**). Endothelium-dependent relaxation induced by acetylcholine was reduced by rotenone and oligomycin, but the significant impairment of the relaxation was observed in response to lower concentrations of acetylcholine only (0.001–1 μM, **Figure 2D**). Due to a considerable impairment of vessel contraction to phenylephrine after incubation with antimycin A, endothelium-dependent relaxation was not investigated in the aorta pretreated with antimycin A. Inhibition of glycolysis by iodoacetate did not affect phenylephrine-induced contractility or endothelium-dependent relaxation (**Figure 5E, F**).

1.3. Analysis of the effects of mitochondrial ETC inhibitors on basal NO-dependent control of vascular tone in the murine aorta

To analyse the regulatory role of NO in the responses to α_1-adrenergic agonist of vessels exposed to mitochondrial ETC inhibitors, aorta contractility to phenylephrine was assessed in aorta pretreated with ETC inhibitors before and after inhibition of NO synthesis and the differences in vascular responses were compared. Firstly, a concentration-dependent contraction to phenylephrine (0.001–3 μM) was assessed in control vessels and treated with ETC inhibitors, then basal NO synthesis was inhibited by incubation with Nω-Nitro-L-arginine methyl ester (L-NAME, 300 μM) alone or with ETC inhibitors for 20 min and vascular contractility to phenylephrine was reassessed.

As shown in **Figure 6**, inhibition of NOS with L-NAME significantly enhanced contractile responses to phenylephrine across all groups when comparing the contraction before and after incubation with L-NAME. However, the degree of this enhancement, calculated as the difference in maximal contraction induced by 3 μM phenylephrine (**Figure 6C**), was significantly reduced in the groups treated with rotenone (10 μM) or oligomycin (10 μg/ml). The increase in contraction in groups treated with rotenone or oligomycin was significantly lower than in control vessels (**Figure 6C**).

The increase in phenylephrine-induced contraction following L-NAME treatment reflected basal NO-dependent control of the vascular tone. The differences observed between groups treated with ETC inhibitors and control suggest that mitochondrial metabolism was required to maintain basal NO production in the murine aorta.

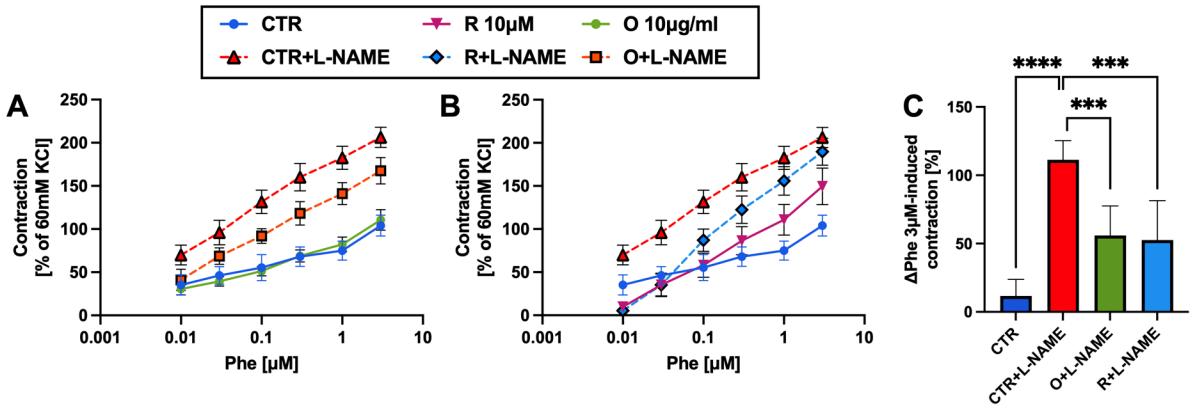

Figure 6. ***The influence of ETC inhibitors on the contribution of basal NO production to phenylephrine-induced contraction in the murine aorta.*** *The aortic rings isolated from 3-month-old C57BL/6 male mice were incubated for 15 min with oligomycin (10 µg/ml) or rotenone (10 µM) in the myograph organ bath. Vascular contractility to increased concentrations of phenylephrine was assessed, then the aortic rings were incubated with L-NAME (300 µM) for 20 min alone (CTR) or together with metabolic inhibitors (O or R), and contractility to phenylephrine was assessed again (**A, B**). The increase in maximal contraction evoked by 3 µM phenylephrine was calculated as a difference between the first contraction and second, after incubation with L-NAME, and compared using one-way ANOVA with the Tukey post-hoc test (**C**). Data represent means ± SEM (n=7), ***p ≤ 0.001.*

1.4. The effects of the inhibitors of ETC and glycolysis on nucleotide content and redox state in the murine aorta

To investigate the role of mitochondrial respiration and glycolysis in maintaining vascular energy homeostasis, the impact of metabolic inhibitors on the levels of ATP, ADP, AMP, NAD^+, $NADP^+$ and NADH was analysed using HPLC in the isolated aorta. To avoid ATP degradation in the tissues, this method was optimised in a few pilot experiments carried out in collaboration with the team of dr hab. Barbara Kutryb-Zając in Gdańsk Medical University. It was found that the key to this was to avoid any step that could unfreeze the samples after collection and then quickly freeze-dry the tissue, which prevented nucleotide degradation. The isolated aorta was divided into 4 fragments incubated in the control buffer or with the metabolic inhibitors: antimycin A, oligomycin or iodoacetate.

As expected, oligomycin significantly reduced the ATP content in the aorta (**Figure 4A**) with no changes in ADP and AMP (**Figure 7B, C**). Antimycin A caused a slight reduction in ATP level (**Figure 7A**), which was not significant. Inhibition of glycolysis with iodoacetate (IAA) did not affect the levels of adenine nucleotides (**Figure 7A**). AMP content showed an increasing trend after the incubations with antimycin A and oligomycin, indicating energy depletion (**Figure 4C**). Both oligomycin and antimycin A caused a significant reduction

in the ATP/ADP ratio and a nonsignificant but apparent decrease in the ATP/AMP ratio. There were also downward trends in the ratios of ATP/ADP and ATP/AMP after incubation with antimycin A and iodoacetate, but they were less pronounced than the effects on ATP/AMP ratio, and the effect of iodoacetate was marginal. The ATP/ADP ratio in the control group was close to 3, confirming that there was no degradation of ATP induced by experimental conditions and the quality of the prepared aorta samples was good. Furthermore, the adenylate energy charge (AEC) was significantly decreased by antimycin A and slightly by oligomycin (**Figure 5F**). AEC is a parameter indicating the cellular energy state, particularly energy stored in the adenine nucleotide pool (Atkinson and Walton, 1967). On the other hand, NAD^+, NADH and $NADP^+$ levels and ratios remained consistent and were not affected by any of the metabolic inhibitors used (**Figure 8**), suggesting preserved redox state despite bioenergetic metabolism inhibition.

In summary, oligomycin had the most severe effect on the vascular bioenergetic status, indicating the critical role of mitochondrial ATP production in maintaining total ATP pools in the vessel wall. Antimycin A exhibited a milder effect on adenine nucleotide levels but was used at a lower concentration (5 μM), corresponding only to partial vascular dysfunction (**Figure 5A**, chapter 1.2). The iodoacetate-related energy disruption was marginal, reflecting that the overall bioenergetic status of the vessel wall relied more on mitochondrial ATP production than glycolytic.

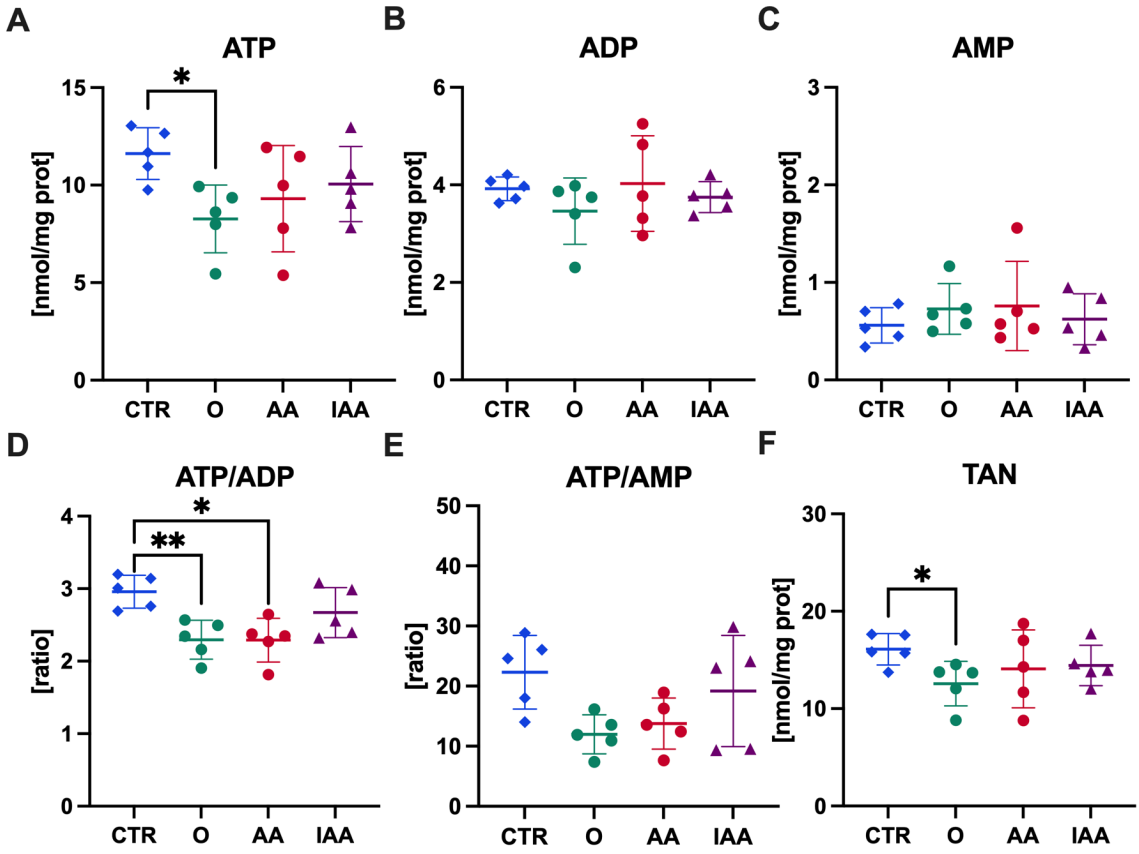

Figure 7. ***The influence of metabolic inhibitors on adenine nucleotide content in the murine aorta.*** *Adenine nucleotides (ATP, ADP, AMP) were measured using HPLC in aortic samples collected from young (3-month-old) C57BL/6 mice incubated for 2h in KH buffer containing oligomycin (O, 10 µg/ml), antimycin A (AA, 5 µM) or iodoacetate (IAA, 20 µM). Data represent means ± SD (n=5), analysed with one-way ANOVA followed by post-hoc Šídák test, *p ≤ 0.05, **p ≤ 0.01 (In cooperation with dr hab. Barbara Kutryb-Zając, Medical University of Gdańsk). TAN – total adenine nucleotides (ATP + ADP + AMP).*

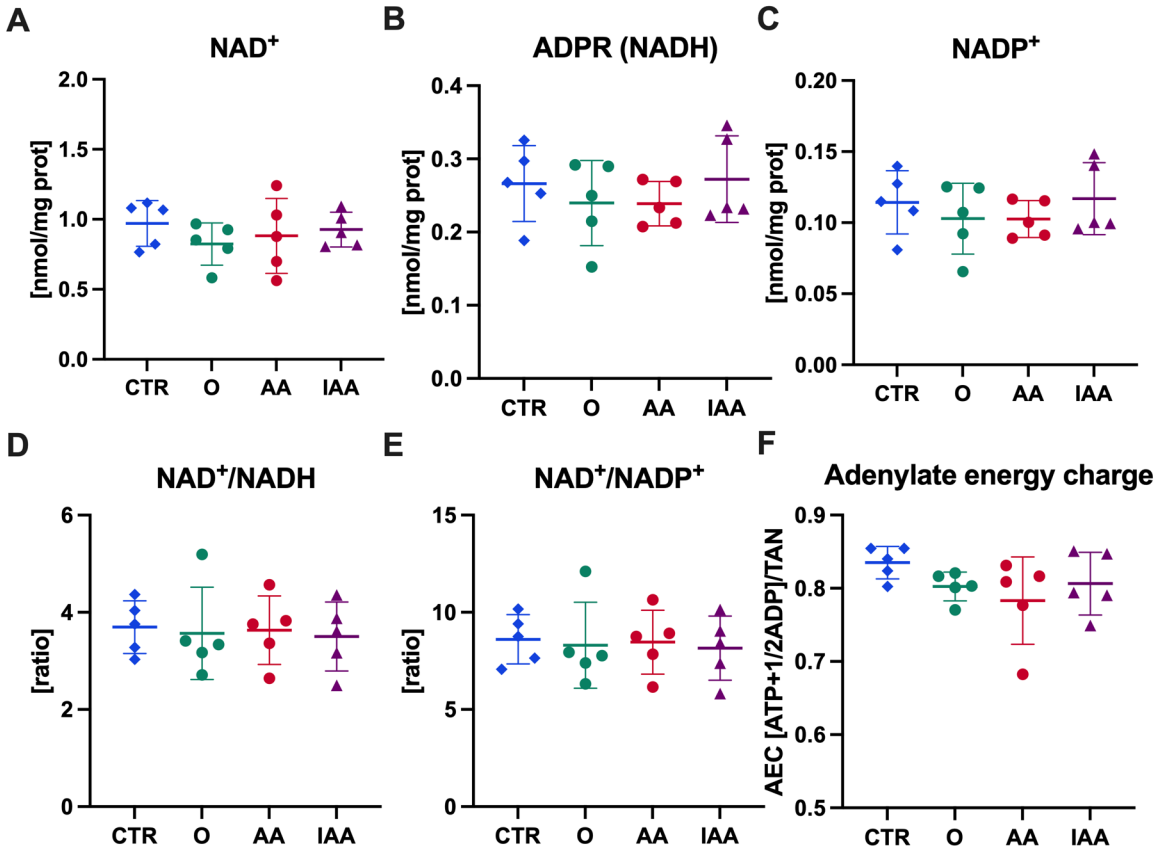

Figure 8. ***Influence of metabolic inhibitors on nicotinamide adenine dinucleotide content in the murine aorta.*** *Adenine nucleotides and nicotinamide adenine dinucleotide in both oxidised (NAD^+) and reduced (NADH) forms were measured using HPLC in aortic samples collected from young (3-month-old) C57BL/6 mice incubated for 2h in KH buffer containing oligomycin (O, 10 µg/ml), antimycin A (AA, 5 µM) or iodoacetate (IAA, 20 µM). Data represent means ± SD (n=5), analysed with one-way ANOVA followed by post-hoc Šídák test, *$p \leq 0.05$, **$p \leq 0.01$ (In cooperation with dr hab. Barbara Kutryb-Zając, Medical University of Gdańsk). AEC – adenylate energy charge.*

1.5. The role of extracellular ATP and purinergic signalling in vascular NO production and vasorelaxation in the murine aorta

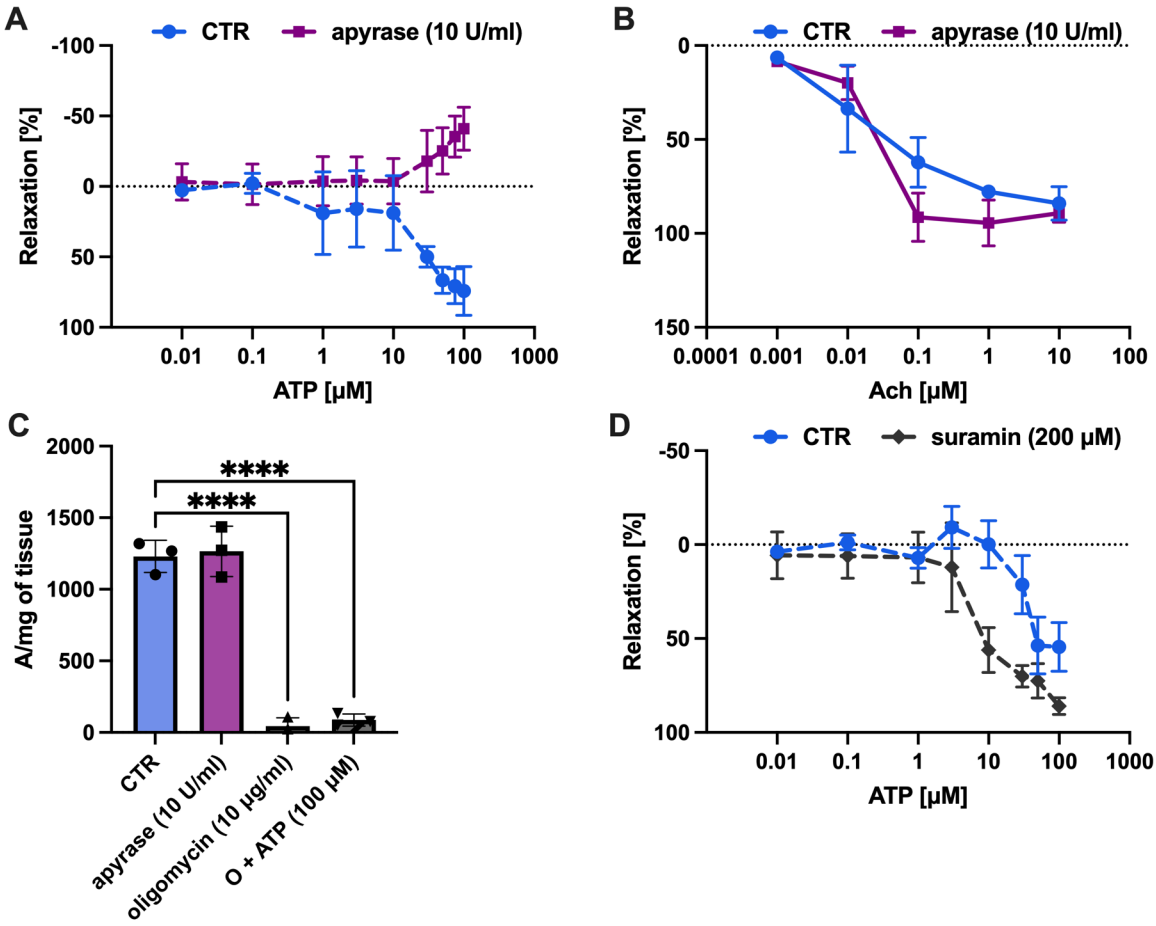

Figure 9. ***The role of extracellular ATP in vascular relaxation and NO production in the murine aorta****. Aortic rings isolated from 3-month-old C57BL/6 male mice were preincubated with apyrase (10 U/ml) for 5 min or suramin (200 μM) for 15 min, and the vasorelaxation to ATP (**A, D**) or Ach (**B**) was assessed (n=2). (**C**) The isolated thoracic aorta was preincubated with apyrase, oligomycin, or oligomycin together with ATP and the NO production was measured with EPR (n=3, in cooperation with dr. Janusz Pyka, JCET), analysed with one-way ANOVA followed by post-hoc Šídák test, ****p ≤ 0.0001. Data represent means ± SEM (graphs A, B, D) or means ± SD (graph C).*

Previous analyses demonstrated that metabolic inhibitors with the most substantial effect on vascular function and NO production, oligomycin and antimycin A, caused notable depletion of ATP in the murine aorta. The potential role of extracellular ATP was investigated to determine whether these effects were solely due to reduced availability of intracellular ATP or could have involved extracellular ATP signalling.

First, extracellular ATP degradation was induced using apyrase, an enzyme that hydrolyses nucleoside triphosphates, to investigate the role of ATP in vascular relaxation. ATP induced concentration-dependent relaxation of aortic rings (**Figure 9A**).

Then, the efficiency of ATP hydrolysis by apyrase was validated by the significant inhibition of vessel relaxation to exogenous ATP (**Figure 9A**). However, no influence of apyrase was observed on vessel relaxation to acetylcholine (**Figure 9B**). This effect was not related to the low enzymatic activity of apyrase, as evidenced by the full inhibition of the vasorelaxant effect of ATP by apyrase (**Figure 9A**). Moreover, apyrase did not affect the production of aortic NO in response to calcium ionophore, as demonstrated by EPR spectroscopy (**Figure 9C**).

To evaluate whether extracellular ATP could rescue oligomycin-induced reduction of NO production in the aorta, ATP was added together with oligomycin, and NO production was assessed with EPR. However, no improvement was observed compared to the aorta incubated with oligomycin alone (**Figure 9C**).

Suramin, a nonspecific antagonist of purinergic receptors P2X and P2Y, was used to study the role of purinergic signalling in aorta vasodilation. Firstly, the vasodilatory response to ATP was tested after preincubation with suramin, but the vessel relaxation was not inhibited by suramin (**Figure 9D**).

In addition, the release of ATP from the vascular wall cells after proinflammatory stimulation in young and old C57BL/6 mice was investigated to estimate the levels of extracellular ATP. Due to the rapid degradation of ATP in extracellular space to ADP, AMP, and then adenosine, a cocktail of inhibitors was used that inhibited the degradation of AMP. Accumulation of extracellular AMP was adopted as a measure of ATP efflux.

The baseline AMP release rate was significantly higher in old mice aorta than in young mice (**Figure 10B**). Proinflammatory stimulation with IL-1β significantly increased the AMP release rate in young mice. In old mice, there was a nonsignificant downward tendency in AMP release in the presence of IL-1β (**Figure 10B**). The basal extracellular AMP accumulated after 2 hours of incubation in the aorta of young mice reached ~5 pmol/mg of tissue. The intracellular concentrations of all adenine nucleotides based on the previous analysis (**Figure 7,** chapter 1.4) were ~11 nmol/mg of protein. The measured intracellular ATP level was ~2000-fold higher than the accumulated extracellular AMP pool, which likely reflects not only the ATP release but the total released pool of ATP, ADP and AMP.

In summary, these findings indicated that extracellular ATP activity was not involved in regulation of NO-dependent vascular function in the murine aorta. The lack of improvement in NO production after adding exogenous ATP to aorta treated with oligomycin further support the conclusion that extracellular ATP was not critical to maintaining NO production. Since oligomycin specifically inhibits ATP synthase, these findings indicate that higher

concentrations of intracellular ATP produced by ETC are required to maintain NO-dependent vascular function and that short-term supplementation with exogenous ATP was insufficient to meet this demand. Furthermore, the observed difference between extracellular AMP accumulation and intracellular ATP pool in the aorta of young mice in basal conditions suggested that the release of ATP have a marginal contribution to vascular ATP pool.

Taken together, described observations implied that the primary activity of ATP produced in the vascular wall was intracellular rather than linked to paracrine signalling in these experimental conditions.

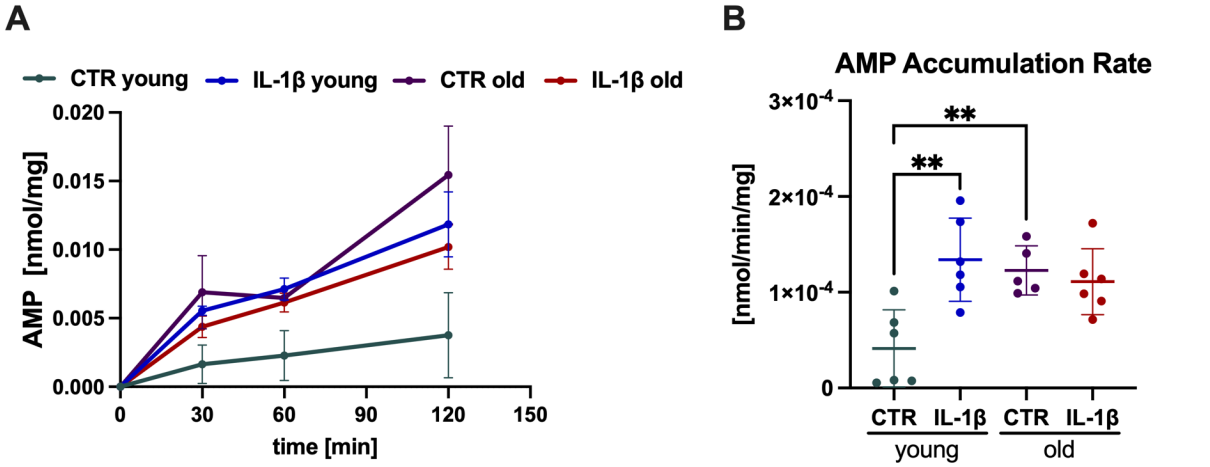

Figure 10. ***Adenine phosphate efflux was measured as AMP accumulation rate from the aorta of young and old C57BL/6 mice after 2h of stimulation with IL-1β.*** *Abdominal aorta isolated from young (3-month-old) and old (28-month-old) C57BL/6 mice was incubated for 2 hours in KH buffer containing 150 μM AOPCP, 10 μM DCF, 10 μM NBTI and stimulated with IL-1β (10 ng/ml). Samples were collected in several time points (0', 30', 60', and 120') and analysed with HPLC for AMP concentrations, representative time-dependent increase in AMP is shown on* ***graph A****. Extracellular AMP efflux rate was calculated per one minute and mg of tissue (****B****). Data represent means ± SEM (n=5–6), analysed with one-way ANOVA followed by post-hoc Šídák test, **p ≤ 0.05, **p ≤ 0.01. (In cooperation with dr hab. Barbara Kutryb-Zając, Medical University of Gdańsk).*

2. METABOLIC AND FUNCTIONAL PROFILE OF OLD VESSELS

2.1. Phenotype of the aorta of old mice assessed with histology

The initial phase of the research on the metabolism and function of the aged vessel wall was to evaluate tissue phenotypes in young (3-month-old) and old (25-month-old) C57BL/6 mice using basic histological assessments. Haematoxylin and eosin (HE) staining was utilised to assess general morphology, revealing a marked increase in smooth muscle cell number and hypertrophy in the aorta of old mice compared to young mice (**Figure 11A, B** – HE panels). In addition, Picro-Sirius Red (PSR) staining was performed to visualise collagen fibres.

The old vessel wall displayed pronounced fibrosis, characterised by enhanced collagen fibre density (**Figure 11A, B** – PSR panels). Quantitative analyses of PSR-stained images demonstrated a significant increase in aortic media thickness (**Figure 11D**) and in relative collagen content (**Figure 11C**) in old C57BL/6 mice compared to young mice. These findings highlight structural remodelling of the aortic wall with ageing, including smooth muscle cell hypertrophy, increased collagen deposition, and medial thickening.

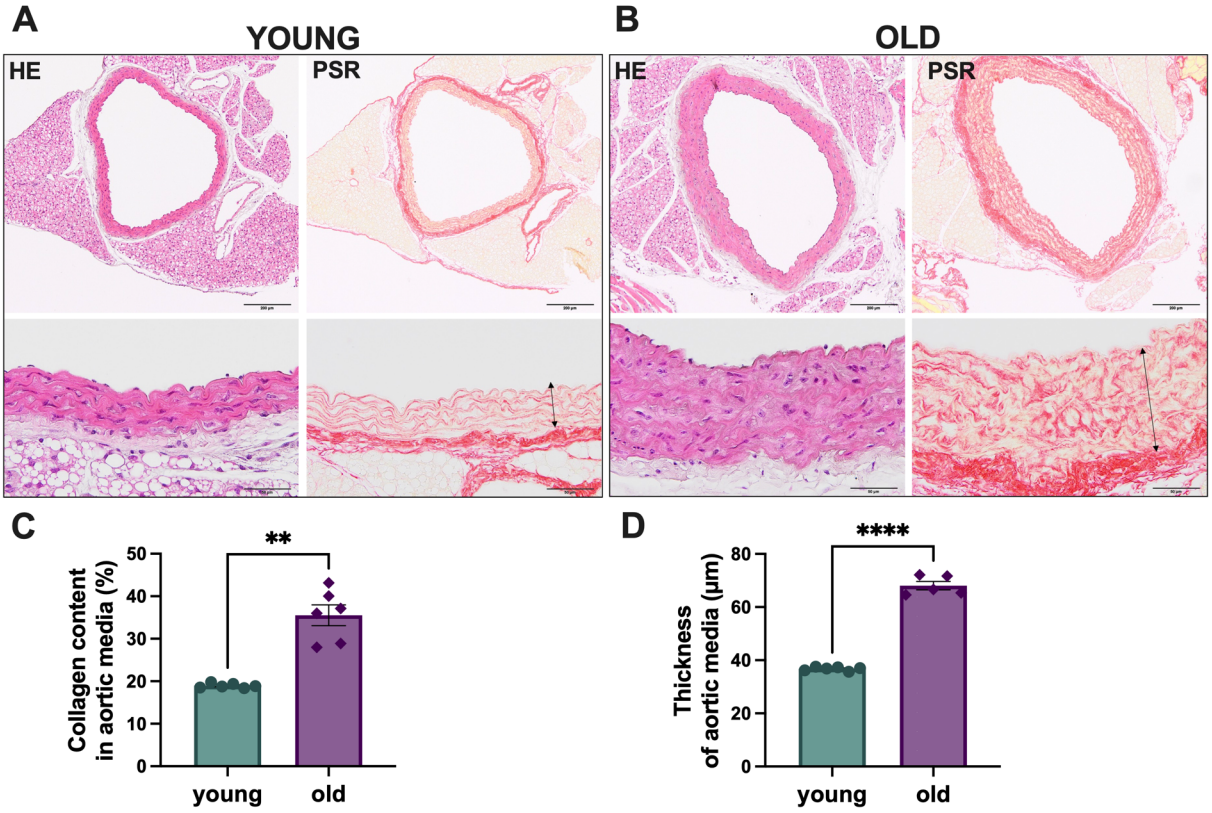

Figure 11. ***Age-dependent remodelling of the aortic wall in old C57BL/6 mice****. Representative images of haematoxylin and eosin (HE) staining (n = 6) and picrosirius red (PSR) staining for collagen fibres (n = 6) in the thoracic aorta of old (25-month-old) mice* ***(B)*** *compared to young (3-month-old) mice* ***(A)*** *at 100x magnification (upper images) and 400x magnification (lower images).* ***(C)*** *Measurement of aortic media thickness based on PSR-stained images, area indicated by arrows in panels A and B.* ***(D)*** *Quantification of the relative collagen content in the media, calculated as the percentage of red pixels in the PSR-stained images. Graphs B and D data are expressed as means ± SEM (n=5–6) and analysed using a t-test, **p ≤ 0.01, ****p ≤ 0.0001. (Figure based on A. Karaś et al., 2024; modified).*

2.2. Analysis of endothelial function in old mice *ex vivo* using wire myography and *in vivo* using MRI imaging

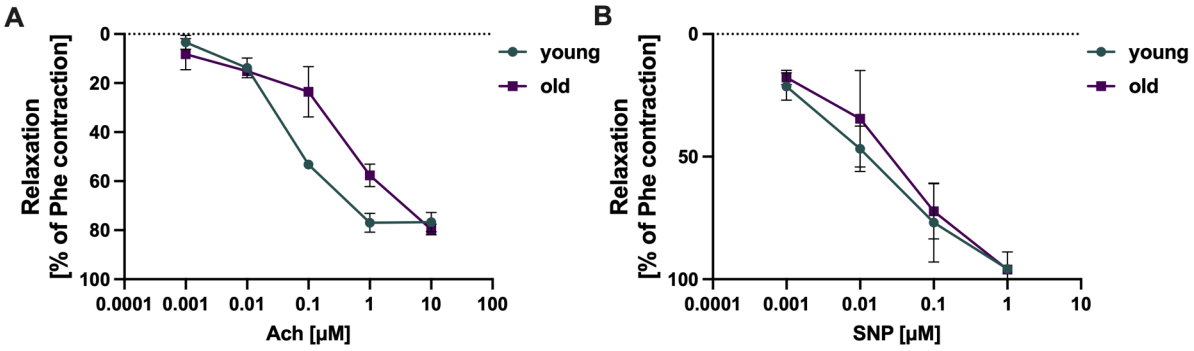

Figure 12. ***Endothelial function in young and old C57BL/6 mice assessed ex vivo in the isolated aorta.*** *Endothelial function was evaluated with wire myography in young (5-month-old) and old (30-month-old) C57BL/6 mice. Endothelium-dependent relaxation of the aortic rings was assessed in response to increasing concentrations of acetylcholine (**A**). Response to sodium nitroprusside (**B,** SNP, 0.001 – 1 µM) was used to assess endothelium-independent vasodilation. Data represent means ± SEM (n=2).*

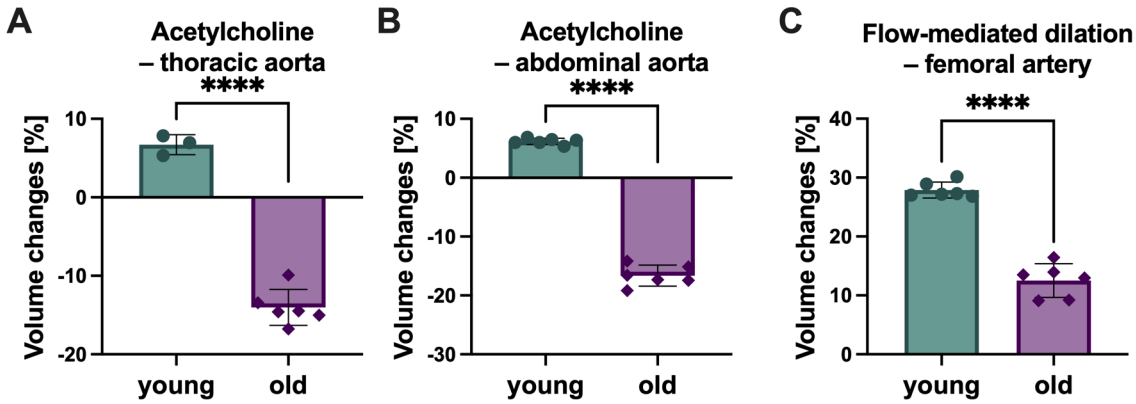

Figure 13. ***Endothelial function in young and old C57BL/6 mice assessed in vivo using magnetic resonance imaging (MRI).*** *The imaging was carried out in young (3-month-old) and old (24-month-old) C57BL/6 mice. Acetylcholine-dependent relaxation was evaluated in the thoracic (**A**) and abdominal aorta (**B**), and flow-mediated dilation was assessed in the femoral artery after short-term vessel occlusion (**C**). Data represent means ± SD (n=3-6), analysed with t-test, ****p ≤ 0.0001 (In cooperation with dr Anna Bar, JCET).*

Endothelial function was investigated in young and old C57BL/6 mice *ex vivo* as acetylcholine-dependent relaxation using wire myography. Endothelial-dependent vasodilation decreased slightly with lower concentrations of acetylcholine in aortic rings isolated from old mice compared to aortic rings of young mice. Still, maximal relaxation induced by 10 µM acetylcholine was comparable in the aorta of young and old mice (**Figure 12A**). Endothelium-independent relaxation in response to SNP was fully preserved in old mice as compared to young mice (**Figure 12**).

On the other hand, MRI analysis of acetylcholine-dependent relaxation revealed severe impairment in old C57BL/6 mice and a switch to vasoconstriction, both in the thoracic aorta (**Figure 13A**) and abdominal aorta (**Figure 13B**). Additionally, flow-mediated dilation was measured in the femoral artery, and it was also impaired in old C57BL/6 mice compared to young mice (**Figure 13C**). Differences between *ex vivo* and *in vivo* analyses may reflect greater sensitivity in assessing vascular function *in vivo* based on magnetic resonance imaging than *ex vivo* assays.

2.3. NOS and arginase activity in the aorta of old mice

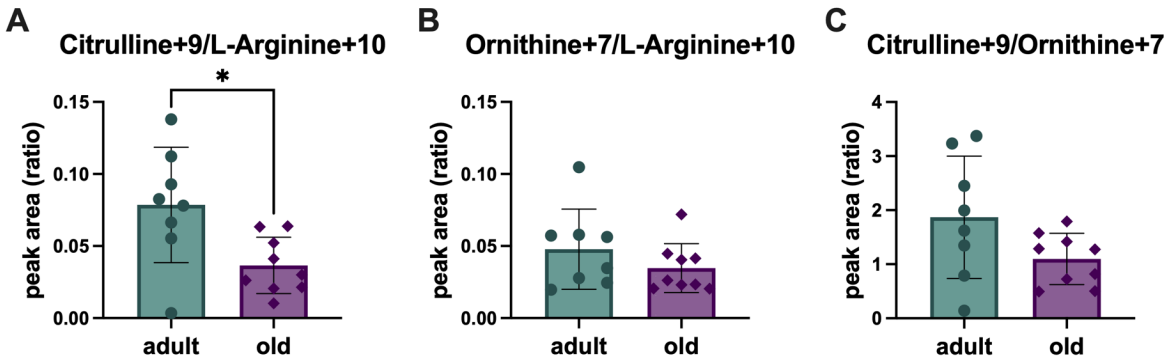

Figure 14. ***Metabolism of labelled L-arginine to citrulline by nitric oxide synthase (NOS) and to ornithine by arginase in the aorta of adult and old C57BL/6 mice.*** *Isolated aorta collected from adult (8-month-old) or old (26-month-old) mice was incubated with* $^{13}C_6$, $^{15}N_4$ *L-Arginine-HCl (Arginine +10) for 24h in RPMI for SILAC containing 1% FBS. For the last 90 min of incubation, calcium ionophore (A23187, 1 µM) was added. The levels of labelled arginine +10,* $^{13}C_6$, $^{15}N_3$ *L-Citrulline (Citrulline +9) and* $^{13}C_5$, $^{15}N_2$ *L-Ornithine (Ornithine +7) were assessed with LC/MS and expressed as ratios reflecting enzymatic activity. Data represent means ± SD (n=8–9), analysed with t-test/Mann-Whitney, *p≤0.05 (Figure based on A. Karaś et al., 2024; modified).*

In addition to functional analyses, another approach was used to assess NO production and nitric oxide synthase (NOS) activity in the aorta of old C57BL/6 mice. The aorta was incubated with labelled L-arginine, NOS activity was stimulated with calcium ionophore, and labelled derivatives of arginine were evaluated with HPLC. The labelled citrulline/arginine ratio was decreased in old mice compared to adult (**Figure 14A**), reflecting diminished NOS activity. The labelled ornithine/arginine ratio (**Figure 14B**), indicating arginase activity, remained unchanged. Furthermore, the labelled citrulline/ornithine ratio (**Figure 14C**) displayed a downward tendency, but the difference was not significant. This ratio could be interpreted as an indicator of relative NOS activity to arginase activity.

These results correspond to age-related endothelial dysfunction described above (chapter 2.2) and may indicate that reduced NO production in the aorta of old mice does not depend on increased arginine utilisation by arginase.

2.4. Evaluation of aortic stiffness in old mice

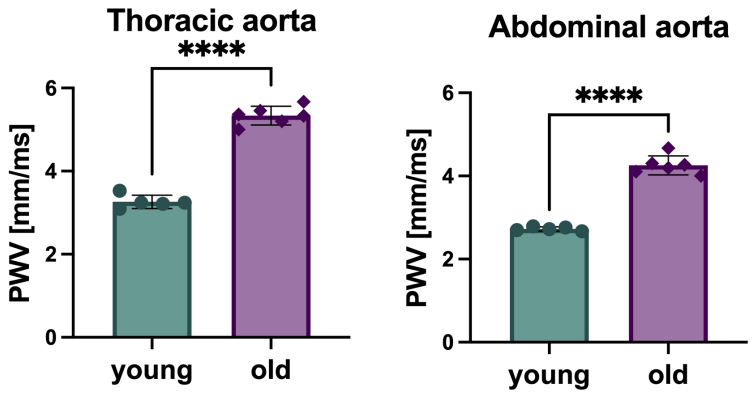

Figure 15. ***Vascular stiffness of the aorta of young and old C57BL/6 mice analysed in vivo.*** *Aortic stiffness was assessed as pulse wave velocity (PWV) using the Doppler system in young (3-month-old) and old (24-month-old) C57BL/6 mice in the thoracic (TA) and abdominal aorta (AA). Data represent means ± SD (n=5–6), analysed with t-test, ****p ≤ 0.001. (Figure based on A. Karaś et al., 2024; modified; in cooperation with dr Anna Bar, JCET).*

Pulse wave velocity (PWV), an indicator of arterial stiffness, was evaluated in young (3-month-old) and old (25-month-old) C57BL/6 mice using the Doppler ultrasound technique. The results demonstrated a significant increase in PWV in old mice compared to the young group in the thoracic and abdominal aorta (**Figure 15**), which reflected increased aortic stiffness with vascular ageing.

2.5. Vascular bioenergetics assessed *ex vivo* in the isolated aorta of old mice

A mitochondrial stress test (MST) and a glycolysis stress test (GST) conducted on isolated aortic rings using Seahorse Analyzer revealed that old and young vessels exhibited distinct functional metabolic profiles. In the aorta of old C57BL/6 mice (25-month-old), significant impairment of spare respiratory capacity and maximal respiration was noted (**Figure 16**) as compared to young C57BL/6 mice (3-month-old). In contrast, the basal level of mitochondrial respiration, evaluated as the basal OCR, was unchanged. ATP-linked OCR reflecting ATP production was also unchanged (**Figure 16**). Furthermore, basal glycolysis, assessed in the GST protocol as basal ECAR, and glycolytic capacity, were reduced in the aortic rings of old mice compared to young mice (**Figure 17**).

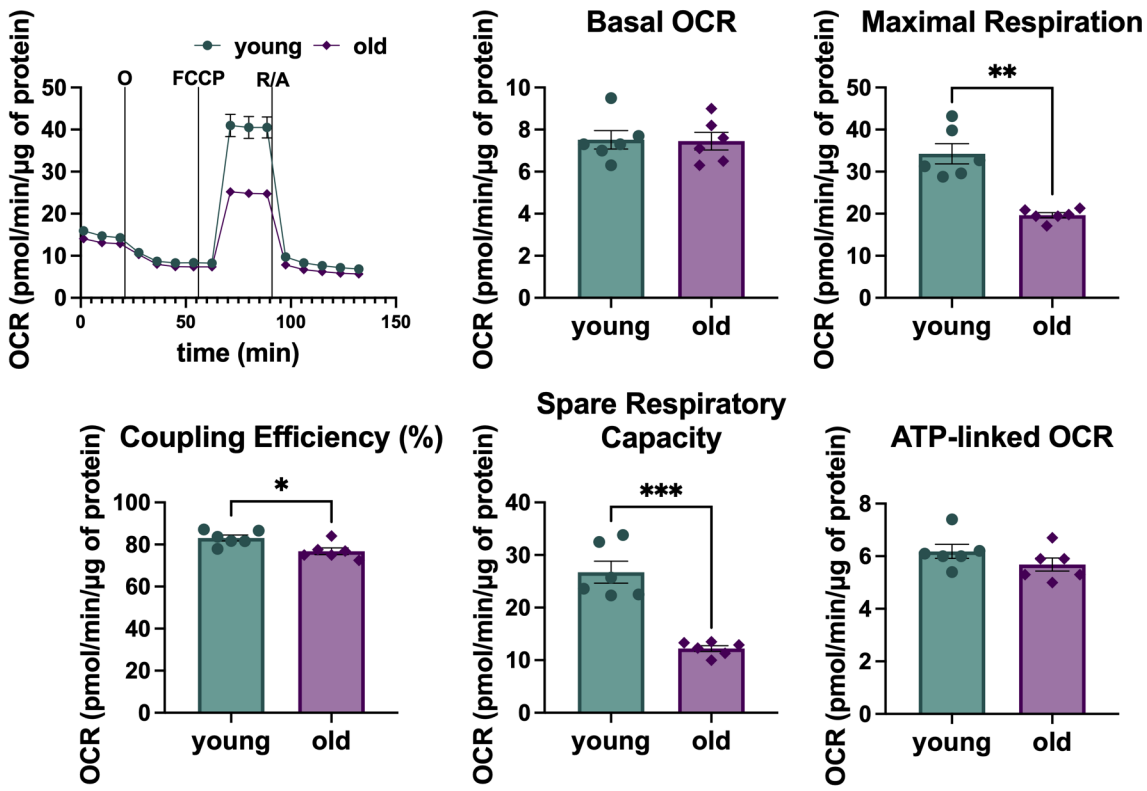

Figure 16. ***Vascular functional metabolic profile (mitochondrial stress test) of young and old C57BL/6 mice evaluated in isolated aortic rings using Seahorse XFe96 Analyzer.*** *The aorta was isolated from 3-month-old or 25-month-old C57BL/6 mice and cut into rings, which were placed on Seahorse Spheroid Microplates. Measurement of OCR was performed with Seahorse XFe96 Analyzer. The bioenergetic parameters were calculated based on the results of the Agilent mitochondrial stress test (MST) procedure. Data represent means ± SEM (n=6). Differences were analysed with t-test, *p ≤ 0.05, **p ≤ 0.01, ***p ≤ 0.001, ****p ≤ 0.001. (Figure based on A. Karaś et al., 2024; modified).*

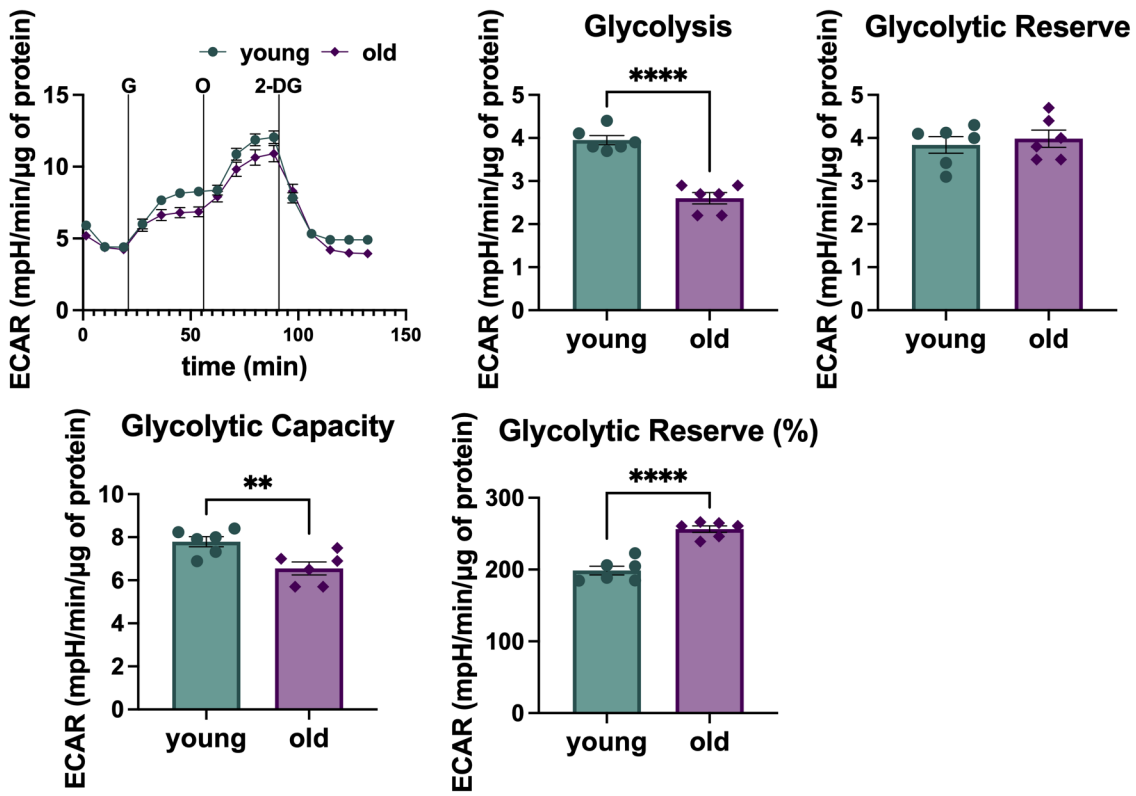

Figure 17. ***Vascular functional metabolic profile (glycolysis stress test) of young and old C57BL/6 mice evaluated in isolated aortic rings using Seahorse XFe96 Analyzer.*** *The aorta was isolated from 3-month-old or 25-month-old C57BL/6 mice and cut into rings, which were placed on Seahorse Spheroid Microplates. The ECAR measurement was performed with a Seahorse XFe96 Analyzer. The bioenergetic parameters were calculated based on the results of the Agilent glycolysis stress test (GST) procedure. Data represent means ± SEM (n=6). Differences were analysed with t-test, **p ≤ 0.01, ****p ≤ 0.001. (Figure based on A. Karaś et al., 2024; modified).*

2.6. Nicotinamide adenine dinucleotide content in the aorta of old mice

The levels of nicotinamide adenine dinucleotide in oxidised (NAD^+) and reduced (NADH) forms were measured in the isolated aorta of young and old C57BL/6 mice using HPLC. Old mice displayed reduced pools in both NAD^+ and NADH in the aorta compared to young mice; however, the redox balance remained unaltered (**Figure 18**).

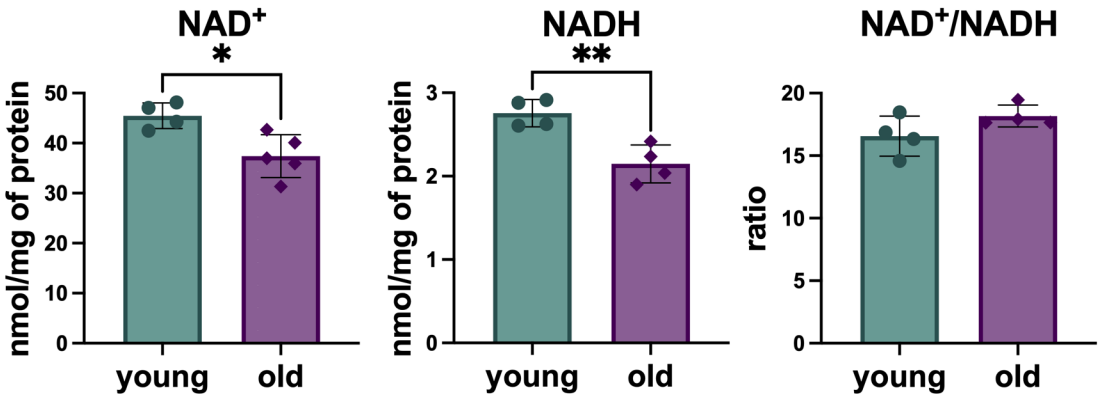

Figure 18. ***Nicotinamide adenine dinucleotide (NAD) levels in the thoracic aorta of young and old C57BL/6 mice.*** *The concentrations of both oxidised (NAD^+) and reduced (NADH) forms were measured using HPLC in aortic samples collected from young (4-month-old) and old (25-month-old) C57BL/6 mice. Data represent means ± SD (n=4), analysed with the t-test, with *p ≤ 0.05, **p ≤ 0.01 (Figure based on A. Karaś et al., 2024; modified).*

3. AGE-DEPENDENT ALTERATIONS IN VASCULAR METABOLISM AND FUNCTIONAL RESPONSES OF THE MURINE AORTA IN VASCULAR INFLAMMATION

3.1. Comparison of the effects of selected proinflammatory cytokines on functional vascular bioenergetic metabolism assessed with Seahorse XFe96 Analyzer

The isolated aorta was incubated with proinflammatory cytokines to check if the *ex vivo* stimulation of isolated vessels could influence vascular metabolism and whether the optimised Seahorse-based approach is sensitive enough to detect acute changes induced by proinflammatory stimulation. Initially, the effects of IL-6 and TNF were compared (**Figure 19**). There was a significant increase in maximal respiration after stimulation with TNF (**Figure 19E**). A slight upward trend in basal mitochondrial respiration (Basal OCR) and and respiration linked to ATP production (ATP-linked OCR) was also observed for both cytokines, but the effect of IL-6 seemed more pronounced (**Figure 19A, B**).

Changes in basal metabolic parameters appeared more intriguing for further studies; therefore, in the second attempt, IL-6 was chosen and compared with IL-1β (**Figure 20**). Stimulation with IL-1β caused significant activation of basal and ATP-linked respiration (**Figure 20E, F**). Accordingly, IL-1β was chosen for further studies on the effect of inflammation on vascular function and metabolism.

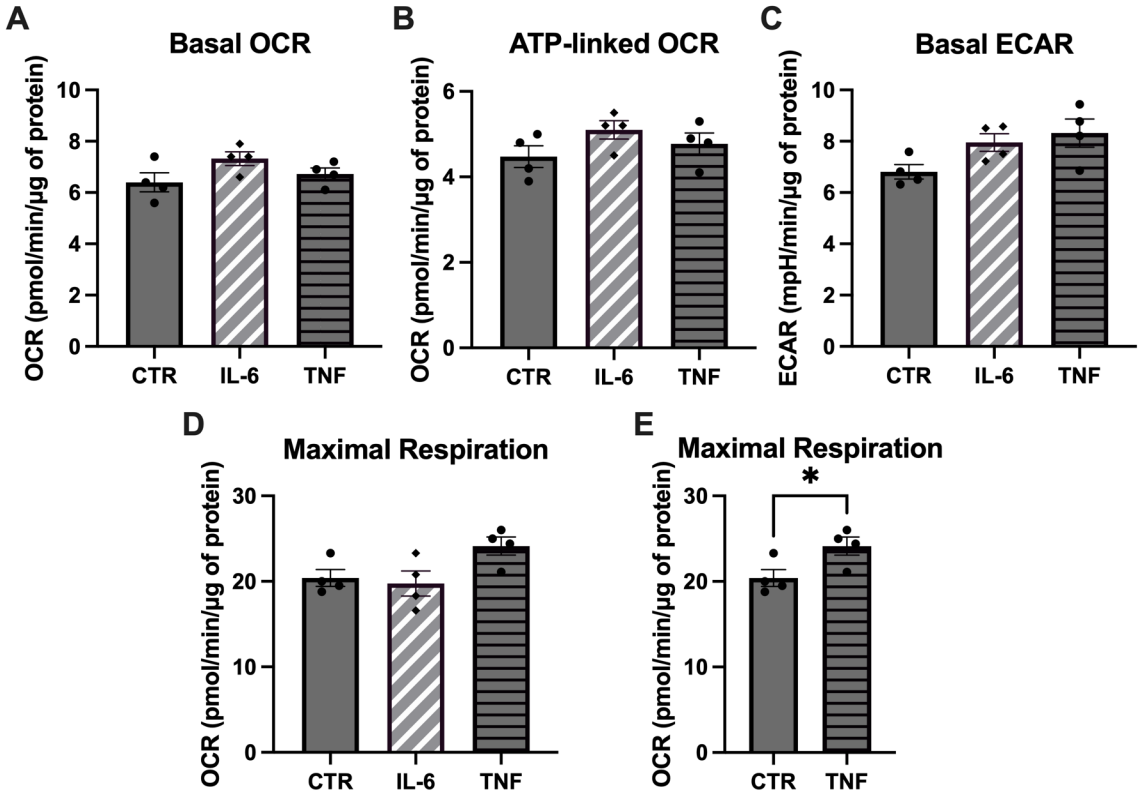

Figure 19. ***Comparison of the effects of stimulation of the isolated aorta with IL-6 and TNF on vascular bioenergetics.*** *The aorta isolated from young (3-month-old) C57BL/6 mice was incubated for 24h in MEM containing 0.1% FBS with IL-6 (10 ng/ml) or TNF (10 ng/ml). OCR and ECAR were measured with Seahorse XFe96 Analyzer according to MST protocol. Data represent means ± SEM (n=4), analysed with ANOVA (graphs* ***A-D****) or t-test (graph* ***E****), *p≤0.05.*

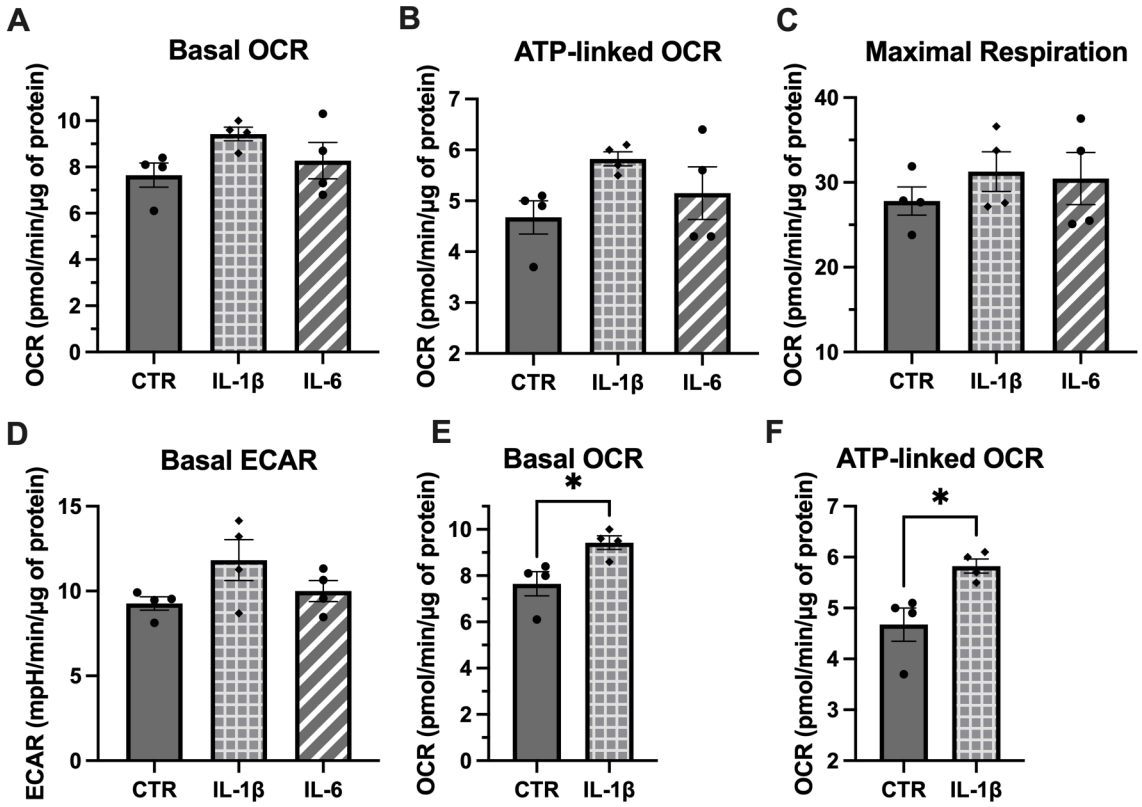

Figure 20. ***Comparison of the effects of stimulation of the isolated aorta with IL-1β and IL-6 on functional vascular bioenergetic metabolism.*** *The aorta isolated from young (3-month-old) C57BL/6 mice was incubated for 24h in medium MEM containing 0.1% FBS with IL-1β (10 ng/ml) or IL-6 (10 ng/ml). OCR and ECAR were measured with Seahorse XFe96 Analyzer according to MST protocol. Data represent means ± SEM (n=4), analysed with ANOVA (graphs* ***A-D****) or t-test (graphs* ***E, F****), *p≤0.05.*

3.2. The effects of IL-1β-induced inflammation on endothelial function and vascular bioenergetic metabolism in the aorta of young mice

To assess if proinflammatory stimulation with IL-1β can impair endothelial function, aorta isolated from young C57BL/6 mice was incubated for 2 hours and 24 hours with IL-1β (1 ng/ml, 3 ng/ml, 10 ng/ml).

Endothelium-dependent relaxation to acetylcholine and endothelium-independent relaxation to SNP were fully preserved in aortic rings incubated for 2 hours with IL-1β (**Figure 21**). In turn, 24 hours of incubation with IL-1β elicited a concentration-dependent impairment of endothelial function (**Figure 22A**). IL-1β at concentrations of 3 ng/ml and 10 ng/ml caused substantial impairment of vasorelaxation to acetylcholine. After the incubation with the lowest concentration of IL-1β (1 ng/ml), relaxation was impaired more modestly, and the difference was not significant. In addition, the highest concentration of IL-1β (10 ng/ml)

also caused diminished endothelium-independent vasodilation induced by SNP (**Figure 22B**), indicating impairment of smooth muscle cell function.

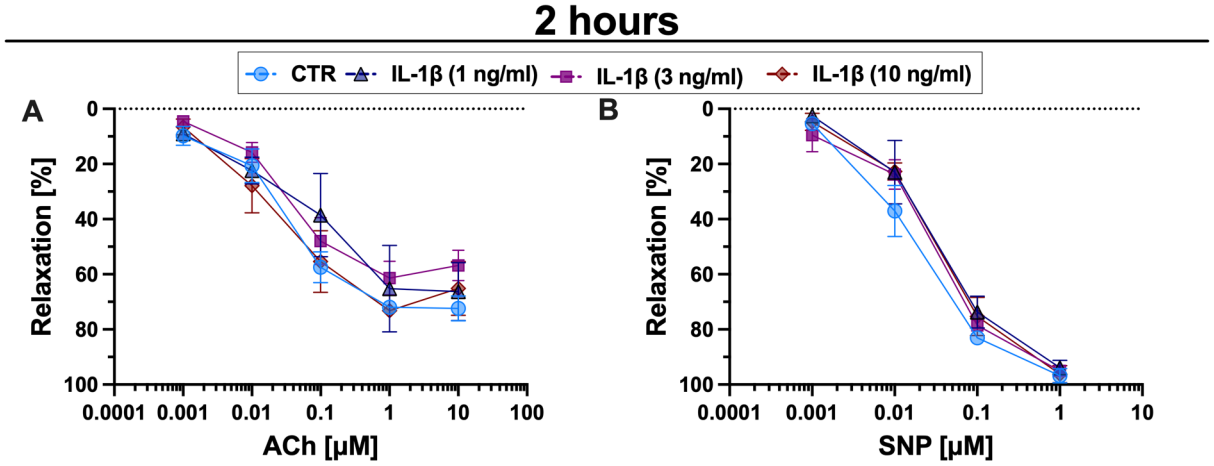

Figure 21. ***Comparison of the effects of IL-1β in different concentrations on vascular function after 2 hours of incubation assessed ex vivo with wire myography.*** *The aorta isolated from 3-month-old C57BL/6 mice was incubated with IL-1β (1 ng/ml; 3 ng/ml; 10 ng/ml) for 2 hours in MEM containing 0.1% FBS. Endothelial function was evaluated with wire myography, and relaxation of the aortic rings was assessed in response to Ach (**A**) for endothelium-dependent vasodilation, or SNP (**B**) for endothelium-independent vasodilation. Data represent the means ± SEM (n=3-6), analysed with two-way ANOVA.*

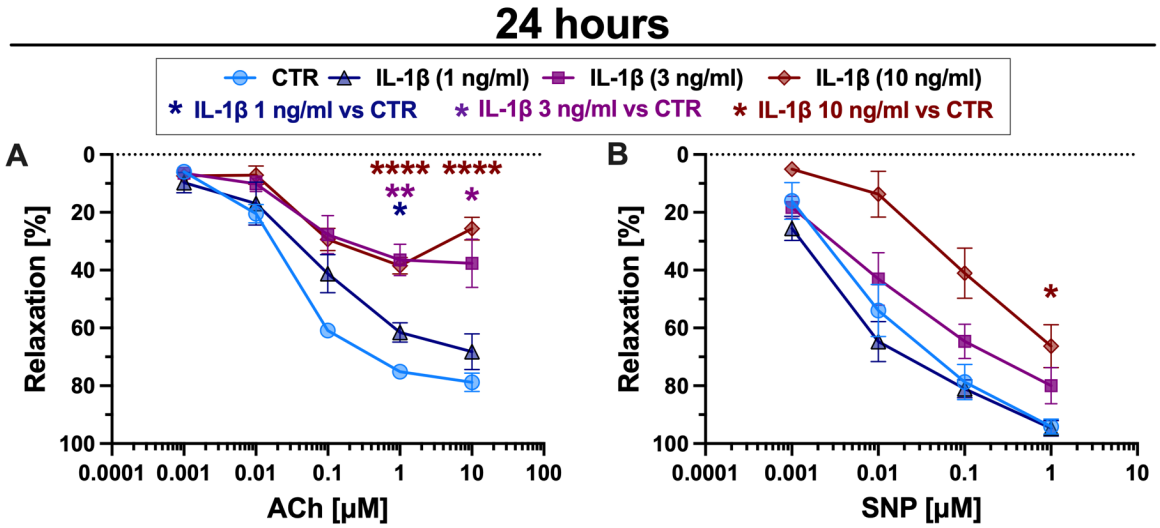

Figure 22. ***Comparison of the effects of IL-1β in different concentrations on vascular function ex vivo after 24 hours of incubation assessed ex vivo with wire myography.*** *The aorta isolated from 3-month-old C57BL/6 mice was incubated with IL-1β (1 ng/ml; 3 ng/ml; 10 ng/ml) for 24 hours in MEM containing 0.1% FBS. Endothelial function was evaluated with wire myography, and relaxation of the aortic rings was assessed in response to Ach (**A**) for endothelium-dependent vasodilation, or SNP (**B**) for endothelium-independent vasodilation. Data represent means ± SEM (n=4–7), analysed with two-way ANOVA, with post-hoc Tukey test, *p≤0.05, **p≤0.01, ****p≤0.0001.*

In the next step, the effect of stimulation with IL-1β on vascular bioenergetics measured *ex vivo* in aortic rings was analysed to compare with endothelial function studies. Therefore, the aorta was incubated with IL-1β for 2 or 24 hours.

After 2 hours of proinflammatory stimulation with IL-1β, aortic rings demonstrated increased basal mitochondrial respiration, respiration linked to ATP production and basal glycolysis measured as basal ECAR (**Figure 23**). Likewise, after 24 hours of stimulation, the activation of mitochondrial respiration was still observed. There was also an increase in basal glycolysis; however, it was not significant (**Figure 24**).

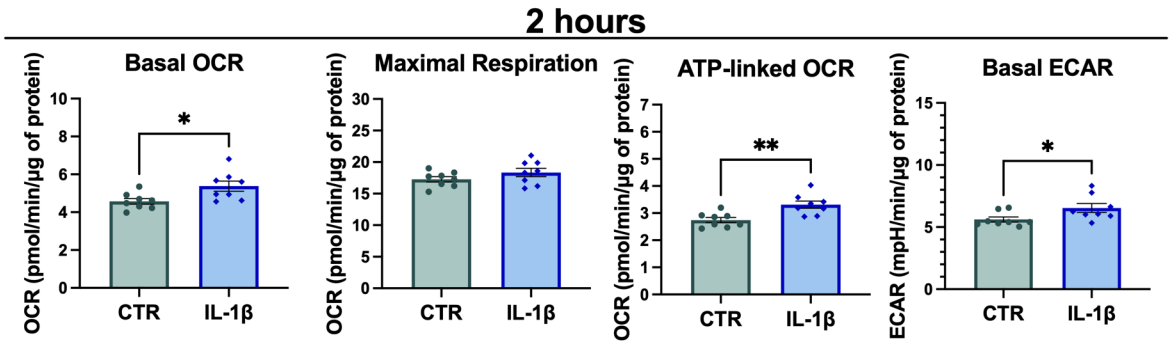

Figure 23. ***Functional vascular bioenergetic response to IL-1β-induced inflammation in the aorta of young mice after 2h of incubation****. The aorta isolated from 3-month-old male C57BL/6 mice was incubated with IL-1β (10 ng/ml) for 2 hours. Vascular bioenergetics was measured with Seahorse XFe96 in aortic rings, mitochondrial stress test (n=8). Data represent the means ± SEM, analysed with t-test, *p≤0.05, ** p≤0.01.*

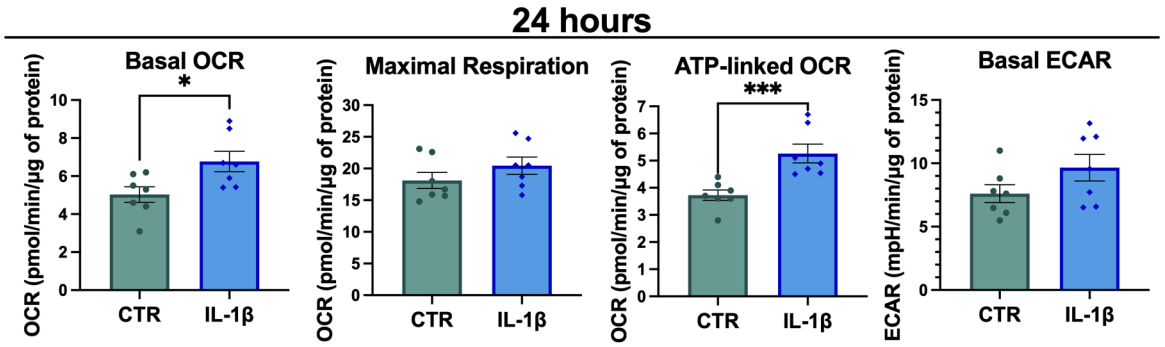

Figure 24. ***Functional vascular bioenergetic response to IL-1β-induced inflammation in the aorta of young mice after 24h of incubation****. The aorta isolated from 3-month-old C57BL/6 mice was incubated with IL-1β (10 ng/ml) for 24 hours. Vascular bioenergetics was measured with Seahorse XFe96 in the aortic rings, mitochondrial stress test (n=8). Data represent means ± SEM, analysed with t-test, *p≤0.05, *** p≤0.001.*

3.3. The effects of IL-1β-induced inflammation on NOS and arginase activity in the aorta of young mice

The effects of 24-hour stimulation with IL-1β on NOS and arginase activity in the aorta were assessed using an HPLC-based approach evaluating the metabolism of labelled L-arginine. The ratio of labelled citrulline to labelled arginine, reflecting NOS activity, was slightly increased after incubation with IL-1β (**Figure 25A**). Stimulation with IL-1β resulted in significant arginase activation, indicated by the increased labelled ornithine/arginine ratio (**Figure 25B**). The decreased labelled citrulline/ornithine ratio caused by IL-1β (**Figure 25C**) reflected a decreased relative NOS to arginase ratio, thereby indicating a predominance of arginine utilisation by arginase during the inflammatory response.

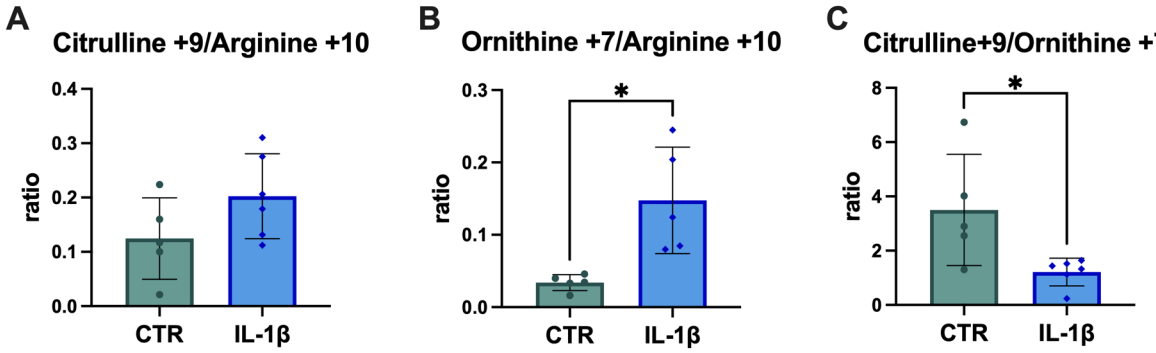

Figure 25. ***The effect of IL-1β on the metabolism of labelled L-arginine to citrulline by nitric oxide synthase (NOS) and to ornithine by arginase in the aorta of young mice.*** *Isolated aorta collected from young mice (3-month-old) was incubated with IL-1β (10 ng/ml) and $^{13}C_6$, $^{15}N_4$ L-Arginine-HCl (Arginine +10) for 24h in RPMI for SILAC containing 1% FBS. For the last 90 min of incubation, calcium ionophore (A23187, 1 μM) was added. The levels of labelled arginine +10, $^{13}C_6$, $^{15}N_3$ L-Citrulline (Citrulline +9) and $^{13}C_5$, $^{15}N_2$ L-Ornithine (Ornithine +7) were assessed with LC/MS and as ratios reflecting enzymatic activity were calculated. Data represent means ± SD (n=5–6), analysed with t-test/Mann-Whitney, *p≤0.05.*

3.4. The effects of IL-1β-induced inflammation on vascular bioenergetics in the aorta of old mice

Vascular metabolism was measured *ex vivo* in aortic rings using Seahorse XFe96 Analyzer, and vascular function was evaluated with wire myography. The aorta isolated from young (3-month-old) or old (22-month-old) C57BL/6 mice was stimulated with IL-1β to analyse the effects of vascular ageing on metabolic and functional responses to inflammation.

Following 24 hours of incubation with IL-1β, the metabolic activation occurred only in young mice, demonstrated as an increase in basal respiration, ATP-linked respiration and basal glycolysis. In contrast, old mice did not respond to inflammation with any changes in bioenergetic parameters (**Figure 26**).

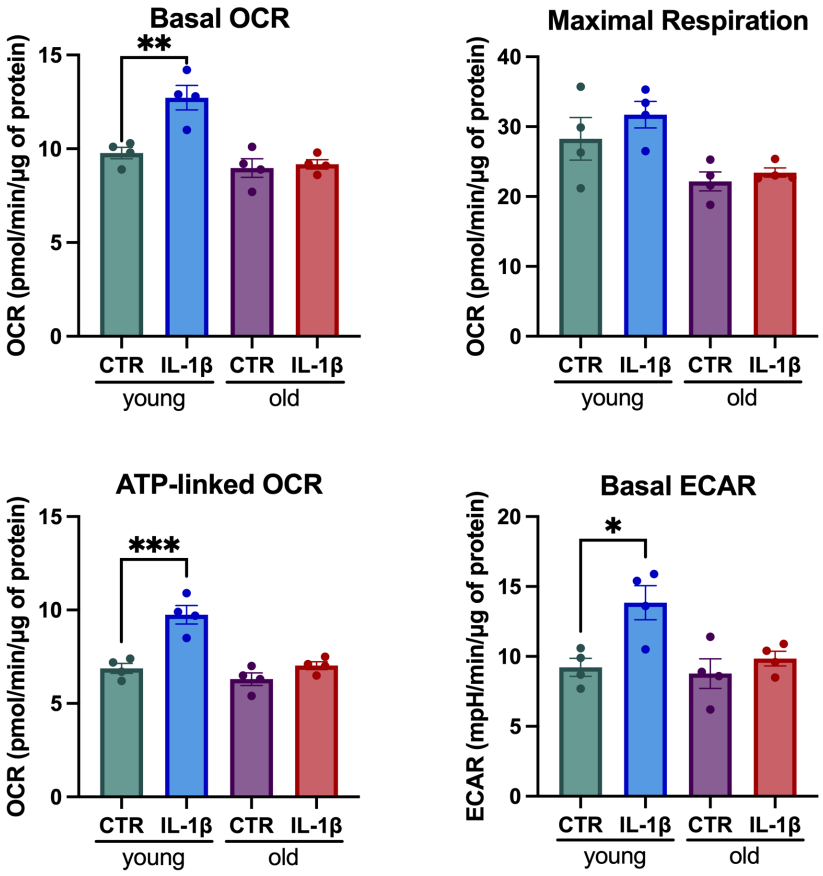

Figure 26. ***Functional vascular bioenergetic response to IL-1β-induced inflammation in the aorta of young and old mice.*** *The isolated aorta of young (3-month-old), and old (22-month-old) C57BL/6 mice was incubated with IL-1β (10 ng/ml) for 24 hours. Vascular metabolism was measured in aortic rings using the Seahorse XFe96 Analyzer. Data represent means ± SEM (n=4), analysed with one-way ANOVA or Kruskal–Wallis test (Max. Resp.), *p≤0.05, ** ≤0.01, ***p≤0.001.*

Furthermore, vascular functional metabolic profile and metabolic response to IL-1β was assessed in middle aged mice (10–12 months), to evaluate the age-dependent progression of changes in vascular metabolism. Vascular functional bioenergetics was assessed in basal conditions in the aorta of 10-month-old mice and compared with 3-month-old mice. No changes in bioenergetic parameters were observed (**Figure 27A**). In contrast to 24-month-old mice (**Figure 16**), spare respiratory capacity was fully preserved at this stage.

Interestingly, the aorta of middle-aged mice (12-month-old) did not respond to stimulation with IL-1β with activation of mitochondrial respiration after 2 or 24 hours of incubation (**Figure 27A**, **B**). Only an increase in basal glycolysis after 24h of stimulation was observed (**Figure 27B**).

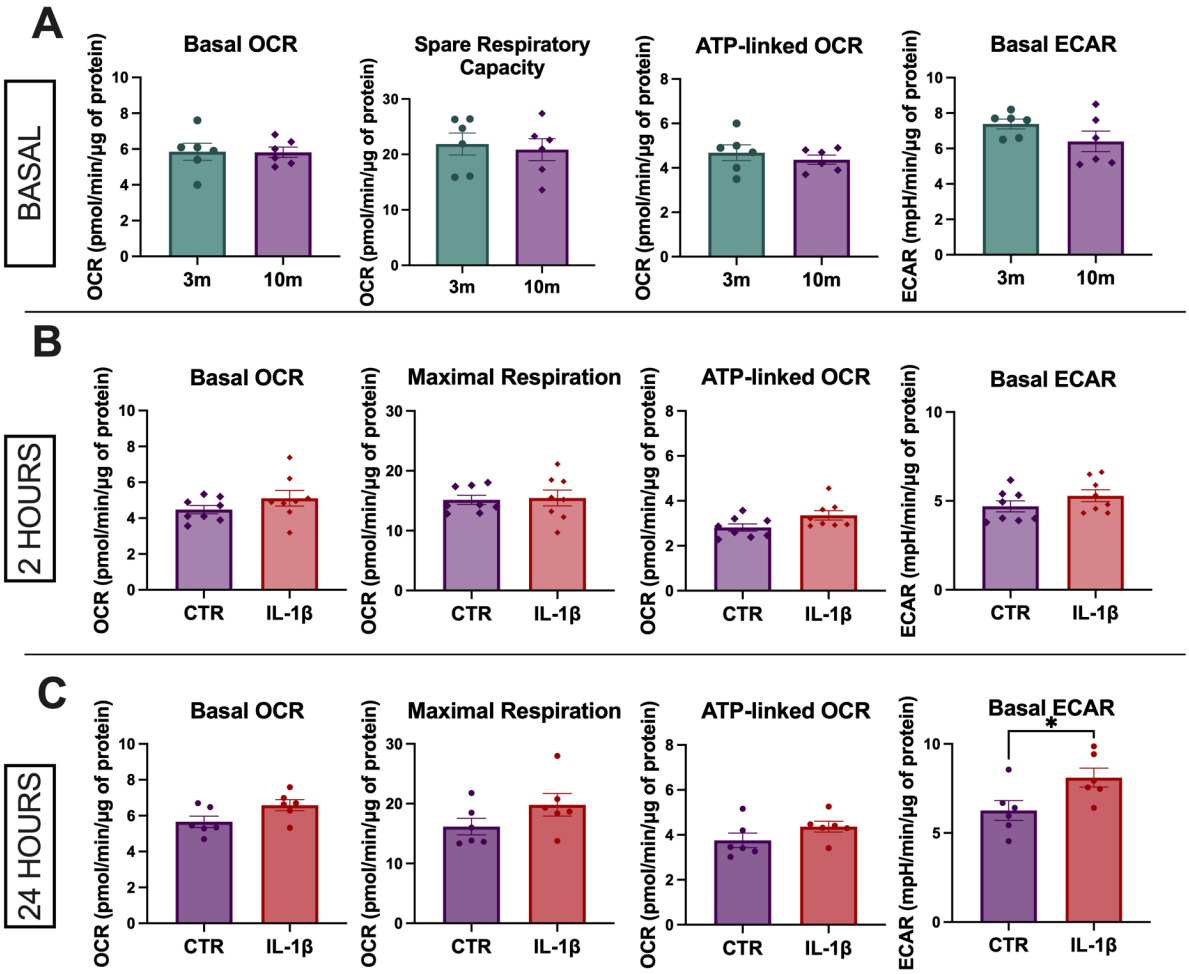

Figure 27. ***Functional vascular bioenergetic profile and the response to IL-1β-induced inflammation in the aorta of middle-aged mice****. (**A**) The aorta was isolated from 10-month-old and 3-month-old C57BL/6 mice and cut into rings, which were placed on Seahorse Spheroid Microplates. Measurement of OCR was performed with Seahorse XFe96 Analyzer. Aorta isolated from 12-month-old C57BL/6 mice was incubated with IL-1β (10 ng/ml) for 2 hours (**panel B**) or 24 hours (**panel C**). Vascular metabolism was measured in aortic rings using the Seahorse XFe96. Data represent means ± SEM (n=6-8). Differences were analysed with t-test, *p ≤ 0.05.*

To summarise, the aorta of middle-aged and old mice exhibited a different metabolic response to inflammation than the aorta of young mice, not exhibiting activation of mitochondrial respiration after stimulation with IL-1β. Interestingly, no changes in basal bioenergetic parameters were detected in middle-aged mice, specifically, the spare respiratory capacity was fully preserved. However, lack of functional activation of mitochondrial respiration in response to proinflammatory stimuli could be an early sign of the loss of metabolic inflexibility.

3.5. Differences in metabolic fluxes after proinflammatory stimulation with IL-1β in the aorta of young and old mice

Targeted fluxomic analysis using $^{13}C_6$ glucose as a tracer was employed to investigate the mechanism of the absence of metabolic activation in the aorta of old mice in response to IL-1β-induced inflammation. Stimulation of the aorta isolated from young (6-month-old) and old (28-month-old) C57BL/6 mice caused multiple differences in the ^{13}C enrichment of the metabolites, indicating a shift in metabolic flux.

The metabolomic analyses were focused mainly on the intermediates of glycolysis, pentose phosphate pathway (PPP), tricarboxylic acid cycle (TCA) and amino acids linked to central metabolic pathways. Results included different isotopomers of each metabolite, with varying numbers of incorporated labelled carbon atoms derived from labelled glucose. The schematic representation of labelled carbon flux and chosen labelling patterns are shown in **Figure 28**. The results analysis was based on manual tracking of the carbon flow, and results were mainly presented as the chosen labelled fractions for which upstream sources of the labelled carbon could be identified. Results were divided into panels and associated with the main pathway. Additionally, a part of the results was calculated as a mean isotopomer distribution (MID), where one fraction is expressed as a percentage of the whole pool of the metabolite isotopomers. The MID-based approach allowed a more comprehensive analysis of the results but indicated labelling patterns rather than absolute quantities. Significantly, unlabelled glutamine was added to the incubation media, except for the labelled glucose as a primary energy source, to assure natural TCA flow and availability of the intermediates. Chosen unlabelled metabolites were also presented to reflect the degree of the TCA dependency on glutamine.

Interestingly, the main effect of the proinflammatory stimulation of the aorta with IL-1β was the activation of the PPP and purine metabolism, both pathways particularly upregulated in old mice.

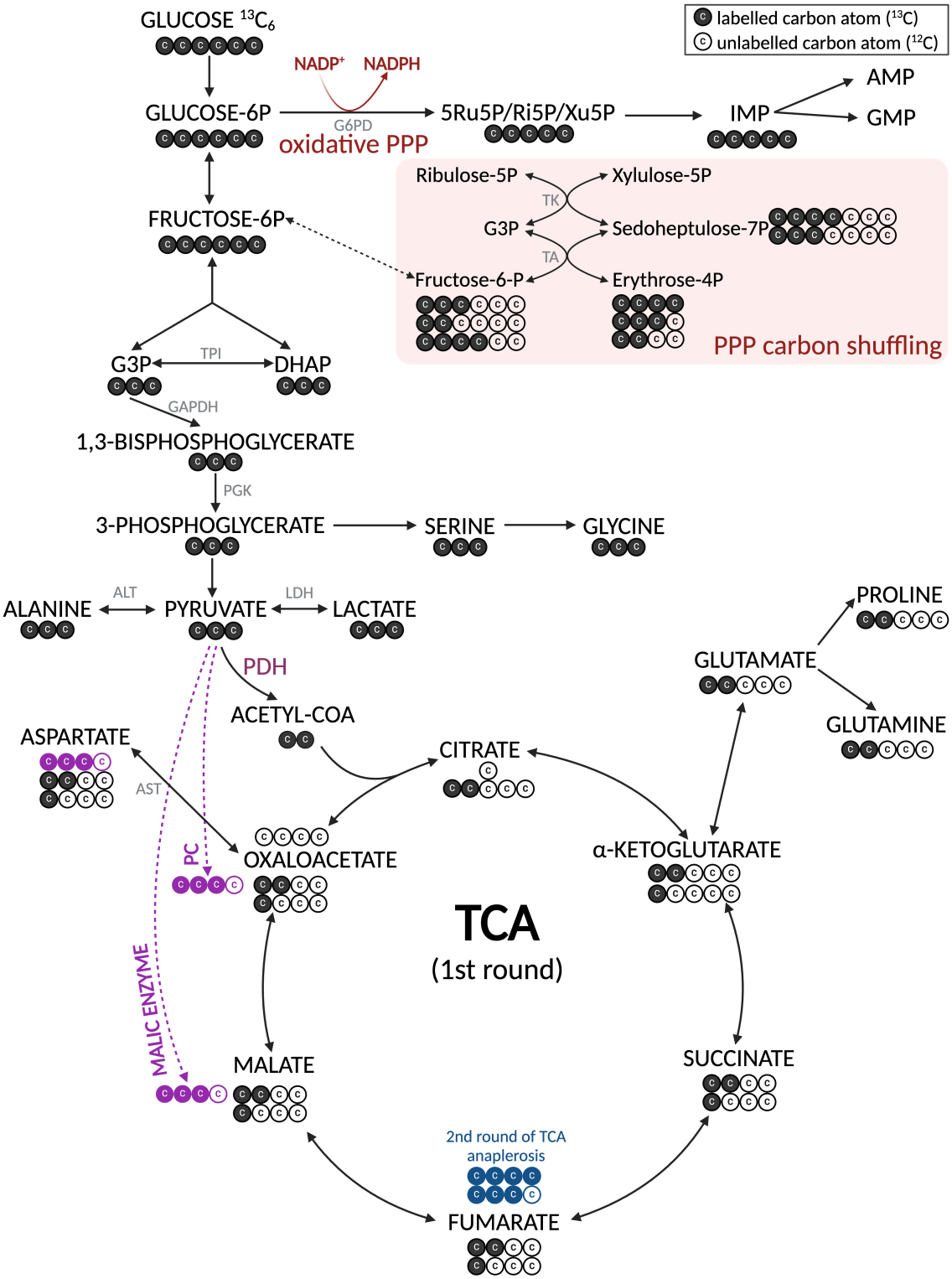

Figure 28. ***Schematic representation of glucose $^{13}C_6$ fluxomics and carbon flow through main metabolic pathways****. Dark circles represent labelled carbon atoms, while white circles represent unlabelled carbon atoms. Violet circles represent potential anaplerotic pathways, blue circles – labelling with 2nd turn of TCA. G3P - Glyceraldehyde-3-phosphate; DHAP – dihydroxyacetone phosphate; Ru5P/Ri5P/Xu5P – Ribose 5-phosphate/Ribulose 5-phosphate/Xylulose 5-phosphate; P – phosphate; PDH – Pyruvate dehydrogenase complex; PC – pyruvate carboxylase; TPI – triphosphate isomerase; GAPDH – glyceraldehyde 3-phosphate dehydrogenase; LDH – lactate deghydrogenase; ALT – Alanine transaminase; AST – aspartate transaminase.*

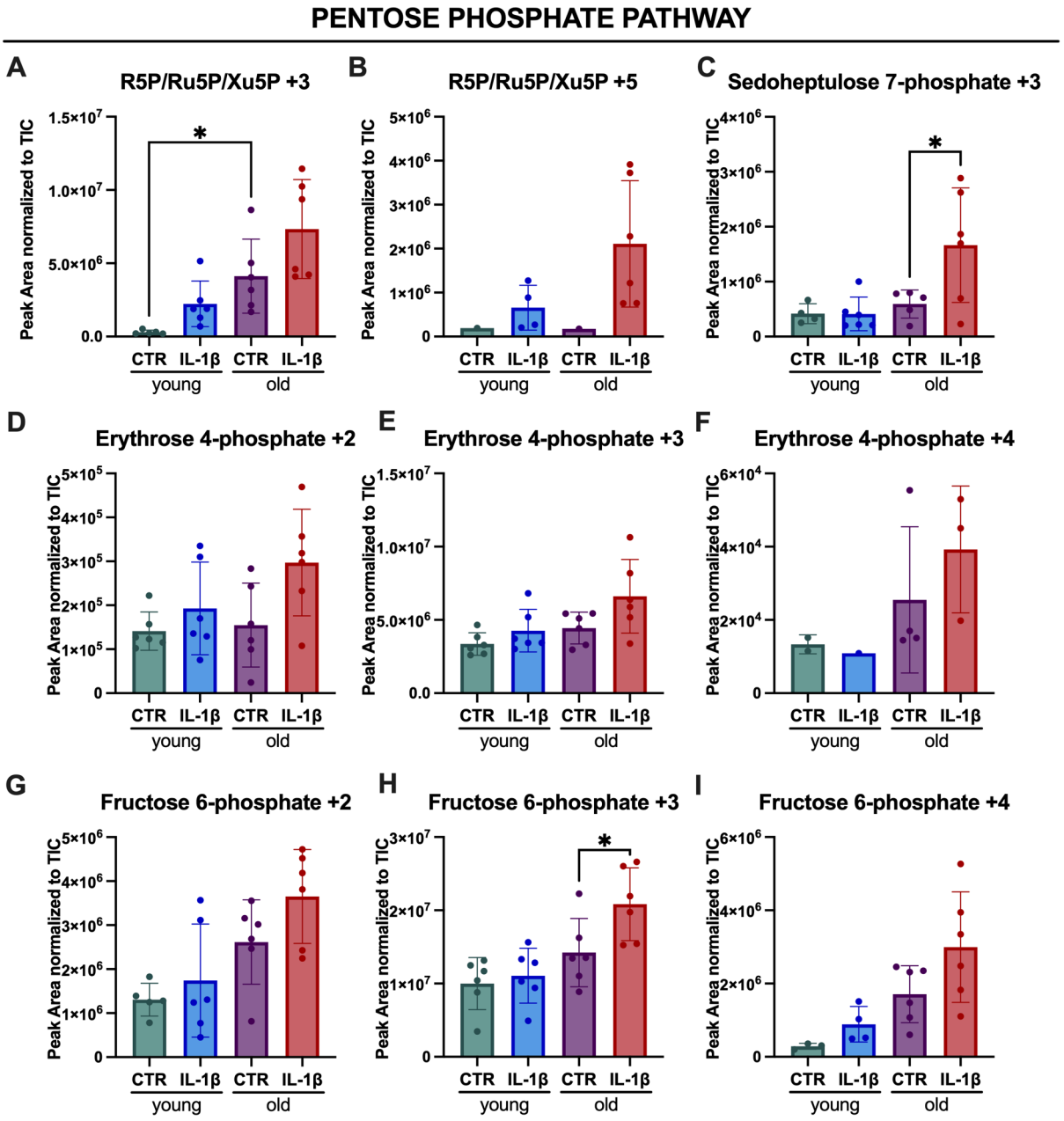

Figure 29. ***Metabolic flux into pentose phosphate pathway (PPP) in the aorta of young and old mice after stimulation with IL-1β.*** *The isolated thoracic aorta of young (6-month-old), and old (28-month-old) C57BL/6 mice was incubated for 22h with IL-1β (10 ng/ml), then for the next 2h with labelled glucose ($^{13}C_6$ glucose, 10 mM) and L-glutamine (2 mM). Metabolite isotopomers with different numbers of incorporated labelled carbons (^{13}C) were analysed using LC/MS. Data represent means ± SD (n=1-6, some isotopomers were not detected in all the groups), analysed with one-way ANOVA followed by post-hoc Šídák test, *p ≤ 0.05. R5P/Ru5P/Xu5P – 5-Ribose 5-phosphate/Ribulose 5-phosphate /Xylulose 5-phosphate.*

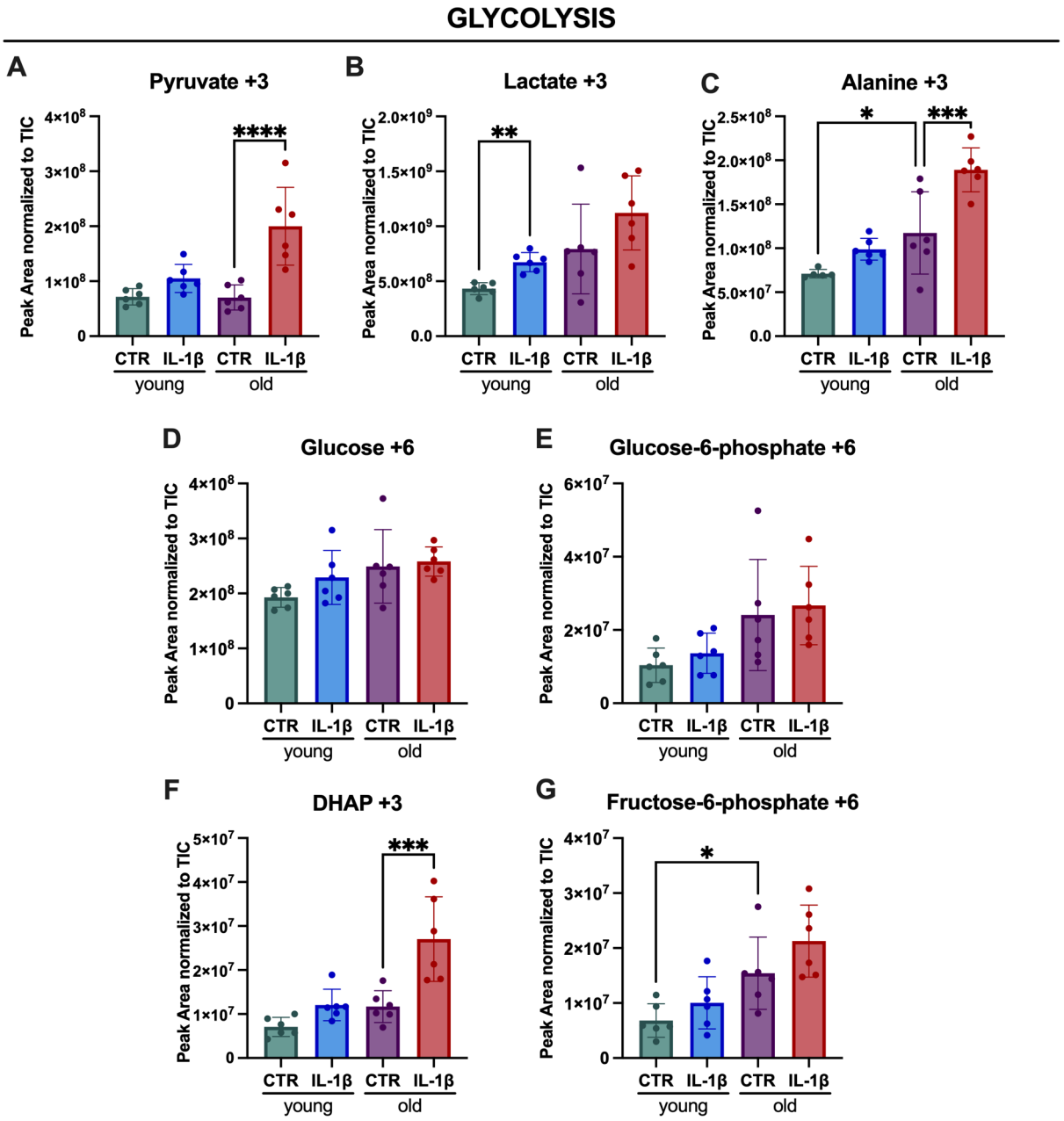

Figure 30. ***Metabolic flux into glycolysis in the aorta of young and old mice after stimulation with IL-1β.*** *The isolated thoracic aorta of young (6-month-old) and old (28-month-old) C57BL/6 mice was incubated for 22h in MEM (0.1% FBS) with IL-1β (10 ng/ml); then was transferred to KH buffer containing IL-1β, labelled glucose ($^{13}C_6$ glucose, 10 mM) and L-glutamine (2 mM), without pyruvate, and incubated for 2h. Samples were snap-frozen in liquid nitrogen, and then metabolite isotopomers with different numbers of incorporated labelled carbons (^{13}C) were analysed using LC/MS. Peak areas were normalised to Total Ion Count (TIC). Data represent means ± SD (n=5-6), analysed with one-way ANOVA followed by post-hoc Šídák test, *p ≤ 0.05, p** ≤0.01, ***p ≤ 0.001, ****p ≤ 0.0001. DHAP – Dihydroxyacetone phosphate.*

3.5.1. Glycolysis and pentose phosphate pathway

In the aorta of old mice, stimulation with IL-1β resulted in higher levels of ribose 5-phosphate/ribulose 5-phosphate/xylulose 5-phosphate (R5P/Ru5P/Xu5P) +3 (3 atoms of incorporated ^{13}C) (**Figure 29A**), pentose 5-phosphate isomers linked to PPP activity. Furthermore, the fully labelled (+5) pool of R5P/Ru5P/Xu5P was detectable in young and old groups in the presence of IL-1β, and higher in old mice (**Figure 29B**). Full labelling of pentose phosphates was derived from the glucose 6-phosphate direct entry into oxidative PPP, strongly reflecting robust activation of NADPH synthesis. In the control groups, fully labelled isotopomer (R5P +5) was detectable only in single samples at very low levels. Furthermore, IL-1β significantly increased sedoheptulose 7-phosphate +3 content in the aorta of old mice (**Figure 29C**), suggesting high activity also in the regenerative phase of PPP. Labelled carbon incorporation into erythrose 4-phosphate (E4P) (+2, +3, +4) also was increased in old mice after stimulation (**Figure 29D, E, F**). Transketolase and transaldolase convert sugar phosphates in the regenerative phase of PPP shuffling carbons, which in this experiment generated multiple ^{13}C enrichment patterns. Accordingly, a variety of partially labelled metabolites of PPP were detected at low levels in single samples, which are partially represented in the **Figure 29** as isotopomers of erythrose 4-phosphate and fructose 6-phosphate.

In the aorta of young mice, PPP intermediates linked to oxidative phase (R5P +3 and +5) were also elevated in the IL-1β-stimulated group compared to the control; however, the differences were more subtle than in the old mice and did not reach statistical significance. On the other hand, metabolites of regenerative phase of PPP, such as sedoheptulose 7-phosphate or erythrose 4-phosphate remained relatively unchanged (**Figure 29C-F**).

In young mice, the +3 fraction of lactate was significantly elevated following proinflammatory stimulation with no significant accumulation of glycolytic intermediates, reflecting efficient glycolytic flux (**Figure 30B**). In the aorta of old mice, lactate +3 showed only a minor increase, and this difference was not significant. In old mice, there was observed accumulation of pyruvate +3 and alanine +3 (**Figure 30A, F**). caused by IL-1β not present in the young group. It may indicate reduced mitochondrial pyruvate oxidation in the aorta of old mice. Furthermore, there was a significant rise in ^{13}C enrichment of DHAP (+3) in old mice following aorta stimulation (**Figure 30C**), possibly related to impaired glycolytic flux downstream. On the other hand, DHAP +3 accumulation could also be related to increased PPP flux, as PPP and glycolysis are interconnected by several intermediates.

For instance, transketolase reaction can produce fructose 6-phosphate (F6P) and glyceraldehyde 3-phosphate (G3P). G3P was not detected in this analysis, but it could be rapidly converted to DHAP by triose phosphate isomerase (TPI). DHAP could be produced also from F6P derived from glycolysis or PPP. In fact, in old mice, after IL-1β, there was an increase in partial F6P labelling, especially +2 and +4 (**Figure 29G, I**) derived from transketolase reactions in PPP. In contrast, F6P fully labelled (+6) was likely derived from labelled glucose, and F6P +3 can be generated both in the glycolytic pathway and PPP.

In summary, young mice exhibited activation of oxidative PPP in the aorta stimulated with IL-1β. Glycolysis was also upregulated, as reflected by an increase in lactate. In the aorta of old mice, the activation of oxidative and regenerative PPP was observed in response to stimulation with IL-1β. In contrast, the glycolytic flux efficiency was found to be impaired following IL-1β stimulation, as evidenced by the accumulation of DHAP and a marginal increase in lactate.

3.5.1. Purine metabolism

Furthermore, PPP activation was also linked to the strong upregulation of *de novo* purine synthesis. A striking rise in IMP and GMP with +5 labelling (**Figure 31A, B**) indicated ribose was derived from PPP. The adenosine and guanosine +5 and +6 fractions demonstrated a robust increase in the old aorta after proinflammatory stimulation (**Figure 31C-F**). In addition, purine degradation also seemed to be upregulated due to an elevation in hypoxantine and xanthine isotopomers with partial labelling (+2 and +3) in the aorta of young and old mice stimulated with IL-1β (**Figure 31G, H**).

Altogether, stimulation with IL-1β caused activation of purine synthesis in the aorta of young and old mice, which was more pronounced in old mice. There was also an increase in purine degradation similar in the aorta of young and old mice.

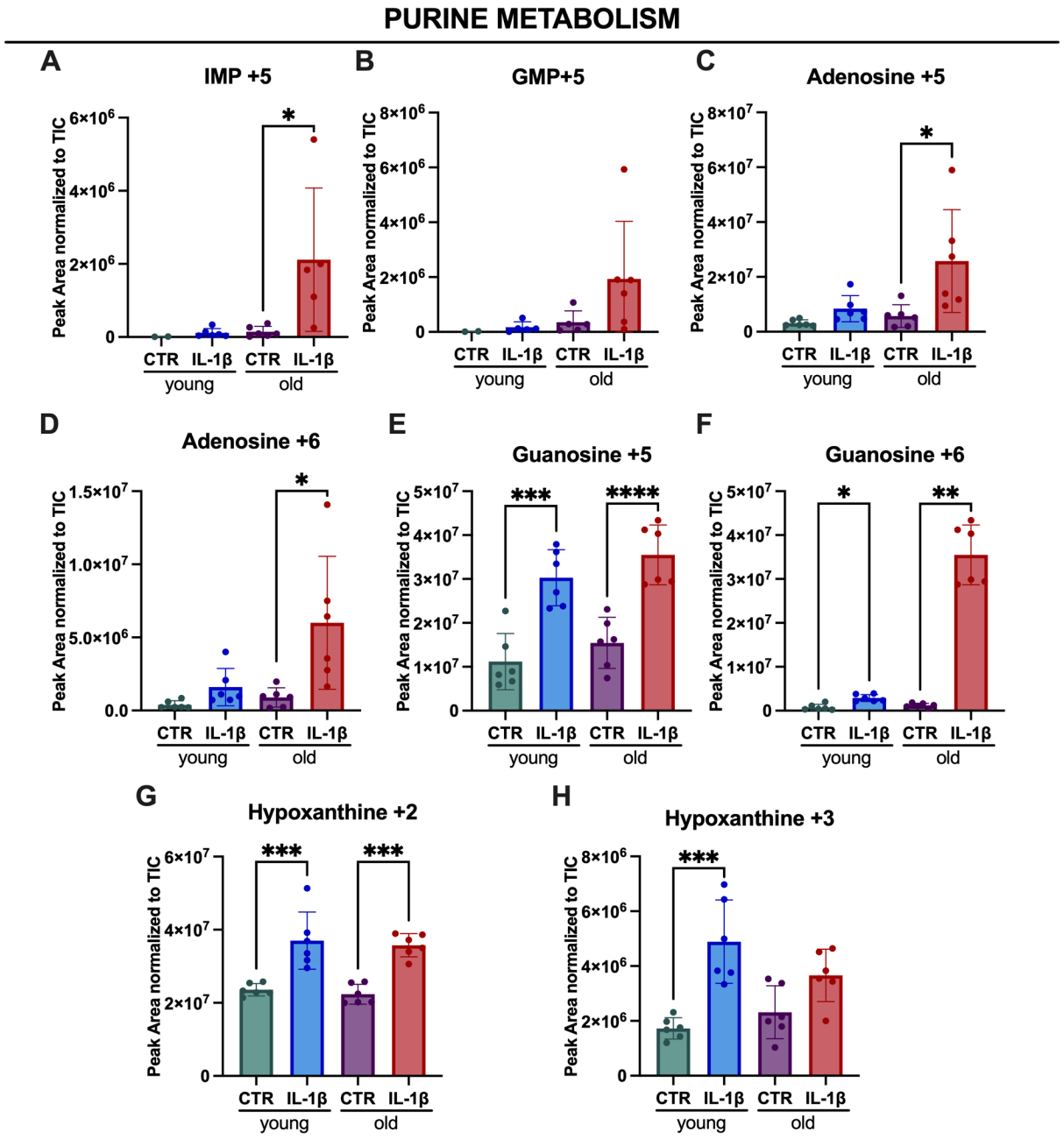

Figure 31. ***Metabolic flux in purine metabolism in the aorta of young and old mice after stimulation with IL-1β.*** *The isolated thoracic aorta of young (6-month-old), and old (28-month-old) C57BL/6 mice was incubated for 22h with IL-1β (10 ng/ml), then for the next 2h with labelled glucose ($^{13}C_6$ glucose, 10 mM) and L-glutamine (2 mM). Metabolite isotopomers with different numbers of incorporated labelled carbons (^{13}C) were analysed using LC/MS. Data represent the means ± SD (n=2-6, some isotopomers were not detected in control groups), analysed with one-way ANOVA followed by post-hoc Šídák test, *p≤0.05, ** ≤0.01, ***p≤0.001, ****p≤0.0001.*

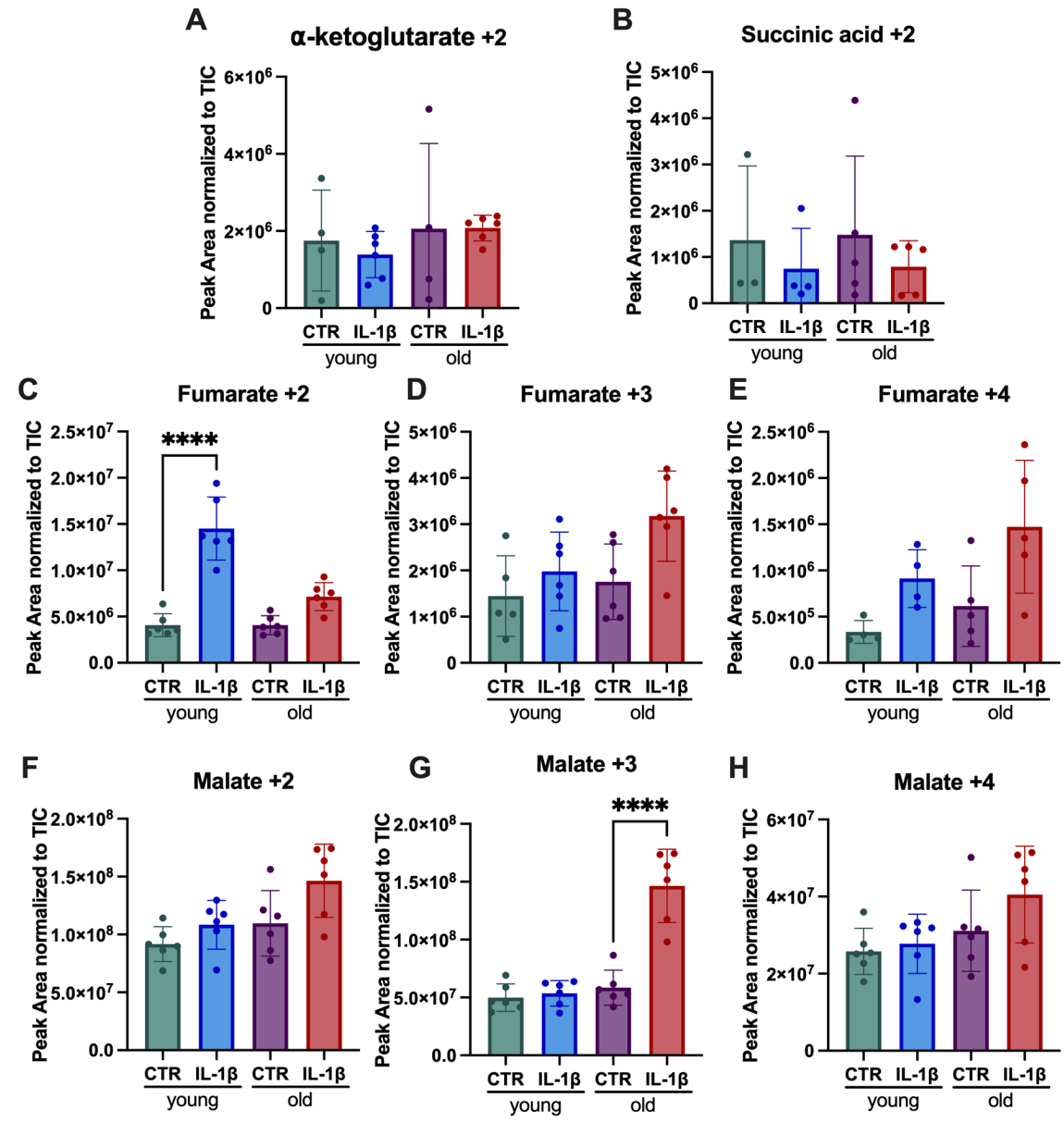

Figure 32. ***Metabolic flux into tricarboxylic acid (TCA) cycle in the aorta of young and old mice after stimulation with IL-1β.*** *The isolated thoracic aorta of young (6-month-old), and old (28-month-old) C57BL/6 mice was incubated for 22h with IL-1β (10 ng/ml), then for the next 2h with labelled glucose ($^{13}C_6$ glucose, 10 mM) and L-glutamine (2 mM). Metabolite isotopomers with different numbers of incorporated labelled carbons (^{13}C) were analysed using LC/MS. Data represent means ± SD (n=3-6), analysed with one-way ANOVA followed by post-hoc Šídák test, *p≤0.05, ** ≤0.01, ***p≤0.001, ****p≤0.0001.*

3.5.1. Tricarboxylic acid cycle (TCA)

Several age-related differences in TCA flux were observed in the metabolic response to vascular inflammation. IL-1β stimulation notably elevated fumarate labelling (+2) in the aorta of young mice (**Figure 32C**). Before entering TCA, pyruvate is oxidised to acetyl-coenzyme A (acetyl-CoA) by pyruvate dehydrogenase complex (PDH) losing one carbon atom; therefore, incorporation of two labelled carbons into TCA intermediates indicates efficient pyruvate oxidation in mitochondria. Nonsignificant elevation in +4 labelling **(Figure 32E**) might indicate the next rounds of TCA incorporating more glucose-derived two-carbon units in the intermediates. No other significant IL-1β-dependent changes in the TCA intermediates were detected in young mice.

In the aorta of old mice, the observed elevation in fumarate (+2) was minor (**Figure 32C**), implying reduced mitochondrial TCA or PDH activity, or inhibition of PDH by pyruvate dehydrogenase kinase (PDK). On the other hand, in the aorta of old mice, in the presence of IL-1β, there was a substantial increase in malate +3 labelling **(Figure 32G**), which indicates an anaplerotic origin, due to the retaining of all three labelled, pyruvate-derived carbons. For instance, it could result from pyruvate carboxylase (PC) activity, which converts pyruvate to oxaloacetate, which could be next converted to malate. Fumarate +3 also demonstrated a rising tendency (**Figure 32D**). The hypothesis of PC-mediated carbon influx to the TCA is also supported by the increase in aspartate +3 in old mice after stimulation with IL-1β (**Figure 35B, C**), which could also be derived from oxaloacetate generated by PC. However, oxaloacetate isotopomers were not detected in this analysis.

To assess the reliance on glutamine utilisation, the levels of unlabelled TCA intermediates were also examined and are shown in **Figure 33**. Notably, unlabelled glutamine was additionally added to the incubation media; accordingly, changes in unlabelled TCA intermediates could be plausibly attributed to glutamine-dependent anaplerosis.

In young mice, IL-1β stimulation resulted in an increase in the level unlabelled glutamine in the aorta, suggesting a decrease in glutamine utilisation. In old mice, the baseline level of glutamine was higher than in young mice and increased significantly after stimulation with IL-1β (**Figure 33A**), which indicates reduced glutamine utilisation also with ageing. IL-1β increased also unlabelled fumarate and malate levels in old mice (**Figure 33D, E**). However, the lack of increase in unlabelled α-ketoglutarate and succinate (**Figure 33B, C**) and higher glutamine levels in the IL-1β-stimulated aorta of old mice suggest rather different source of unlabelled furmarate and malate, e.g., unlabelled pyruvate.

The elevated unlabelled malate and fumarate levels in the aorta of old mice by IL-1β are in line with an increase in malate +3 and fumarate +3 **(Figure 32G, H)** and further support the hypothesis about enhanced anaplerotic activity in the aorta of old mice in the presence of IL-1β.

In summary, young mice exhibited accelerated TCA flux in the aorta in response to IL-1β. In contrast, this effect was not observed in old mice, which demonstrated impaired pyruvate oxidation and increased anaplerotic carbon entry to TCA following stimulation with IL-1β. However, the source of anaplerotic support of TCA was not glutamine, but glucose-derived pyruvate.

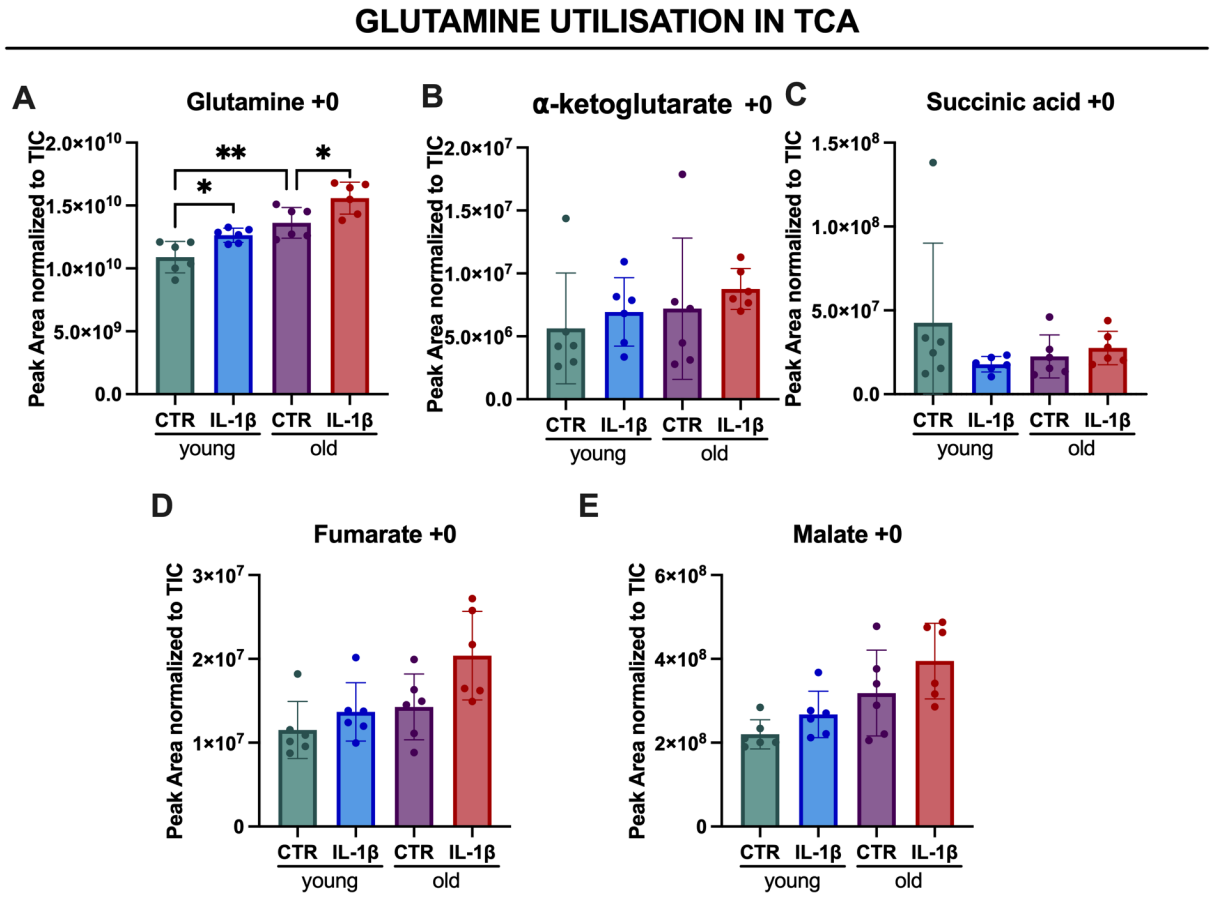

Figure 33. ***The levels of unlabelled glutamine and TCA intermediated in the aorta of young and old mice after stimulation with IL-1β.*** *The isolated thoracic aorta of young (6-month-old), and old (28-month-old) C57BL/6 mice was incubated for 22h with IL-1β (10 ng/ml), then for the next 2h with labelled glucose ($^{13}C_6$ glucose, 10 mM) and L-glutamine (2 mM). Metabolite isotopomers with different numbers of incorporated labelled carbons (^{13}C) were analysed using LC/MS. Data represent means ± SD (n=6), analysed with one-way ANOVA followed by post-hoc Šídák test, *p≤0.05, ** ≤0.01.*

3.5.2. Amino acid metabolism

Moreover, in young and old mice, there was increased proline ^{13}C carbon enrichment (**Figure 34A–C**), in the aorta of young and old mice stimulated with IL-1β, with higher levels in old mice. No changes in glutamate labelling (**Figure 35D–F**) suggest that proline was derived from other precursors than glutamate, e.g., ornithine. Increased proline synthesis is NADPH-dependent, which aligns with the increased oxidative activity of PPP. An increase in serine and glycine levels with +2 incorporated carbons was also observed in young mice and was even more significant in old mice (**Figure 34D, F**). These findings might indicate that 3-phosphoglycerate shunts into the serine biosynthesis pathway, which could be influenced by PPP activity. Glycine is a carbon donor in purine synthesis and can be utilised for NADPH generation. Glutamine +3 levels are significantly lower in the aorta of old mice in the presence of IL-1β (**Figure 35H)**, which suggest decreased glutamine synthesis from TCA intermediates. It could be explained by higher levels of intracellular glutamine (**Figure 33A**) resulting from reduced utilisation of glutamine from incubation media, or carbon redirection from TCA towards aspartate synthesis rather than glutamine. This hypothesis is supported by the increase in aspartate +3 in the aorta of old mice after IL-1β stimulation (**Figure 35C)**. Other amino acids exhibited stable flux after IL-1β stimulation, and no differences between groups were observed.

In summary, increased synthesis of serine, glycine and proline in response to IL-1β stimulation in the aorta of young and old mice indicates enhanced biosynthetic activity in response to inflammation, which was facilitated in old mice.

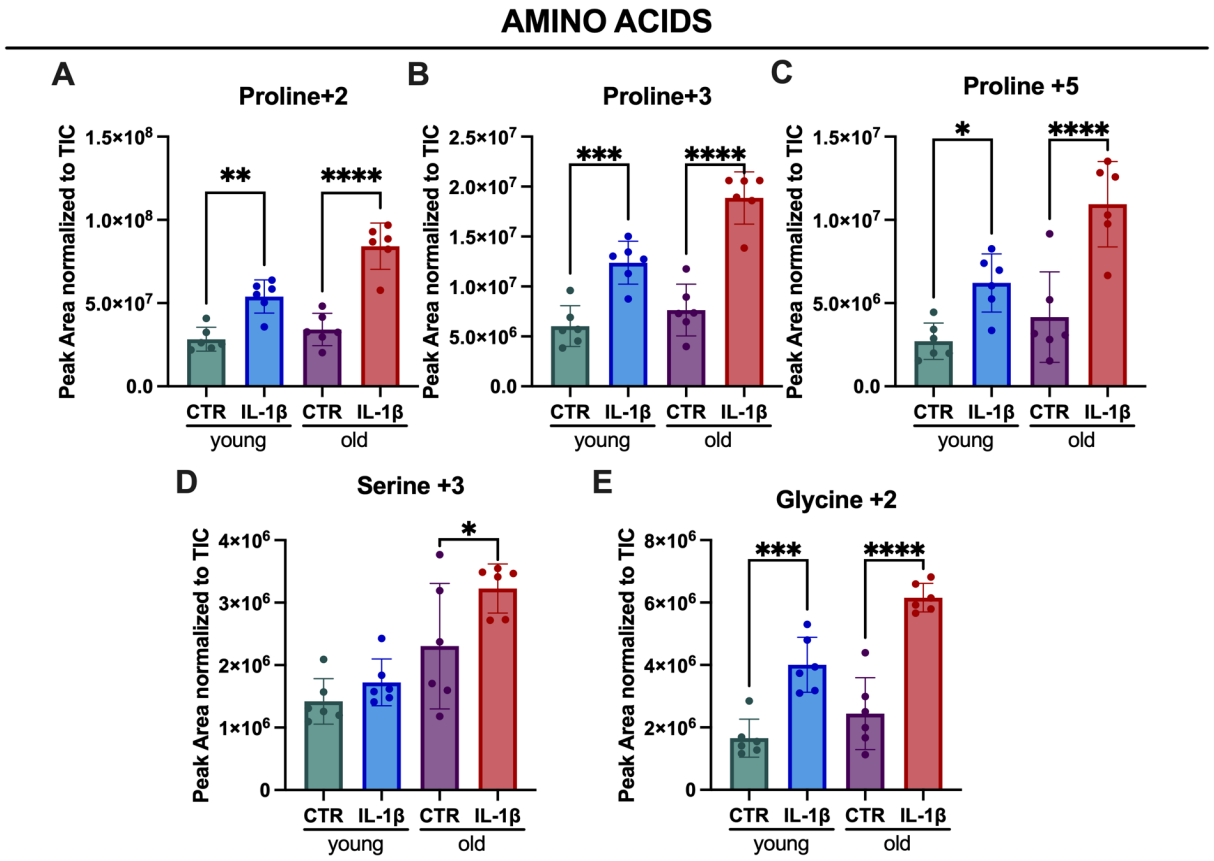

Figure 34. ***Metabolic flux into serine/glycine synthesis pathway and proline synthesis in the aorta of young and old mice after stimulation with IL-1β.*** *The isolated thoracic aorta of young (6-month-old), and old (28-month-old) C57BL/6 mice was incubated for 22h with IL-1β (10 ng/ml), then for the next 2h with labelled glucose ($^{13}C_6$ glucose, 10 mM) and L-glutamine (2 mM). Metabolite isotopomers with different numbers of incorporated labelled carbons (^{13}C) were analysed using LC/MS. Data represent means ± SD (n=6), analysed with one-way ANOVA followed by post-hoc Šídák test, *p≤0.05, ** ≤0.01, ***p≤0.001, ****p≤0.0001.*

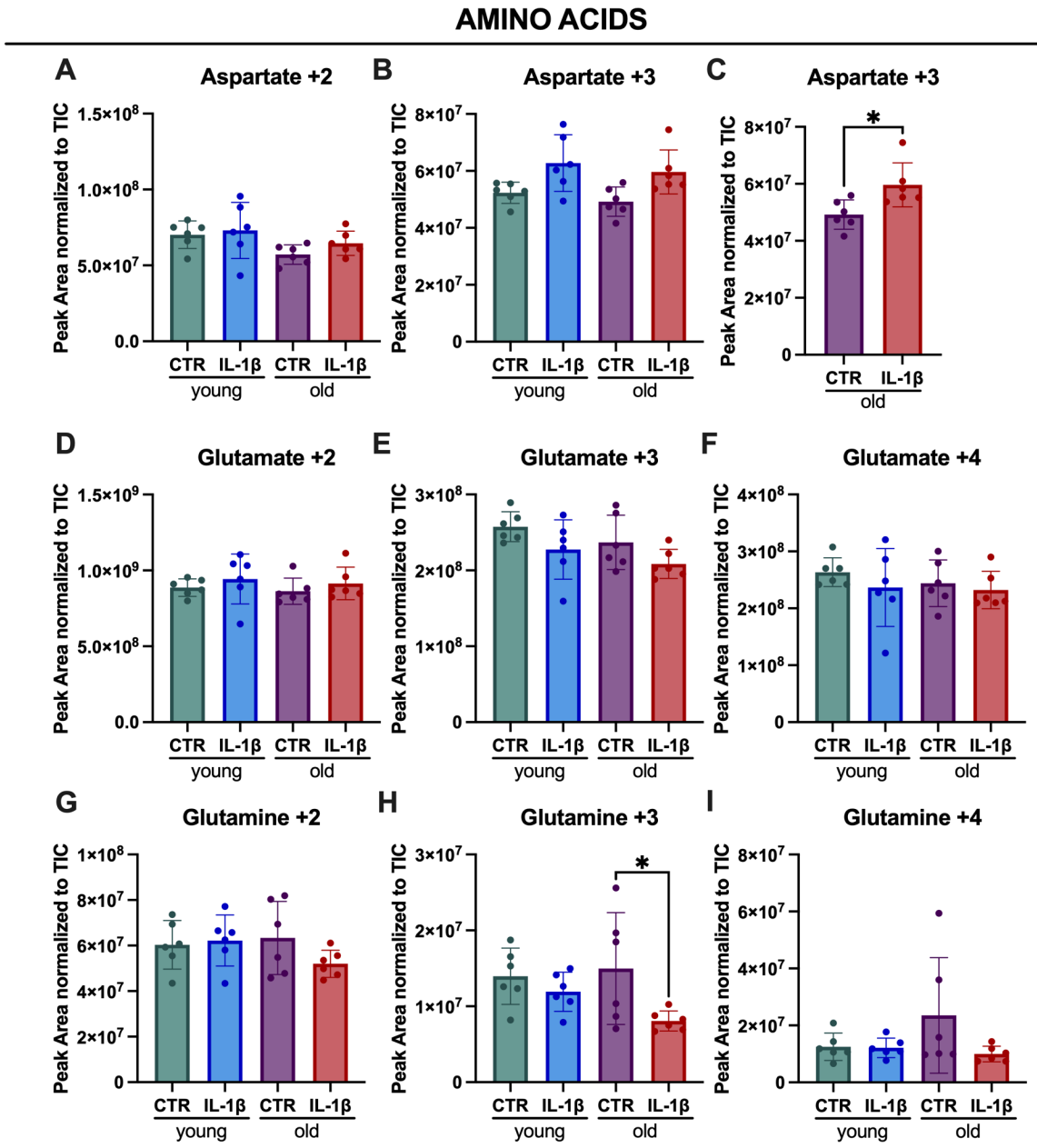

Figure 35. ***Metabolic flux into glutamate, glutamine and aspartate synthesis in the aorta of young and old mice after stimulation with IL-1β.*** *The isolated thoracic aorta of young (6-month-old), and old (28-month-old) C57BL/6 mice was incubated for 22h with IL-1β (10 ng/ml), then for the next 2h with labelled glucose ($^{13}C_6$ glucose, 10 mM) and L-glutamine (2 mM). Metabolite isotopomers with different numbers of incorporated labelled carbons (^{13}C) were analysed using LC/MS. Data represent means ± SD (n=6), analysed with one-way ANOVA followed by post-hoc Šídák test, or t-test (CTR vs IL-1β for young and old separately, graph B) * p≤ 0.05, **p ≤ 0.01, ***p ≤ 0.001, ****p ≤ 0.0001.*

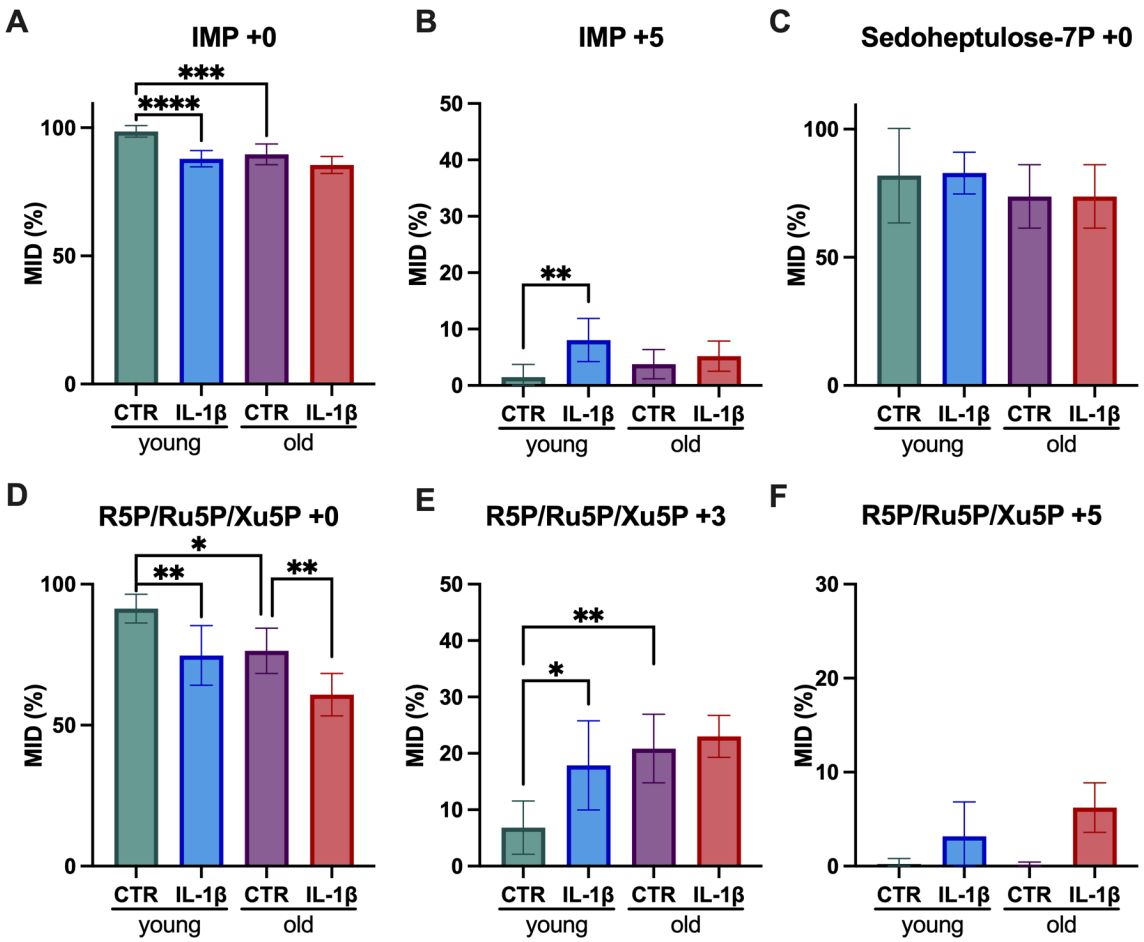

Figure 36. ***Mass isotopomer distribution (MID) of PPP metabolites in the aorta of young and old mice after stimulation with IL-1β.*** *The isolated thoracic aorta of young (6-month-old), and old (28-month-old) C57BL/6 mice was incubated for 22h with IL-1β (10 ng/ml), then for the next 2h with $^{13}C_6$ glucose (10 mM) and L-glutamine (2 mM). MID was calculated as a percentage of fractions with different numbers of incorporated labelled carbons (M+0, M+3, M+5) of the sum of all isotopomers of the metabolite. Data represent means ± SD (n=6), analysed with one-way ANOVA followed by post-hoc Šídák test, *p ≤ 0.05, **p ≤ 0.01, ***p ≤ 0.001, ****p ≤ 0.0001.*

3.5.1. Reprogramming of basal vascular metabolism in the aorta of old mice

Ageing appeared to change the metabolic flux without proinflammatory stimuli; differences between young and old control groups were noted. The R5P/Ru5P/Xu5P +3 labelled fraction was significantly increased in the old control compared to the young control (**Figure 29A**), suggesting a shift in glucose utilisation towards PPP with ageing under basal conditions, which is further enhanced by inflammatory stimuli. The results calculated as a percentage of a labelled fraction to the pool of all metabolite isotopomers (MID – mass isotopomer distribution) further support this conclusion (**Figure 36**). The data revealed a significant decline in the unlabelled pools of IMP and R5P/Ru5P/Xu5P (**Figure 36A, D**) complemented by an increase in the percentage of +3 fraction of R5P/Ru5P/Xu5P in the old control group

compared to the young control (**Figure 36E**). There was also a nonsignificant downward trend in the unlabelled fraction of sedoheptulose 7-P and an increasing trend in IMP +5.

In summary, old mice exhibited metabolic reprogramming in the aorta as compared to young mice. A shift towards increased PPP activity was observed, reflected by higher incorporation of labelled carbons into PPP intermediates in the aorta of old mice compared to young mice, and diminished relative proportions of unlabelled fractions within total PPP metabolite pools.

3.6. The effect of inflammation on bioenergetic nucleotide levels and redox status of the aorta of young and old mice

To gain further insight into the energy and redox status of the aorta isolated from young and old mice following proinflammatory stimulation, the levels of ATP, ADP, AMP, NAD^+, NADH and $NADP^+$ were assessed using HPLC. Due to their instability and low tissue concentrations, these compounds were not detected during the fluxomic assessment. Nevertheless, the levels of NADPH were unfortunately insufficient to allow detection in any of the samples and complement the fluxomic analysis in the context of PPP activation. The isolated aorta was divided into 4 fragments, which were incubated for 2 hours and 24 hours with IL-1β (10 ng/ml) or without as a control.

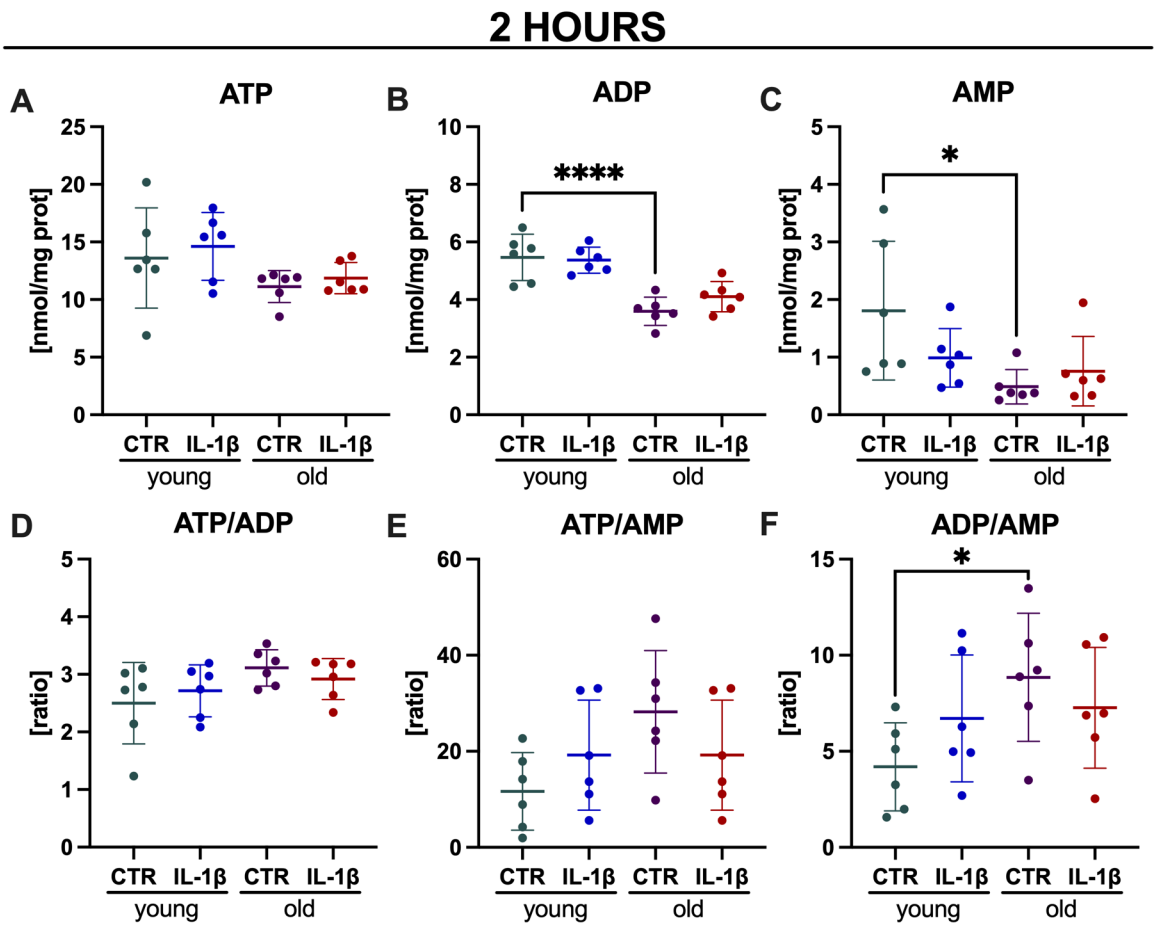

Figure 37. ***Adenine nucleotides content in the aorta of young and old mice after 2h of stimulation with IL-1β.*** *Adenine nucleotides were measured using HPLC in aortic samples collected from young (4-month-old) and old (28-month-old) C57BL/6 mice incubated for 2h in MEM containing IL-1β (10 ng/ml). Data represent means ± SD (n=5–6), analysed with one-way ANOVA followed by post-hoc Šídák test, **p ≤ 0.05, ****p ≤ 0.0001. (In cooperation with dr hab. Barbara Kutryb-Zając, Medical University of Gdańsk).*

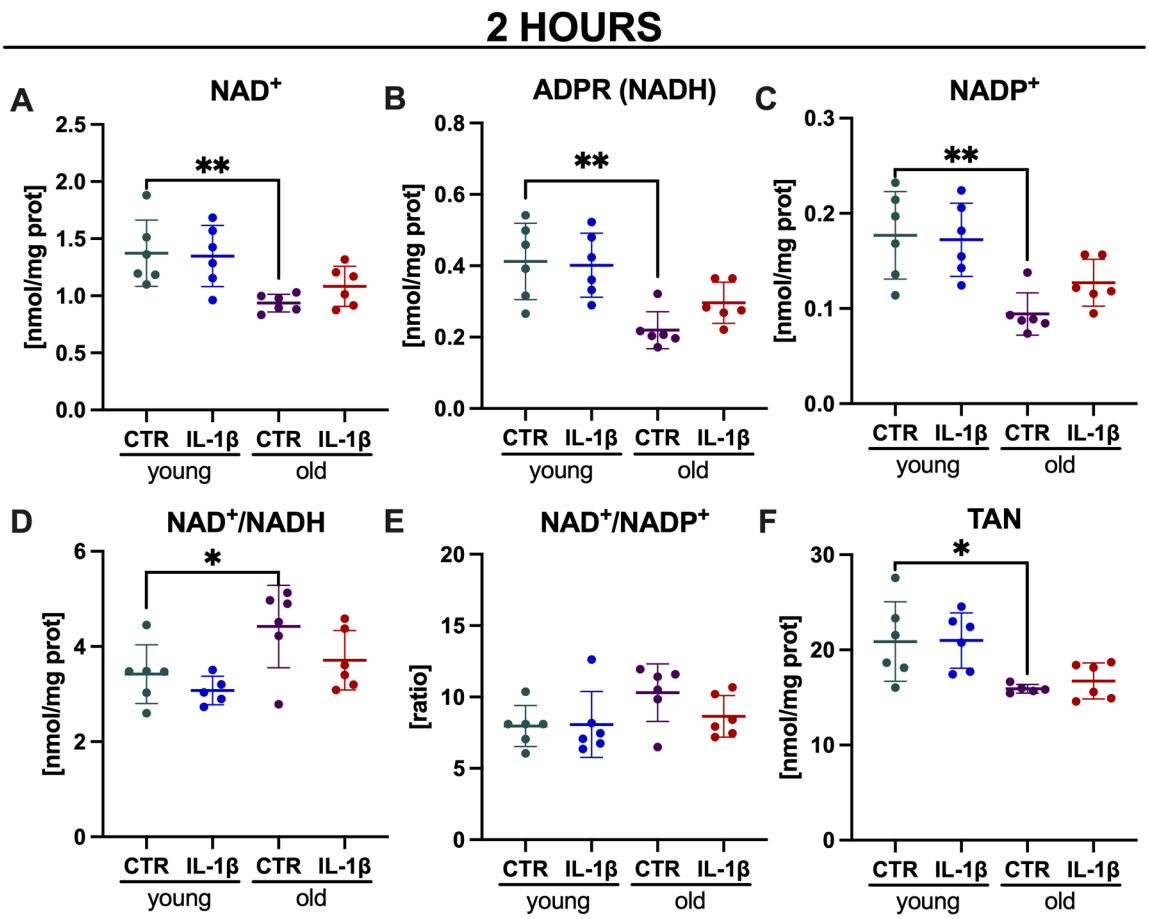

Figure 38. ***Nicotinamide adenine dinucleotide content in the aorta of young and old mice after 2h of stimulation with IL-1β.*** *Adenine nucleotides and nicotinamide adenine dinucleotide in both oxidised (NAD^+) and reduced (NADH) forms were measured using HPLC aortic samples collected from young (4-month-old) and old (28-month-old) C57BL/6 mice incubated for 2h in MEM containing IL-1β (10 ng/ml). Data represent means ± SD (n=5–6), analysed with one-way ANOVA followed by post-hoc Šídák test, **$p \leq 0.05$, **$p \leq 0.01$. Outliers detected by Grubbs test ($\alpha = 0.05$) were removed. (In cooperation with dr hab. Barbara Kutryb-Zając, Medical University of Gdańsk). TAN – total adenine nucleotides (ATP + ADP + AMP).*

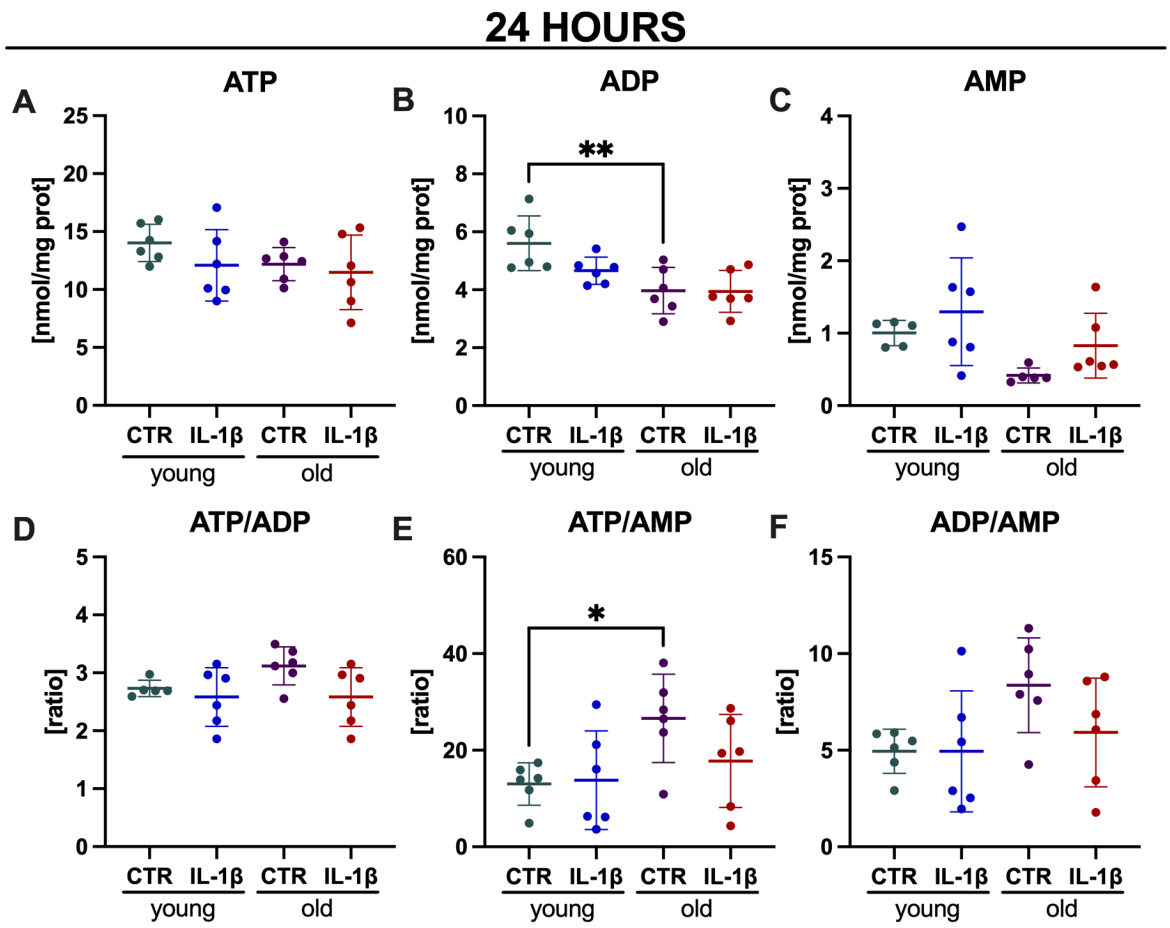

Figure 39. ***Adenine nucleotides content in the aorta of young and old mice after 24h of stimulation with IL-1β.*** *Adenine nucleotides were measured using HPLC in aortic samples collected from young (4-month-old) and old (28-month-old) C57BL/6 mice incubated for 24h in MEM containing IL-1β (10 ng/ml). Data represent means ± SD (n=5–6), analysed with one-way ANOVA followed by post-hoc Šídák test, **p ≤ 0.05, ****p ≤ 0.0001. Outliers detected by the Grubbs test (α = 0.05) were removed. (In cooperation with dr hab. Barbara Kutryb-Zając, Medical University of Gdańsk).*

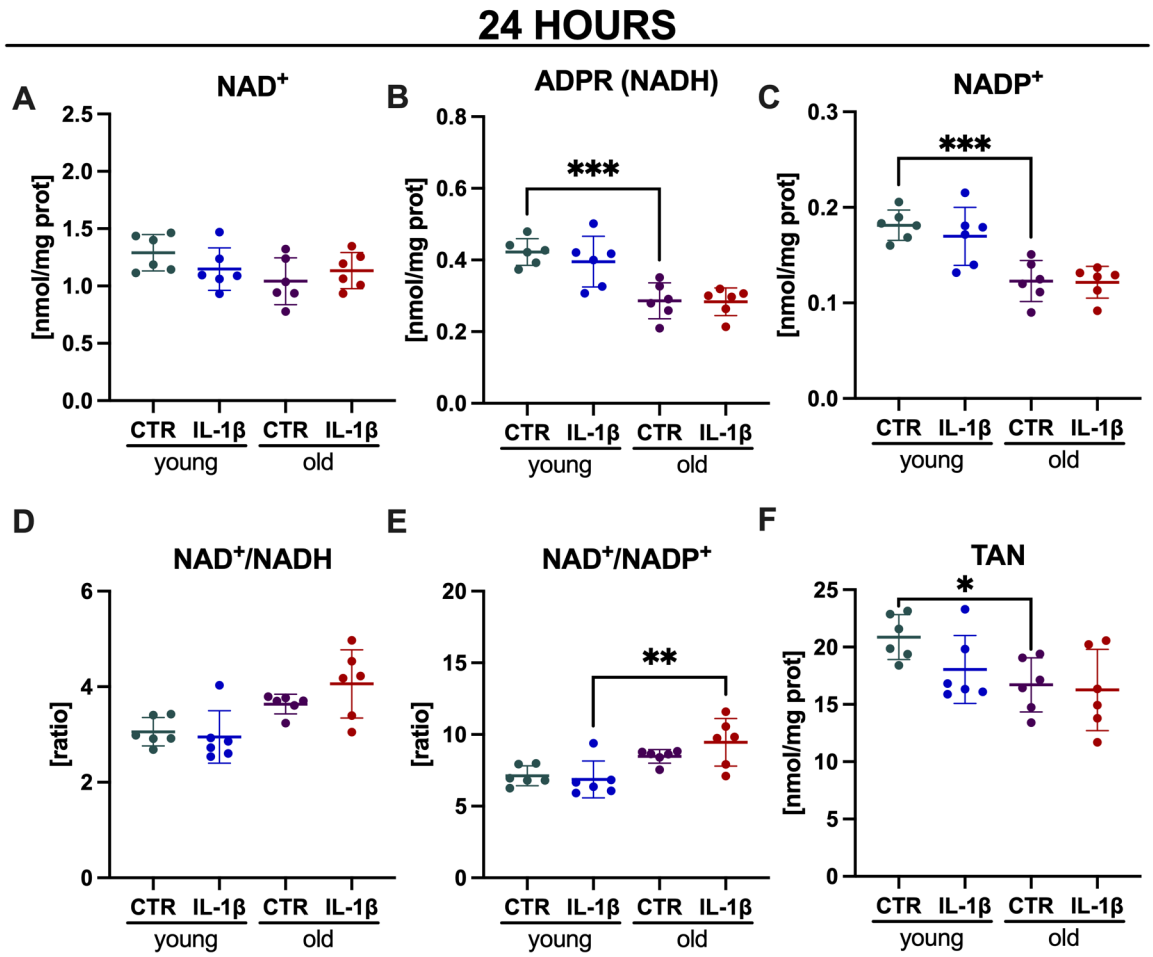

Figure 40. ***Nicotinamide adenine dinucleotide content in the aorta of young and old mice after 24h of stimulation with IL-1β.*** *Adenine nucleotides and nicotinamide adenine dinucleotide in both oxidised (NAD^+) and reduced (NADH) forms were measured using HPLC aortic samples collected from young (4-month-old) and old (28-month-old) C57BL/6 mice incubated for 24h in MEM containing IL-1β (10 ng/ml). Data represent means ± SD, (n=5–6), analysed with one-way ANOVA followed by post-hoc Šídák test, **$p \leq 0.05$, **$p \leq 0.01$, ***$p \leq 0.001$ (In cooperation with dr hab. Barbara Kutryb-Zając, Medical University of Gdańsk). TAN – total adenine nucleotides (ATP + ADP + AMP).*

In the aorta of young mice, nucleotide pools displayed minimal fluctuations after proinflammatory stimulation for 2 and 24 hours with IL-1β. 2 hours of incubation with IL-1β resulted in a minor increase in ATP and a decrease in AMP (**Figure 37A, C**). IL-1β caused increasing tendencies in ATP/ADP, ATP/AMP and ADP/ AMP ratios (**Figure 37D, E, F**) in the aorta of young mice. However, none of these differences were statistically significant. These observations suggested the activation of metabolism to meet increased energy demands, consistent with the functional analysis with Seahorse XF after 2 hours (**Figure 23**, chapter 3.2). After 24h of stimulation with IL-1β, there was a minor decrease in ATP and ADP and an increase in AMP levels in the aorta of young mice (**Figure 39**), which could suggest increased

energy consumption. No differences in NAD^+, NADH and $NADP^+$ levels and redox state were observed after 2h (**Figure 38**). After 24 hours of stimulation with IL-1β, there was a subtle, nonsignificant decrease in total adenine nucleotide pool (TAN) and NAD levels (**Figure 40**), likely linked to increased glycolytic and biosynthetic NAD^+ utilisation. Despite this, the preserved NAD^+/NADH ratio suggested efficient metabolic turnover.

In the aorta of old mice, there was a decrease in ADP and AMP in the control group compared to the young control, after IL-1β nucleotide levels showed minimal changes (**Figure 37, Figure 39**) in the aorta of old mice. However, after 2 and 24 hours of stimulation with IL-1β, there was a decline in ATP/ADP, ATP/AMP, and ADP/AMP ratios in the aorta of old mice (**Figure 37, Figure 39**). This observation indicates that old mice fail to upregulate pathways for ATP production in the aorta, prioritising PPP activation instead. Consequently, ATP consumption exceeded synthesis in response to inflammation. Due to the considerable dispersion of the results, those tendencies were not statistically significant. Yet, the observed pattern seemed consistent with previous findings (described in chapters 3.4–3.5), which demonstrated that ageing vessel wall display the metabolic shift and dysfunctional mitochondrial metabolism.

Old mice exhibited lower NAD^+ and NADH pools at the baseline (**Figure 38A, B; Figure 40B**), which was already shown in chapter 2.6 (**Figure 18**). $NADP^+$ pool was also decreased (**Figure 38C, Figure 40C**). Furthermore, old mice displayed a higher baseline NAD^+/NADH ratio in the aorta than young mice under control conditions; after 2 hours of incubation, this difference reached statistical significance (**Figure 38D**). An increase in baseline NAD^+/NADH ratio in the aorta of old mice as compared to young mice could be interpreted as impaired TCA activity, which generates NADH. This observation differs from the previous analysis described in the chapter 2.6, showing that old, 25-month-old mice, in comparison to young mice, displayed unchanged NAD^+/NADH ratio; only a decrease in both NAD^+ and NADH levels was noted (**Figure 18**). However, the mice used in experiments described in the current chapter were older (28-month-old), and the age difference likely explains the observed change in the redox state, reflecting the progressive decline in mitochondrial function within the vascular wall during advanced ageing.

Proinflammatory stimulation with IL-1β after 2h moderately decreased the NAD^+/NADH ratio in the aorta of old mice (**Figure 38D**). This effect was associated with a minor elevation in both NAD^+ and NADH; therefore, it could be related to acute activation of glycolysis or even partial TCA flux in response to inflammation. On the contrary, 24 hours of stimulation with IL-1β increased the NAD^+/NADH ratio compared to the control in the aorta of old mice (**Figure 40D**), suggesting impairment of oxidative metabolism and NADH generation.

3.7. The effect on pharmacological modulation of PPP on endothelial function in young and old mice

The results of the fluxomic analysis described in chapter 3.5 indicated that the main effect of IL-1β on the vascular metabolism in old mice is the activation of the PPP and purine synthesis. A pharmacological blockade of these pathways was used to test the role of their IL-1β-induced activation in vascular function. Aorta taken from young (5-month-old) or old (30-month-old) mice was incubated with IL-1β combined with methotrexate (MTX, 10 μM) or dehydroepiandrosterone (DHEA, 500 μM). Methotrexate is an inhibitor of tetrahydrofolate dehydrogenase, the enzyme responsible for the production of tetrahydrofolate, which is essential for the synthesis of a purine precursor – IMP. In addition, dehydroepiandrosterone was chosen to inhibit the PPP upstream as an inhibitor of glucose 6-phosphate dehydrogenase (G6PD), the rate-limiting enzyme of PPP.

When incubated with IL-1β at a concentration of 10 ng/ml, a substantial impairment of phenylephrine-dependent contraction was observed. In young mice, dehydroepiandrosterone notably improved aortic contractility in the presence of IL-1β in young mice, yet the difference did not reach statistical significance due to the low repetition number (**Figure 41A**). In contrast, methotrexate did not influence phenylephrine-dependent contraction in the aorta of young mice stimulated with IL-1β.

In the aorta of old mice, IL-1β-induced impairment of vascular phenylephrine-dependent contractility was largely reversed by both methotrexate and dehydroepiandrosterone, for dehydroepiandrosterone the difference was statistically significant (**Figure 41B**). Methotrexate mainly affects purine synthesis downstream from PPP. Therefore, its beneficial effect in the aorta of old mice but not young mice was consistent with the results from the previous analysis, indicating considerably greater activation of purine metabolism in the aorta of old mice.

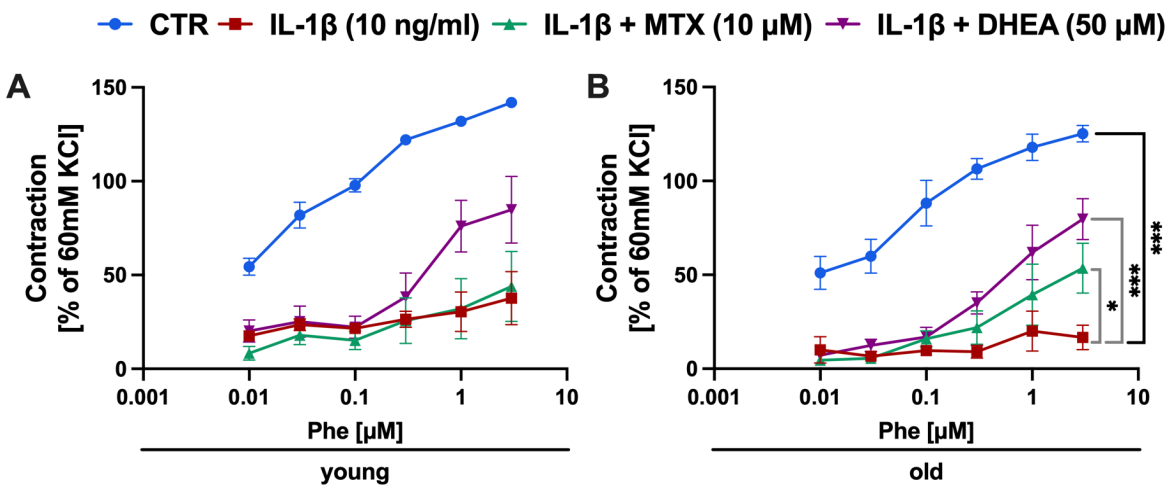

Figure 41. ***The effect of methotrexate and dehydroepiandrosterone on IL-1β-induced impairment of vascular contractility.*** *The aorta isolated from young (5-month-old) or old (30-month-old) C57BL/6 mice was incubated for 24h with IL-1β (10 ng/ml) and IL-1β supplemented with methotrexate (MTX, 10 μM) or dehydroepiandrosterone (DHEA, 50 μM). Vascular contractility was evaluated with wire myography using increasing concentrations of phenylephrine. Data represent means ± SEM (n=3), analysed with two-way ANOVA and post-hoc Tukey test, *p ≤ 0.05, ***p ≤ 0.001.*

Due to the substantial impairment of phenylephrine-induced contraction in response to IL-1β at a concentration of 10 ng/ml, endothelium-dependent vasodilation could not be reliably assessed in these experiments. Therefore, the IL-1β concentration was reduced to 1 ng/ml in the next stage, to achieve vascular dysfunction to an extent comparable to previous experiments (**Figure 22**, chapter 3.2). Under these conditions, no impairment of phenylephrine-induced contraction was observed in the aorta of young mice in the presence of IL-1β (1 ng/ml) (**Figure 42A, B**). Endothelium-dependent vasodilation was impaired in response to stimulation with IL-1β (1 ng/ml) both in the aorta of young and old mice (**Figure 42C, D**). Of note, the IL-1β-induced endothelial dysfunction was more severe in the aorta of old mice (**Figure 42C, D**). Furthermore, in the aorta of old mice, stimulation with IL-1β impaired also endothelium-independent vasodilation in response to SNP (**Figure 42F**) and phenylephrine-induced contractility was also modestly impaired (**Figure 42B**).

In the aorta of young mice, endothelial function impaired by IL-1β was not restored by dehydroepiandrosterone or methotrexate (**Figure 42C**).

In the aorta of old mice, dehydroepiandrosterone markedly improved endothelium-dependent relaxation in the presence of IL-1β (**Figure 42D**). Maximal endothelium-dependent relaxation reached statistical significance compared to both control and IL-1β groups.

Methotrexate displayed a non-significant tendency to improve endothelial function in the aorta of old mice in the presence of IL-1β. Furthermore, both dehydroepiandrosterone and methotrexate improved endothelium-independent vasodilation in the presence of IL-1β in old mice, but this difference was not significant (**Figure 42F**).

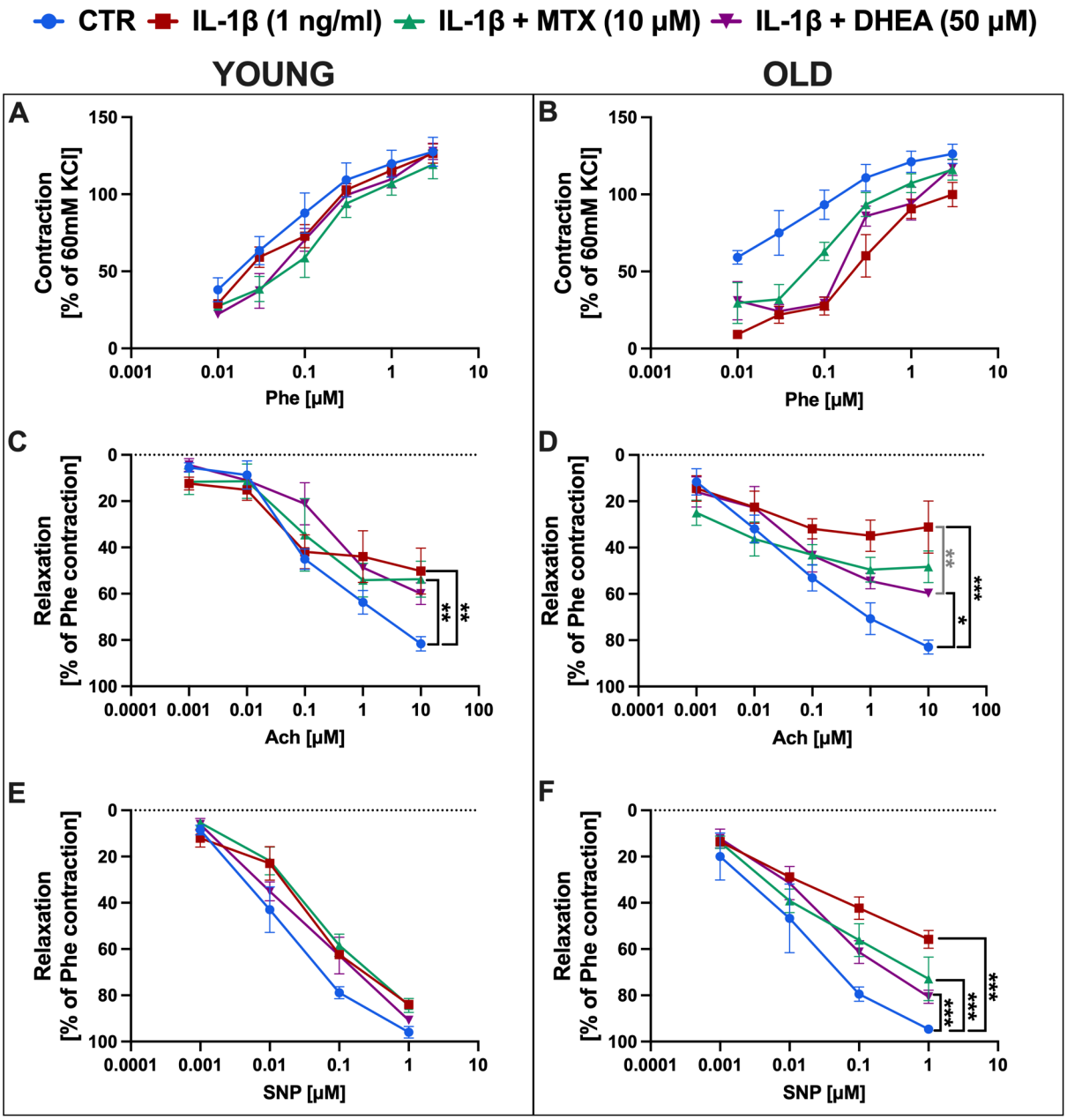

Figure 42. ***The effect of methotrexate and dehydroepiandrosterone on IL-1β-induced impairment on endothelium-dependent vasodilation****. The aorta isolated from young, 5-month-old (A, C, E) or old, 30-month-old C57BL/6 mice (B, D, F) was incubated for 24h with IL-1β (1 ng/ml) and IL-1β supplemented with methotrexate (MTX, 10 μM) or dehydroepiandrosterone (DHEA, 50 μM). Vascular contractility was assessed in response to increasing concentrations of phenylephrine (**A, B**) and relaxation in response to acetylcholine (**C, D**) or SNP (**E, F**) using wire myography. Data represent means ± SEM (n=4), analysed with two-way ANOVA and post-hoc Tukey test, *p ≤ 0.05, **p ≤ 0.01, ***p ≤ 0.001.*

It was noted that in 30-month-old mice the extent of endothelial dysfunction caused by IL-1β is more pronounced than in young mice (3-month-old). Subsequently, vascular functional response to IL-1β was assessed in the aorta isolated from 18-month-old mice and compared to aorta from young, 3-month-old mice (**Figure 43**). 18-month-old mice were used to represent an earlier stage of vascular ageing to determine whether endothelial dysfunction in response to inflammation develops gradually or exhibits a rapid decline in advanced age of mice (30 months).

IL-1β (1 ng/ml) impaired vascular contractility to phenylephrine significantly only in the 18-month-old group **(Figure 43B**). Notably, endothelial dysfunction caused by IL-1β was comparable for both age groups (**Figure 43C**). On the other hand, reduced vasorelaxation to SNP was observed only in old mice (**Figure 43D**).

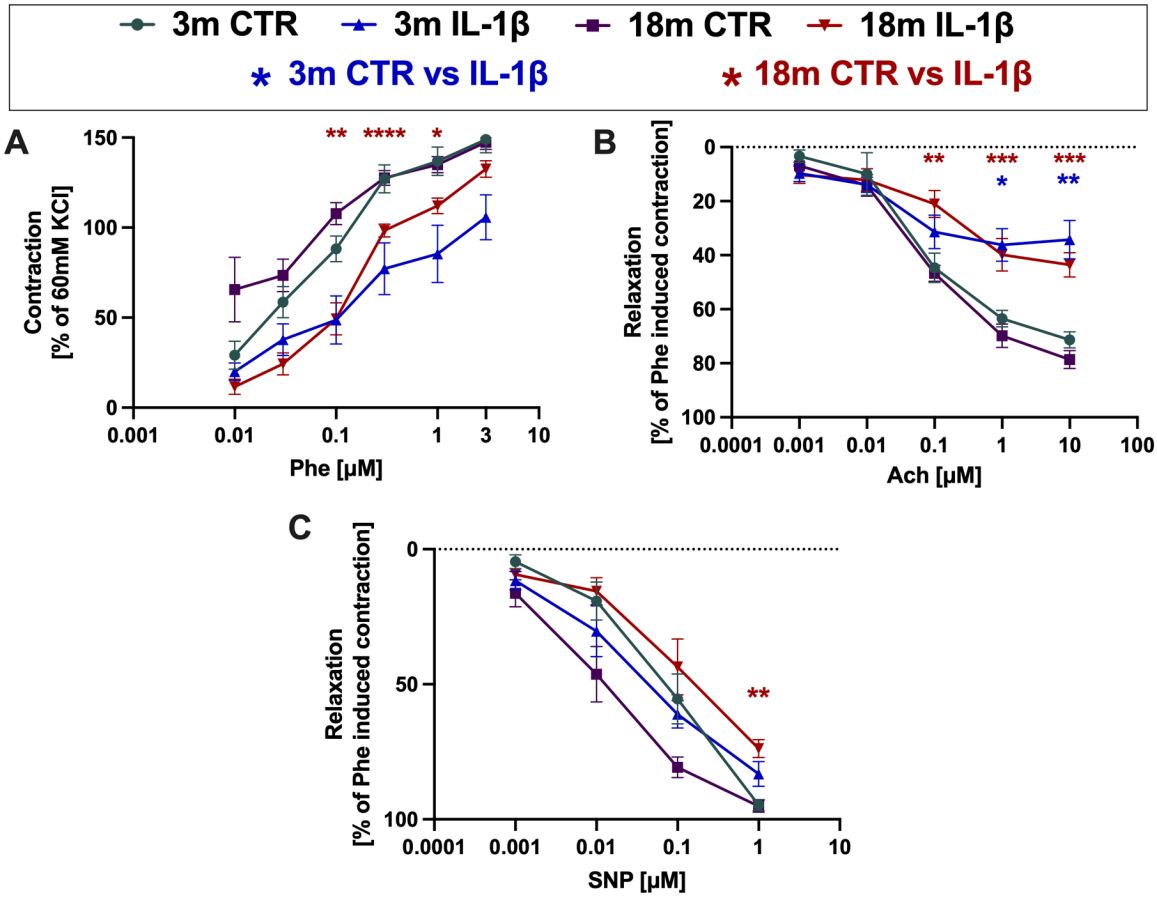

Figure 43. ***The effect of IL-1β-induced inflammation on vascular function in 3-month-old and 18-month-old C57BL/6 mice.*** *The isolated aorta of young (3-month-old) or old (18-month-old) C57BL/6 mice was incubated with IL-1β (1 ng/ml) for 24 hours, and vascular function was assessed with wire myography. The vascular contractility was assessed in response to phenylephrine (**A**), endothelium-dependent vasodilation was assessed in response to acetylcholine (**B**) and endothelium-independent vasodilation in response to SNP (**C**). Data represent means ± SEM (n=6-7), analysed with two-way ANOVA, with post-hoc Tukey test, *p ≤ 0.05, **p ≤ 0.01, ****p ≤ 0.0001.*

In summary, inhibition of PPP with dehydroepiandrosterone, significantly improved endothelial function, endothelium-independent relaxation and vascular contractility in the aorta of old mice stimulated with IL-1β. Inhibition of purine synthesis pathway with methotrexate also had a beneficial effect for vascular function in inflammation in the aorta of old mice, but the effect of methotrexate was less pronounced than inhibition of PPP. In contrast, in the aorta of young mice, dehydroepiandrosterone only modestly improved phenylephrine-dependent contraction and had no effect on endothelial function in the presence of IL-1β. No effect of methotrexate was observed in the aorta of young mice.

Furthermore, the severity of IL-1β-dependent endothelial dysfunction was more pronounced in 30-month-old mice as compared with young, 3-month-old mice, but for 18-month-old mice the degree of endothelial dysfunction was comparable with the young group. On the other hand, endothelium-independent vasodilation and contraction to phenylephrine was more impaired in 18-month-old group in response to IL-1β, that might indicate that VSMC-dependent function is earlier affected by age than endothelial function in the setting of acute vascular inflammation.

Importantly, the impairment of vascular bioenergetic response to inflammation in mice was observed as early as at 12 months of age. It suggests that the impairment of bioenergetic flexibility preceded the impairment of endothelial-dependent and vascular smooth muscle-dependent vascular function in inflammation and could be an early contributor rather than a consequence of age-dependent decline in vascular function.

V. DISCUSSION

The findings of this PhD thesis demonstrated that vascular mitochondrial bioenergetic metabolism plays a crucial role in maintaining the NO-dependent vascular function. Furthermore, it has been established that vascular bioenergetic metabolism is affected by ageing and inflammation, which has consequences for the NO-dependent endothelial functional response.

In particular, the present PhD thesis demonstrated that oxidative phosphorylation, but not glycolysis, was a prerequisite for NO production and endothelium-dependent vasodilation in the murine aorta. Furthermore, it was shown that vascular oxidative bioenergetic metabolism played a pivotal role not only in maintaining basal NO-dependent endothelial function but also in preserving the endothelial function during the processes of ageing and inflammation. One of the most interesting findings was to reveal that ageing induced a decline in metabolic flexibility of the vessel wall, defined as the ability to activate bioenergetic reserves in response to stress conditions, which was evident even in the conditions that did not affect basal vascular bioenergy metabolism. This finding suggests that a decline in vascular, metabolic flexibility in response to acute proinflammatory stimuli may contribute to the chronic impairment of vascular function during inflammation and ageing, identified recently as the process of inflammageing.

In the following chapters of the discussion, the details of the findings of this PhD will be discussed, such as the role of ATP in endothelium-dependent vasodilation (chapters 1–2), the impact of ageing on endothelial function and metabolism (chapter 3), the role of activation of pentose phosphate pathway in inflammation-induced vascular dysfunction in the aorta of young and old mice (chapters 6–7), and the potential bioenergetic mechanisms of mitochondrial dysfunction in the aorta of old mice (chapters 8–11).

An important methodological aspect of this study that needs to be emphasised is the use of a specially adapted experimental approach for assessing bioenergetics of the vessel wall directly in isolated murine aorta in relation to endothelial function. To date, most studies focused on vascular metabolism have been performed using primary cell cultures or isolated mitochondria. However, such models provide limited insight into vascular wall physiology, mainly due to the fact that primary endothelial cells may change their phenotype during isolation and culture. In fact, previous studies demonstrated that endothelial cells undergo dedifferentiation, and *in vitro* research may not accurately reflect their phenotype *in vivo* (Lacorre et al., 2004).

Furthermore, *ex vivo* analysis in the tissues could include mechanisms based on metabolite crosstalk between cells, which could provide more insight into the metabolic regulations of vascular function, as many metabolites have been proven to have signalling properties (Haas et al., 2016). For the purpose of this research, a unique approach of functional measurement of vascular bioenergetics in isolated aortic rings *ex vivo* using Seahorse XFe96 was optimised (Karaś et al., 2024). The results obtained using this experimental approach were referred to, among others, the results of functional studies in the classical myograph system, measurements of NO production by EPR, and fluxomic analyses identifying the details of metabolomic reprogramming in the vessels in response to inflammation and ageing. This combination of methods was instrumental in drawing the conclusion of this PhD thesis, providing a deeper understanding of connections between NO production, endothelium-dependent vasodilation, vascular mitochondrial respiration and the details of the activity of various metabolic pathways, underscoring the need for a multimethodological approach on functional and biochemical levels to understand the vascular metabolic reprogramming in the vasculature.

1. The role of vascular bioenergetic metabolism in maintaining endothelium-dependent vasodilation

To date, several studies have been conducted on the regulatory role of oxidative metabolism and glycolysis in vascular function and NO release. However, there is no consistent conclusion in the literature about the relationship between specific metabolic pathways and endothelial function.

In the rabbit aorta, mitochondrial electron transport chain (ETC) inhibitors, rotenone, inhibiting complex I, and antimycin A, an inhibitor of complex III, reduced endothelium-dependent relaxation stimulated with acetylcholine or calcium ionophore irreversibly (Griffith et al., 1987, 1986). Rodman et al. confirmed the inhibitory effect of rotenone and antimycin A on acetylcholine-dependent vasodilation in rat aorta. However, in contrast to the previous findings, the inhibitors had a marginal impact on relaxation in response to calcium ionophore (Rodman et al., 1991). Other groups also observed complete inhibition of acetylcholine-dependent relaxation in rat and rabbit aorta caused by rotenone, but the effect was fully reversible (Cappelli-Bigazzi et al., 1997) or partially reversible (Weir et al., 1991). Relaxation to calcium ionophore was shown to be reduced in rabbit aorta by rotenone (Cappelli-Bigazzi et al., 1997).

On the contrary, inhibition of glycolysis with two different inhibitors, iodoacetate and 2-deoxyglucose (2-DG), did not affect vasorelaxation (Cappelli-Bigazzi et al., 1997). In contrast, other studies showed that inhibition of glycolysis with 2-DG had a moderate effect on vasorelaxation but was observed in the absence of glucose or after more prolonged incubation in the rat and rabbit aorta (Griffith et al., 1986; Weir et al., 1991). Furthermore, different findings confirmed the inhibitory effects of rotenone and antimycin A on vasorelaxation in rat aortic rings, but inhibition of glycolysis with 2-DG in the presence of glucose also modestly reduced vasorelaxation in this report (Rodman et al., 1991). Conversely, the rabbit pulmonary arteries were only mildly affected by inhibiting oxidative metabolism with the use of rotenone or antimycin A (Rodman et al., 1991).

The effects of oligomycin, an ATP synthase inhibitor, can be more confidently attributed to ATP generation, as it was shown to not induce the production of reactive oxygen species in isolated vessels (Wilson et al., 2023), unlike antimycin A and rotenone (L. Wang et al., 2015). There were reports showing that oligomycin impaired acetylcholine-dependent vasodilation in rat aorta, but in contrast to rotenone and antimycin A, with a delay and by approximately 50% (Griffith et al., 1986). Recent studies also used the experimental approach with the inhibition of ATP production with oligomycin, proving that mitochondrial ATP production was required for NO-dependent endothelial function by promoting calcium release (Wilson et al., 2023). Differences in literature in attributing the role of glycolysis and oxidative metabolism to endothelium-dependent vasodilation may arise from variations in vascular responses depending on the vascular bed, vessels of different animal species, differences in used inhibitors or, finally, various experimental conditions. Nevertheless, the prevailing consensus among studies using inhibitors of oxidative mitochondrial metabolism is that they demonstrated full or partial inhibition of acetylcholine-dependent vasodilation. The results of the previous studies vary primarily in terms of the degree and reversibility of the inhibition, and there is less agreement about the effects on vasodilation evoked by different agents, e.g., calcium ionophore. Yet, based on this literature, it can be postulated that in most of the reports, oxidative metabolism contributed to endothelial vasodilatory function (Cappelli-Bigazzi et al., 1997, 1997; Griffith et al., 1986; Rodman et al., 1991; Weir et al., 1991; Wilson et al., 2023), but still some studies refuted this conclusion (Griffith et al., 1987) as discussed below. Still, the role of glycolysis in endothelial function remains more unclear due to the contradictory findings.

In contrast to the previous studies, in the research presented in this PhD thesis, the role of bioenergetic pathways on NO-dependent endothelial function was evaluated not only using *ex vivo* measurement of vasodilation, but it was also verified using direct NO measurement in the isolated aorta. NO production was measured using electron paramagnetic spectroscopy (EPR) and spin-trapping with colloid iron diethyldithiocarbamate complex ($Fe^{2+}(DETC)_2$) (Fink et al., 2006). NO is an unstable gasotransmitter, and reliable NO assessment is challenging and primarily based on indirect assessment such as nitrate derivatives measurement with Griess assay, fluorescent imaging or analysis of NOS activity. EPR spectroscopy is considered one of the most specific methods to measure NO in tissues (Csonka et al., 2015; Hogg, 2010) and colloid iron diethyldithiocarbamate complex spin trap was proven to be highly sensitive to detect NO in murine vessels in studies by our group and by others (Bar et al., 2019; Khoo et al., 2004; Przyborowski et al., 2018).

In the present PhD thesis, inhibitors of ETC such as antimycin A, rotenone, and oligomycin affected both endothelium-dependent vasodilation and NO production, suggesting the critical role of mitochondrial OXPHOS in NO-dependent vascular function. Whereas inhibition of glycolysis with iodoacetate did not affect endothelium-dependent vasodilation or NO production in the murine aorta, suggesting minor reliance of endothelial NO-dependent vasodilation on glycolytic ATP production.

Differences between the effects of particular inhibitors of ETC were noted in the present PhD thesis. Rotenone, antimycin A, and oligomycin displayed a consistent inhibitory effect on NO production stimulated with calcium ionophore in the murine aorta. On the other hand, antimycin A significantly impaired vascular contractility, unlike rotenone and oligomycin. This observation is in line with previous research, proving that inhibition of complex III reduces contractility in isolated arteries *via* inhibition of calcium influx (Saarti et al., 2021). Oligomycin and rotenone caused impairment in endothelium-dependent vasodilation, an effect that was however observed only in response to lower acetylcholine concentrations. In order to further confirm this finding, the effects of rotenone and oligomycin on basal, unstimulated NO production were assessed indirectly as the difference in the magnitude of phenylephrine-induced contraction before and after NOS inhibition with L-NAME, which reflected the contribution of basal NO to the modulation of vascular tone. The NOS-dependent increase in maximal contraction induced by phenylephrine was significantly lower after the inhibition of ETC complexes with rotenone or oligomycin, which can be interpreted as an impairment in basal NO production induced by rotenone or oligomycin pretreatment.

The results presented in this PhD thesis do not confirm previous conclusions made by Griffith et al., showing that basal endothelium-dependent relaxing factor release was not dependent on mitochondrial ATP production (Griffith et al., 1987). These contradictory results may be attributed to the differences in experimental approaches. Griffith et al. assessed endothelium-dependent relaxation using NO scavenging with haemoglobin. Additionally, an inhibitor of cyclic guanosine monophosphate phosphodiesterase was used (MB22948), which prevents cGMP degradation and amplifies the relaxant effect of NO. Vasodilation in response to MB22948 was abolished when haemoglobin was added, showing that the amplified relaxation was due to NO activity. The haemoglobin approach adopted by Griffith et al. was less specific than L-NAME used in the present work because haemoglobin might interact with other endothelium-derived factors, and the observed effect might not depend only on NO.

To sum up, inhibitors of mitochondrial ETC, antimycin A, rotenone and oligomycin all inhibited vascular NO production in the murine aorta. On the functional level, antimycin A impaired vascular contractility to phenylephrine, likely due to changes in calcium signalling. Rotenone and oligomycin had a noticeable effect on acetylcholine-dependent vasodilation in pre-contracted aorta but caused a prominent impairment of NO-dependent regulation of vascular tone assessed based on NO-dependent modulation of phenylephrine-induced vasocontraction.

2. The role of ATP in maintaining endothelium-dependent vasodilation

In the present PhD thesis, the measurement of intracellular adenine nucleotides in the murine aorta after incubation with inhibitors of ETC or glycolysis revealed that oligomycin and antimycin A, which significantly affected endothelial function, also depleted vascular ATP pool and decreased ATP/ADP ratio. Conversely, inhibition of glycolysis with iodoacetate did not considerably influence ATP levels in the isolated aorta. These results suggest that overall vascular bioenergetics relied more on mitochondrial ATP production than glycolytic, and depletion of the vascular ATP pool by inhibitors of ETC resulted in decreased NO production.

Additionally, it was investigated whether the dependence of endothelial function on oxidative metabolism could be linked to extracellular ATP signalling. The results demonstrated that the addition of ATP did not reverse the detrimental effect of oligomycin on NO production. Furthermore, ATP degradation by apyrase did not affect acetylcholine-dependent vasodilation nor NO production in the aorta, and estimated ATP efflux was marginal.

Consequently, within the experimental setting, the impact of ETC inhibitors on endothelial NO-dependent function appeared to be independent of extracellular ATP-mediated signalling. This series of experiments clearly suggested that the most feasible explanation for the impairment of endothelial function dependent on oxidative metabolism is the depletion of the intracellular ATP pool, which is crucial for maintaining vascular function. The mechanism proposed by Wilson et al. implied their dependence on calcium signalling (Wilson et al., 2023). Nevertheless, there is a need to consider divergences in obtained outcomes, total inhibition of NO production by inhibitors of ETC after stimulation with calcium ionophore, and the moderate effect on acetylcholine-dependent vasodilation. These findings are in contrast to the pronounced effects observed during analysis of basal NO-dependent function, raising a question of whether the ATP-dependence of the mechanisms of vasodilation in the murine aorta is more complex than the regulation of calcium vascular signalling.

Due to technical limitations, it was not possible to measure NO production with EPR after stimulation with acetylcholine and compare the effects with calcium ionophore. However, the acetylcholine-dependent vasodilation assessment in isolated aorta *ex vivo* is closer to the physiological condition than the NO measurement after stimulation with calcium ionophore. It is important to note that calcium ionophore was demonstrated to cause relaxation *via* acute calcium release (Furchgott, 1983) but also by non-specific membrane permeabilisation (Xue et al., 1999) and displayed cytotoxic effects (Segal and Ingbar, 1982). Future studies using an approach which allows to directly measure NO after stimulation with acetylcholine would be valuable to validate the role of mitochondrial oxidative metabolism in NO production and the observed effects on acetylcholine-mediated vasodilation.

Previous studies also demonstrated that the effects of inhibitors on mitochondrial respiration vary significantly depending on the type of the vessel and the organism (Griffith et al., 1986; Rodman et al., 1991). The mechanism dependent on calcium release was proposed on the basis of research performed on mesenteric arteries, and the effect of oligomycin on acetylcholine-dependent vasodilation was more pronounced (Wilson et al., 2023), than the effect observed in the aorta in this study. It is thus hypothesised that ATP may mediate multiple mechanisms influencing vascular tone, which may vary depending on the type of vessel, and further studies are required to test this hypothesis using a comparison of the effects of metabolic inhibitors in macro- and microcirculation.

Of note, endothelial cells are connected with vascular smooth muscle cells by gap junctions (Schmidt et al., 2016), and it was demonstrated that gap junction loss or inhibition impaired endothelium-dependent relaxation (Alonso et al., 2010; Tang and Vanhoutte, 2008;

Zhang et al., 2019). Therefore, it is highly likely that vascular smooth muscle cell metabolism provides metabolites for the endothelial cells through gap junctions, which are required to sustain NO-dependent function. For instance, phosphatidylinositol 4,5-bisphosphate (PIP_2) was demonstrated to play a role in vasodilation (Dabertrand et al., 2021). Except for calcium or PIP_2, there are a couple of potential metabolites which could possibly be released or transported from vascular smooth muscle and could influence endothelial function, e.g., cofactors for NOS (NADPH, tetrahydrobiopterin, flavin adenine dinucleotide or flavin mononucleotide), or substrate for NOS (L-arginine). In the present PhD thesis, experiments using an activator of protein kinase C, phorbol ester, were performed to assess the effects of metabolic inhibitors on calcium-independent contraction, but the attempts to evoke contraction in response to phorbol ester failed. Non-specific inhibitors of gap junctions, carbenoxolone and enoxolone, were also tested to assess their effect on acetylcholine-dependent relaxation in the murine aorta. Both compounds caused a significant impairment of the vascular responses. However, the deleterious effect of those compounds was attributed to their amphiphilic structures and surfactant-like properties (Pedraza et al., 2006), causing a firm foam during myograph experiments. Accordingly, those experiments should be repeated using other, more specific inhibitors with different chemical structures or knock-out mice. Accordingly, further studies are required to explore the role of intercellular metabolic communications between smooth muscle cells and endothelial cells and the contribution of these mechanisms to the bioenergetic requirements for NO-dependent function of endothelium.

In this context, the apparent limitation of the experimental approach used in this study was that inhibition of metabolic pathways in the murine aorta affected both endothelial cells and vascular smooth muscle cells. ATP and other purines can be released and up-taken by other cells (Lohman et al., 2012), and depletion of the overall vascular pool of ATP is more relevant to the physiological vascular function. Naturally, ATP could have other extracellular sources, but we excluded the contribution of extracellular ATP to the vasodilation in the aorta. Interestingly, endothelial cells are proven to rely on glycolytic ATP production (De Bock et al., 2013; Dobrina and Rossi, 1983). However, the inhibition of glycolysis in the isolated vessels, both in the present study and previous reports (Cappelli-Bigazzi et al., 1997), did not affect vascular function. It raises the question of whether the source of required ATP or other OXPHOS-derived metabolites to control the NO-dependent function is indeed mainly endothelium-derived or whether metabolic flow from vascular smooth muscle cells to endothelial cells also plays a role.

To sum up, this study provides further evidence to support the hypothesis that mitochondrial oxidative metabolism significantly contributes to endothelial NO-dependent function in the murine aorta, whereas glycolytic ATP production appears to play a relatively minor role. The results of this research suggest that extracellular ATP signalling is not likely to be the underlying mechanism but rather that intracellular ATP depletion or other bioenergetic processes are more relevant for maintaining endothelial function.

3. The influence of ageing on vascular function and bioenergetic metabolism

To better understand what bioenergetic mechanisms could contribute to the development of endothelial dysfunction, the PhD research was focused on two key causes of endothelial dysfunction, ageing and inflammation and analysed how they affected vascular bioenergetic metabolism. Mitochondrial dysfunction in the vascular wall has already been proven to contribute to the ageing-related impairment of vascular phenotype (Fleenor et al., 2012; LaRocca et al., 2014b; Tyrrell et al., 2020a) *via* multiple mechanisms, including impaired autophagy (Larocca et al., 2012), oxidative stress (Fleenor et al., 2012) or mitochondrial DNA damage (Foote et al., 2018).

However, although mitochondrial dysfunction was also linked to impaired cell bioenergetics, the role of metabolic alterations in vascular ageing is still not fully understood. Of note, inhibition of complex I of ETC with rotenone was shown to induce stiffening of aortic rings isolated from young mice (LaRocca et al., 2014a), indicating a key role of impaired mitochondrial bioenergetics in the development of vascular stiffness.

In this study, the aorta of old mice exhibited an apparent phenotype of the aged vessel, including endothelial dysfunction, increased stiffness and vascular remodelling associated with vascular smooth muscle hypertrophy and collagen deposition. Endothelial dysfunction was also associated with reduced NOS activity but was independent of arginine utilisation by arginase. Furthermore, analysis of the functional bioenergetic metabolism of isolated aorta using the Seahorse XFe96 Analyzer revealed that old mice exhibited impaired mitochondrial respiratory capacity, basal glycolysis and glycolytic capacity (Karaś et al., 2024).

The vascular NAD pool also decreased with age, as shown in the present PhD thesis and in the recent report (Karaś et al., 2024), which may partially explain the observed impaired functional metabolic reserve. This observation aligns with previous reports showing a decrease in NAD availability with age in different tissues (Gomes et al., 2013a; Massudi et al., 2012). However, in response to IL-1β, in older mice (28 months old), there was a significant increase in the NAD^+/NADH ratio as compared to young mice despite a depleted NAD pool.

Of note, at 24 months of age, the redox balance in the basal conditions remained still preserved in the murine aorta despite impaired NO-dependent function (Karaś et al., 2024). These results might suggest no direct link between NAD content and NO-dependent function, but more insightful analysis of NAD content separately in mitochondria and in cytoplasm would be needed to understand this phenomenon in detail.

Noteworthy, the NAD^+/NADH ratio may be informative regarding the metabolic/redox vascular status. In old mice (28-month-old), an increased NAD^+/NADH ratio was observed under basal conditions as compared with young mice and it was further increased in response to inflammation. Such alterations in the redox state are often indicative of a relative decrease in NADH to NAD^+ resulting from accelerated utilisation of NADH in activated OXPHOS.

However, this explanation appears unconvincing considering the vascular bioenergetic profile of mice in advanced age. Old mice at 24 months of age displayed preserved basal level of mitochondrial respiration with a decline in spare respiratory capacity; therefore, it is likely that 28-month-old mice exhibit a similar bioenergetic profile, or even further impairment of basal respiration in the vascular wall. Thus, NADH relative decline may result from its consumption in order to maintain minimal basal oxidative metabolism, with the NADH pool markedly depleted with age. Consequently, low availability of NADH may be rate-limiting under increased energy demand conditions, which could further reduce respiratory capacity or even impair basal respiration in the aorta of 28-month-old mice. Additionally, reduced glycolytic or TCA flux could also contribute to the increase of NAD^+/NADH ratio due to decreased generation of NADH by enzymes such as GAPDH (glycolysis), or TCA enzymes, isocitrate dehydrogenase, α-ketoglutarate dehydrogenase complex or malate dehydrogenase (Xie et al., 2020).

On the other hand, NAD deficiency could also be a reasonable explanation for impaired glycolytic capacity. A glycolytic enzyme, GAPDH, requires NAD as a cofactor, and its deficiency can create a bottleneck in glycolytic flux. To sum up, NAD deficiency can not only be an underlying cause of the reduced metabolic reserve capacity and dysfunctional bioenergetic metabolism but also a consequence of impaired bioenergetic metabolism, possibly creating a vicious cycle promoting metabolic inflexibility and further impairment of vascular function.

Of note, NAD deficiency was associated with age-dependent mitochondrial and vascular dysfunction (Csiszar et al., 2019). NAD precursors had beneficial effects on vascular ageing, reducing arterial stiffening and endothelial dysfunction (Picciotto et al., 2016) and exhibiting anti-atherogenic influence (Kiss et al., 2019). The protective effects of NAD

are linked to the activation of sirtuins (Csiszar et al., 2009; Mouchiroud et al., 2013) and the enhancement of mitochondrial oxidative metabolism (Cantó et al., 2012; Gomes et al., 2013b).

To sum up, the age-related impairment of vascular function was associated with metabolic dysfunction, as evidenced by impaired glycolysis and respiratory capacity. Impairment of metabolic reserve could be attributed to NAD deficiency, which plays a key role in bioenergetic metabolism and has already been shown to contribute to vascular dysfunction. However, the results presented in this PhD thesis highlight another potential mechanism related to NAD that may contribute to vascular ageing – namely, the impairment of vascular metabolic reserve. Considering the reduced ability of the aged vessel wall to meet increased energy demands in response to proinflammatory stimulation, it is hypothesised that external factors commonly present in ageing, such as proinflammatory factors, may further compromise mitochondrial function and, consequently, vascular health.

Thus, a key objective of this PhD thesis was to explore the impact of inflammation on the metabolism and function of the vessel wall, with a focus on assessing the vascular metabolic responses to proinflammatory stimulation with IL-1β and, in particular, on the comparison of this response on functional and metabolic levels in young and old mice.

4. The effect of inflammation on vascular function

Vascular inflammation is a known factor contributing to the development of endothelial dysfunction (Daiber and Chlopicki, 2020; Sprague and Khalil, 2009). IL-1β is one of the key cytokines driving the inflammatory response, and due to its detrimental influence on vascular function (Sprague and Khalil, 2009), IL-1β is considered a therapeutic target for cardiovascular disease (Libby, 2017; Ridker et al., 2011). Furthermore, circulating IL-1β is elevated with ageing and correlated with a higher risk of various diseases (Walker et al., 2022).

Ex vivo stimulation of murine aorta with IL-1β caused impairment of endothelium-dependent vasodilation after 24h of incubation but not after 2h of incubation. Interestingly, the degree of the dysfunction was comparable in the aorta of young (3-month-old) and aged mice (18-month-old). However, at the more advanced age of mice (30-month-old), the endothelial dysfunction caused by IL-1β was more pronounced as compared to younger groups. These observations are consistent with previous reports showing that IL-1β causes endothelial dysfunction in isolated vessels (Vallejo et al., 2014) and endothelial cells (Mateuszuk et al., 2020; D. Wang et al., 2015).

Furthermore, the results revealed that IL-1β affected endothelial function after longer incubation time, but not short incubation time, and that in old animals, response to IL-1β caused more severe endothelial dysfunction. It was, therefore, of salient importance for this PhD thesis to correlate these functional findings with metabolomic readouts.

5. The effect of inflammation on the functional bioenergetic profile of the murine aorta

Previous studies investigating the effect of induced inflammation on endothelial cell bioenergetic metabolism found that proinflammatory stimulation accelerated glycolysis and mitochondrial respiration in cultured cells (Junaid et al., 2020; Schnitzler et al., 2020; Xiao et al., 2021). In this PhD thesis, the effect of stimulation with IL-1β was investigated in the isolated aortic rings *ex vivo* to evaluate overall bioenergetic changes of the vascular wall on a tissue level and compare the metabolomic response to vascular inflammation in the young and aged vessel wall. The primary effect of IL-1β-induced inflammation in the aorta of young mice was found to be the activation of mitochondrial OXPHOS, ATP-linked oxygen consumption and glycolysis, which was consistent with previous studies. Furthermore, the metabolic response of young vessels to IL-1β was comparable after 2 hours and 24 hours of incubation, which suggests prolonged metabolic activation in response to inflammatory stimuli. Interestingly, the activation of vascular mitochondrial respiration was not observed in aortic rings taken from middle-aged (10-12 months) and old mice (22 months). In old mice, the lack of the metabolic response to IL-1β could be explained by the impairment of spare respiratory and glycolytic capacity confirmed before (Karaś et al., 2024), which causes the inability to upregulate bioenergetic metabolism in response to increased energy demand, for instance, during inflammation.

The lack of activation of mitochondrial respiration in response in middle-aged mice (12-month-old) to IL-1β could be interpreted as an early impairment of metabolic flexibility, which still was partially compensated by glycolysis. Notably, impairment of spare respiratory capacity was not detected in 10-month-old mice. It could be attributed to the difference in age of mice used in these experiments, which was rather minor (2 months). However, the difference in the assessment was a more likely explanation. Spare respiratory capacity in the MST test is calculated based on the difference between basal and maximal respiration, which is induced by FCCP, an uncoupler of mitochondrial OXPHOS. The effect of FCCP is not dependent on any regulatory mechanisms, and the IL-1β-induced activation is dependent on inflammatory signalling. The analysis of metabolic response to IL-1β could be more sensitive to early impairment of mitochondrial function.

Interestingly, ATP levels in the aorta of old mice were not significantly altered compared to young mice. An ageing-dependent decrease in ATP effective utilisation has already been demonstrated in the heart, and relatively preserved ATP levels have been observed (Yaniv et al., 2013). Following proinflammatory stimulation, there was a nonsignificant decrease in ATP/ADP and ATP/AMP ratios in the aorta of old mice. Old mice did not exhibit activation of mitochondrial respiration in the aorta in response to inflammation. The glycolytic flux seemed to be partially impaired (accumulation of DHAP, nonsignificant increase in lactate), and it was not likely to provide sufficient ATP production. It could be attributed to the shift of the cellular focus toward maintaining redox balance and antioxidant defence (NADPH production *via* PPP) rather than processes requiring high ATP consumption.

The observed impairment in phenylephrine-induced contraction and endothelium-dependent vasodilation in the aorta of aged mice may reflect decreased ATP consumption by vascular smooth muscle and endothelial cells. However, the facilitated endothelial dysfunction in old mice is most likely independent of ATP depletion, due to the nonsignificant changes in ATP levels.

Taken together, these findings indicate that there is a progressive decline in vascular bioenergetics with ageing. Specifically, the responses of isolated murine aorta to proinflammatory stimuli, but not the basal parameters, provided clear-cut evidence for this decline. Young mice exhibited activation of mitochondrial respiration and glycolysis in the aorta after stimulation with IL-1β, while middle-aged mice failed to upregulate mitochondrial respiration, but glycolysis remained activated. Finally, old mice did not display any bioenergetic response to induced inflammation. Interestingly, in young mice, metabolic activation was visible as soon as after 2 hours of stimulation and persisted also 24 hours. This observation suggests the key role of early metabolic reprogramming in response to proinflammatory stimuli, possibly determining the delayed functional outcome of vascular inflammation. Indeed, recent studies indicate that lack of resolution determines chronic inflammation in ageing . This phenomenon could also be related to vascular metabolism and, in particular, to the impaired vascular metabolic flexibility in response to acute proinflammatory stimuli that could lead to unresolved chronic vascular inflammation. Further studies on the metabolic mechanisms of vascular inflammation resolution are needed to confirm or refute this hypothesis.

6. The effect of inflammation on bioenergetic metabolism: the role of pentose phosphate pathway overactivation in the aorta of old mice

The key metabolic effect of proinflammatory stimulation with IL-1β of the aorta of young and old mice was the activation of the PPP. PPP is an alternative branch of glucose metabolism in which the main products are NADPH and ribose. Ribose is a precursor for purine synthesis *de novo*. NADPH is utilised in antioxidant defence, NO production, activity of NADPH oxidase (NOX), a ROS-producing enzyme, and various biosynthetic pathways, for instance, synthesis of steroids and fatty acids. Glutathione reductase, the main antioxidant defence enzyme, requires NADPH to reduce glutathione, which in turn can neutralise ROS. Accordingly, activation of PPP can affect all of the mechanisms mentioned above.

Proinflammatory stimulation with IL-1β caused activation of the oxidative part of PPP corresponding to glucose 6-phosphate dehydrogenase (G6PD) activity producing NADPH, and the increase in ribose 5-phosphate labelling in the aorta of young and old mice reflected G6PD activation. These results are in line with previous studies that demonstrated PPP activation in endothelial cells and vascular smooth muscle cells during inflammation (Peiró et al., 2016; Spolarics and Wu, 1997; Xiao et al., 2021). Furthermore, research on aortic smooth muscle cells and rat mesenteric arteries confirmed that activation of PPP in response to IL-1β causes increased NADPH production, leading to the activation of NOX (Peiró et al., 2016). While the activation of oxidative PPP in the response to IL-1β was more facilitated in the aorta of old mice, the redirection of glucose metabolism towards PPP was also present in old mice without proinflammatory stimuli, suggesting PPP baseline activation with ageing. Previous studies confirmed that the baseline expression of proinflammatory cytokines, including IL-1β, is elevated in the aorta of aged C57BL/6 (Fleenor et al., 2012). Thus, chronic metabolic reprogramming exhibited by old mice in the aorta, including PPP activation, could possibly reflect inflammaging.

Moreover, IL-1β-induced inflammation also activated the synthesis of glycine. Importantly, glycine is a precursor for glutathione synthesis, and its upregulation may indicate compensatory activation of glutathione synthesis to counteract inflammatory oxidative stress. Glycine deficiency was shown to downregulate glutathione synthesis, which was reversed by glycine supplementation (Rom et al., 2022; Sekhar et al., 2011) and accordingly reduced vascular inflammation (Rom et al., 2022). These findings indicate the key role of glycine for glutathione-mediated protection from oxidative stress, and the upregulation of its synthesis might be a compensatory mechanism in response to inflammation.

Of note, glycine was suggested recently to be a precursor of the cytoprotective action of hydrogen cyanide (CN) (Zuhra and Szabo, 2022); however, it remains still unclear whether CN could be generated during vascular proinflammatory response and if increased glycine synthesis plays a role in this mechanism.

Serine biosynthesis was also increased in response to IL-1β-induced vascular inflammation. Serine is a precursor of glycine and originates from glycolytic intermediate, 3-phosphoglycerate. The increase in serine and glycine synthesis suggests redirection of glycolytic intermediates towards glutathione (Zhou et al., 2017) and purine biosynthesis (Fan et al., 2019) or possibly other pathways.

The important finding of this PhD thesis was that IL-1β-induced inflammation caused endothelial dysfunction in the aorta of young and old mice, which seemed to intensify in advanced age. Previous studies have confirmed that the overactivation of PPP induces endothelial dysfunction by a NOX-dependent mechanism (Peiró et al., 2016). It was also demonstrated that inhibition of PPP reduced endothelial dysfunction, but only in the presence of high glucose concentration (22 mM) (Peiró et al., 2016). The overactivation of G6PD was also involved in ROS-mediated age-related renal injury (Han et al., 2024). The described underlying mechanism was linked to excessive production of NADPH (Han et al., 2024; Peiró et al., 2016), which exceeded its utilisation by glutathione reductase for antioxidant defence and thus fuelled NOX activity and ROS generation rather than scavenging (Peiró et al., 2016). Another study also demonstrated that G6PD-deficient mice displayed reduced oxidative stress in response to angiotensin II (Matsui et al., 2005).

On the contrary, multiple studies demonstrated the protective role of PPP during inflammation. For instance, inhibition of G6PD was shown to promote the endothelial inflammatory response in isolated endothelial cells (Xiao et al., 2021). Furthermore, overexpression of G6PD in endothelial cells increased NADPH production but reduced oxidative stress in response to inflammation and enhanced endothelial NO production (Leopold et al., 2003).

These contradictory results indicate the key role of metabolic balance in the vascular wall that was identified in the present PhD thesis. It is generally accepted that PPP plays a protective role in inflammation if the produced NADPH can be effectively used by glutathione reductase for antioxidant defence; furthermore, NADPH is also required for endothelial NO production as a cofactor. Those mechanisms can be maintained if NADPH does not reach high concentrations, triggering its utilisation primarily by NOX and ROS production, and there are sufficient levels of glutathione and glutathione reductase. Furthermore, to maintain the

protective function of PPP, glucose utilisation by PPP shall not exceed the need to preserve the mitochondrial oxidative metabolism. Yet, under certain conditions, such as proinflammatory stimuli in the old vasculature, the overactivation of PPP can potentially contribute to the amplification of oxidative stress and redirection of the metabolism away from mitochondrial oxidative metabolism and subsequently resulting in detrimental response to inflammation, leading to more severe endothelial dysfunction as indicated by the results presented in the present PhD thesis and described in the chapter below.

7. The effect of inhibition of pentose phosphate pathway on vascular function in the aorta of young and old mice

The critical finding of this PhD thesis research was that inhibition of PPP with dehydroepiandrosterone partially reversed the IL-1β-induced endothelial dysfunction, but only in the aorta of old mice. These results seem to contrast with the known protective effects of PPP in the endothelial cells and led to the alternative proposal of the underlying mechanisms that are discussed below and illustrated in **Figure 44**.

Dehydroepiandrosterone is an inhibitor of the main rate-limiting enzyme of PPP – G6PD, that reduces overactivation of the PPP and NADPH production (Camporez et al., 2011). In the aorta of old mice, dehydroepiandrosterone significantly rescued contractile and endothelial dysfunction induced by IL-1β.

In young mice, the beneficial effect of dehydroepiandrosterone was observed only on phenylephrine-induced contraction after stimulation with a higher concentration of IL-1β. It could be hypothesised that under these experimental conditions, the stimulation with IL-1β resulted in a significantly aggravated inflammatory response, which was reflected by severe impairment of phenylephrine-dependent contractility. Under these conditions, the metabolic balance could be disrupted even in young mice, and PPP could be overactivated. On the other hand, although inhibition of NADPH generation likely facilitates inflammation-induced oxidative stress, endothelial function was not further impaired in young mice using lower concentration of IL-1β. This observation suggests that excessive generation of ROS was not the primary mechanism underlying the development of endothelial dysfunction in response to proinflammatory stimulation in young mice. Different outcomes of PPP modulation in the aorta of young and old mice imply that the moderate activation of PPP observed in young mice was insufficient to contribute to endothelial dysfunction.

PPP overactivation appears to have different functional consequences in the aged vessel wall, which can be attributed to significant overactivation of NADPH production, reflected as the increase in full labelling of ribulose 5-phosphate. The detrimental mechanisms linked to excess NADPH production triggered by PPP enhanced overactivation, could be a likely underlying cause of the significant improvement of endothelial function by inhibition of G6PD in old mice. As was shown by Perió et al. in hyperglycaemia conditions, when NADPH generation exceeded its utilisation by glutathione reductase for antioxidant defence, it could be used by NOX for generating ROS and aggravation of oxidative stress (Peiró et al., 2016). Such shift in NADPH utilisation could contribute to endothelial dysfunction, inhibition of G6PD could restore redox balance and promote antioxidant mechanisms. Noteworthy, overexpression of NOX was demonstrated to cause aortic fibrosis and stiffening (Canugovi et al., 2019); accordingly, increased NOX activity triggered by ageing-related metabolic reprogramming could potentially contribute to arterial stiffness and deterioration of vascular function with ageing.

The beneficial effect of dehydroepiandrosterone on downregulating oxidative stress during inflammation has already been demonstrated in vascular smooth muscle cells in response to angiotensin II or IL-6 (Chen et al., 2014), and in endothelial cells in response to high glucose concentration (Huerta-García et al., 2012). Furthermore, another study demonstrated that dehydroepiandrosterone can restore reduced NO availability and improve endothelial function *via* mechanisms related to PPP and downregulation of NOX, and also a PPP-independent mechanism, inducing eNOS phosphorylation at Ser1177, which plays a regulatory role (Camporez et al., 2011). Yet, few studies investigated whether the protective effect of dehydroepiandrosterone could be related to bioenergetic consequences of PPP inhibition independent from NADPH production.

Importantly, in contrast to earlier research in which PPP overactivation was triggered by hyperglycaemia and the resultant elevated glucose uptake, this was not the case in this study. Therefore, the findings of the present study suggest an alternative underlying cause. In fact, no significant increase in fully labelled glucose levels was observed in the aorta of aged mice; fully labelled glucose 6-phosphate exhibited a nonsignificant increasing trend in both aged control and IL-1β stimulated groups compared to young mice. Although the glucose uptake was possibly also increased in the aorta of aged mice, the primary reason for the consequences of the inflammatory PPP overactivation in old mice may be related to inflammaging. Importantly, dehydroepiandrosterone did not cause improvement of endothelium-dependent vasodilation in young mice, which suggests that in old mice, the observed effects were

associated with deterioration of metabolic balance, a phenomenon not present in young mice. Hypothesised metabolic mechanisms of dehydroepiandrosterone-mediated improvement of endothelial function in old mice are illustrated in **Figure 44**. It should be noted that except for PPP overactivation in response to inflammation, the aged mice initially exhibited altered bioenergetic metabolism and impaired glycolytic and respiratory capacity in the aorta. Excessive glucose redirection towards PPP could further impair mitochondrial respiration in response to inflammation; moreover, pyruvate oxidation was found to be impaired in response to proinflammatory stimuli in the aorta of old mice. Most likely, except for PPP activity, mechanisms related to impaired mitochondrial oxidative metabolism contribute to vascular dysfunction during inflammation. To sum up, excessive NADPH generation in response to inflammation is one of the multiple bioenergetic mechanisms underlying pronounced endothelial dysfunction in the aorta of old mice, which was not fully rescued after the inhibition of PPP. Other mechanisms contributing to the improvement of endothelial function in response to IL-1β in old mice might have also been linked to increased pyruvate oxidation in response to the inhibition of PPP and redirection of glucose flux towards mitochondrial respiration.

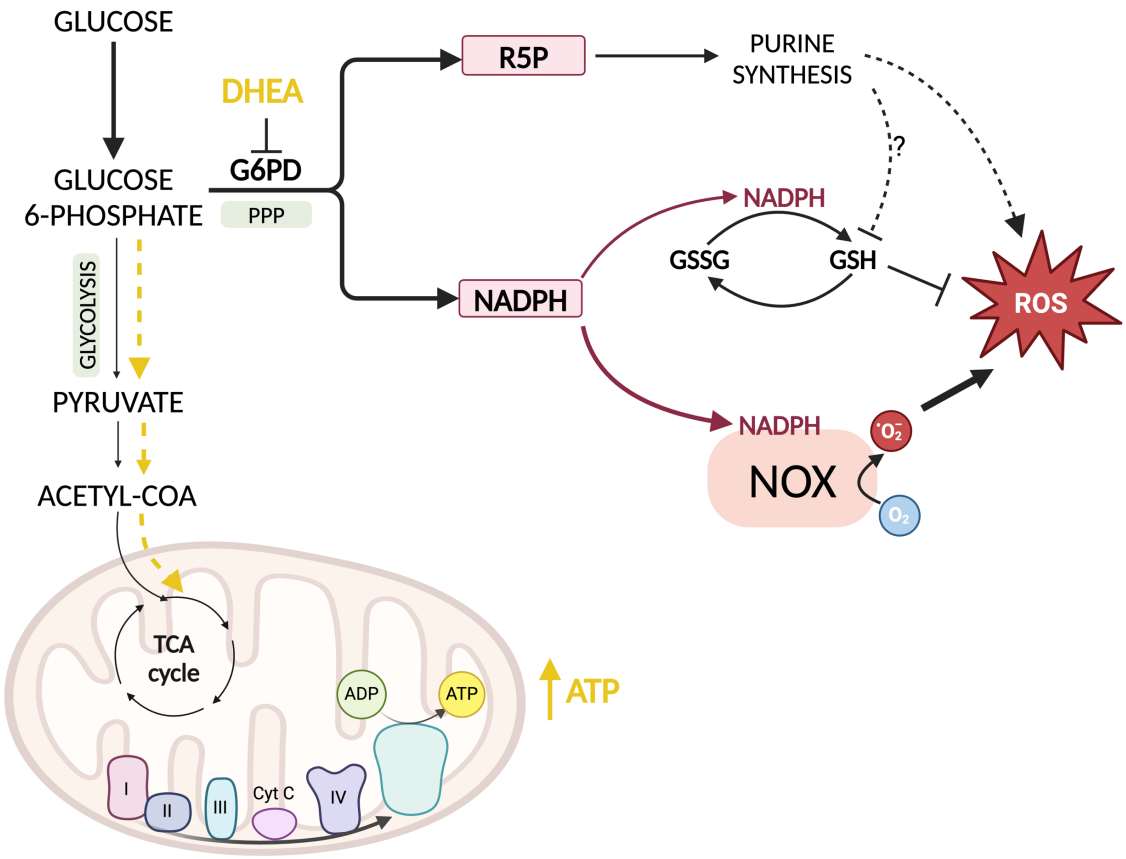

Figure 44. ***Hypothesised mechanisms of protective effect of dehydroepiandosterone (DHEA) in the aorta of old mice stimulated with IL-1β****. Thicker arrows indicate predominant metabolic flux in the aorta of old mice, thinner arrows indicate impaired metabolic flux, and yellow arrows indicate hypothesised enhanced metabolic flux after inhibition of PPP with DHEA. G6PD – glucose 6-phosphate dehydrogenase; DHEA – dehydroepiandosterone; R5P – ribose 5-phosphate; GSH – reduced glutathione; GSGG – oxidised glutathione; NOX – NADPH oxidase.*

8. The effect of inflammation on bioenergetic metabolism: TCA anaplerosis and mitochondrial dysfunction in the aorta of old mice

Both young and old mice displayed the activation of PPP and purine metabolism in the aorta in response to inflammation. Notably, the shift of glucose utilisation by PPP was more pronounced in old mice, and it was also associated with a reduction of the efficiency of pyruvate oxidation and a lack of activation of mitochondrial respiration. It may explain the differences between young and old mice in the severity of endothelial dysfunction and the response to PPP inhibition during proinflammatory stimulation.

The accumulation of pyruvate +3, lactate +3 and alanine +3, together with an increase of malate +3 caused by stimulation with IL-1β in the aorta of old mice, was probably associated with reduced PDH complex activity and anaplerotic carbon entry into TCA.

Ageing has already been associated with reduced activity of the PDH complex in various tissues (Consitt et al., 2016; Nakai et al., 1997); however, this effect has not been extensively investigated in the vascular wall. This finding is consistent with the impairment of mitochondrial capacity observed in the aorta of aged mice. The underlying cause of reduced vascular mitochondrial respiratory capacity with ageing could be related to NAD deficiency and impaired pyruvate oxidation, which can represent a bottleneck to TCA flexibility.

Pyruvate oxidation is also regulated by pyruvate dehydrogenase kinase (PDK), which inactivates PDH through phosphorylation (Zhang et al., 2014). There are four isoforms of PDK; studies on rat tissues demonstrated that PDK1 is expressed mainly in the heart, PDK2 and PDK3 in the majority of the tissues and PDK4 mainly in skeletal muscle and the heart (Bowker-Kinley et al., 1998). Vascular smooth muscle cells were demonstrated to express all isoforms of PDK, but specifically, PDK4 was implicated in vascular calcification (Lee et al., 2015) and was found critical in ischemia-reperfusion mediated renal damage (He et al., 2024; Khang et al., 2024), in LPS-induced mitochondrial and myocardial injury in cardiomyocytes (Chen et al., 2024a, 2024b).

It remains unclear whether the reduced PDH activity in the aorta of aged mice following proinflammatory stimulation results from the lower expression of PDH or its inactivation by PDK. Notably, in previous studies, PDK4 expression was downregulated in response to inflammatory stimuli in endothelial cells, which allowed the enhancement of mitochondrial OXPHOS, confirmed to depend on pyruvate oxidation (Xiao et al., 2021). Furthermore, overexpression of PDK4 reduced the increase in mitochondrial OXPHOS in response to inflammation and aggravated the inflammatory response (Xiao et al., 2021). In addition, the pharmacological inhibition of PDK with dichloroacetate (DCA) *in vivo* and subsequent enhancement of mitochondrial respiration has been demonstrated to reduce vascular inflammation (Forteza et al., 2023; Xiao et al., 2021). Yet, this mechanism was not investigated in the cells of the aged vascular wall. It could be hypothesised that impaired downregulation of PDK expression in response to inflammation resulting in inhibition of PDH could contribute to decreased mitochondrial respiratory capacity and the inability to increase OXPHOS in response to inflammation in the aorta of aged mice.

Interestingly, the basal level of mitochondrial respiration and ATP production was preserved in the aorta of old mice compared to young mice, and the baseline metabolic flux did not indicate any impairment of TCA activity. Furthermore, no accumulation of pyruvate or lactate was observed under control conditions in old mice. It may suggest that the aged vascular wall exhibits minimal pyruvate oxidation to sustain the baseline TCA cycle

and OXPHOS activity to meet resting energy demands or relies on compensatory anaplerotic pathways. However, adapting the TCA flux to increased energy demand in response to proinflammatory stimuli may be supported by several potential anaplerotic pathways compensating for reduced PDH activity in inflammatory conditions, including pyruvate carboxylase activity, malic enzyme activity, increased glutamine utilisation or fatty acid oxidation.

Although glutamine was added to incubation in metabolic flux experiments and could be converted to α-ketoglutarate and fuel the TCA cycle, it does not seem like the primary mechanism under these conditions. In fact, there was no observed decrease in unlabelled glutamine in old mice, and no changes in levels of α-ketoglutarate or succinate were detected.

Pyruvate can fuel TCA by bypassing oxidation by PDH; it can be converted to oxaloacetate by pyruvate carboxylase or to malate by malic enzyme. Pyruvate carboxylase activity seems to be the most likely explanation for the anaplerotic adaptation of old mice, as the enzyme is located in mitochondria and was previously reported to play a role in TCA anaplerosis (Bornstein et al., 2023; Cappel et al., 2019). Although the malic enzyme is located in the cytosol, which makes it less likely to support TCA, and there is less data about its role in pyruvate carboxylation, its contribution cannot be entirely excluded.

The accumulation of fumarate +3, malate +3 and aspartate +3, and also in unlabelled fumarate and malate, was observed in the aorta of old mice in the presence of IL-1β. If the flexibility of TCA was impaired, PC-derived oxaloacetate could accumulate and be converted to malate or aspartate—increases in malate +3 and aspartate +3 support this hypothesis.

A similar conclusion was made previously in research about the impact of acute cold stress on metabolic flux based on malate preserving three labelled carbons, which indicated bypassing PDH oxidation (Bornstein et al., 2023). Oxidation of fully labelled pyruvate by PDH to acetyl-CoA caused a loss of one labelled carbon.

9. The effect of inflammation on bioenergetic metabolism: pyruvate carboxylase and arginase activity

Interestingly, PC was demonstrated to play important role in supporting TCA activity, fat oxidation and mitochondrial respiration in the liver (Cappel et al., 2019). The main allosteric activator of PC is acetyl-CoA, which is particularly important in response to increased fatty acid oxidation during fasting, PC can replenish oxaloacetate to support TCA and gluconeogenesis in the liver (Selen et al., 2022).

PC-mediated anaplerosis was also found to be important source of carbons in the TCA in brown adipose tissue, which was further facilitated during and acute cold stress (Bornstein et al., 2023). The role of PC was also attributed to replenishing TCA intermediates with fatty acid oxidation as the main source of acetyl-CoA. Thus, it could be concluded that PC activation in the aorta of old mice in response to proinflammatory stimuli could be a compensative mechanism to sustain basal TCA activity and mitochondrial respiration during stress conditions. Further research is required to elucidate whether acute inflammation is also associated with increased fatty acid oxidation in the aorta of aged mice, or whether PC-dependent anaplerosis is solely a consequence of impaired pyruvate oxidation.

On the other hand, PC activity has been demonstrated to support aspartate accumulation and activate argininosuccinate shunt, redirecting arginine utilisation to ureagenesis and reducing NO synthesis (Fu et al., 2020). Furthermore, PC deficiency was also associated with impairment of ureagenesis (Cappel et al., 2019; Marin-Valencia et al., 2010), which was reversed by aspartate supplementation (Cappel et al., 2019), thereby confirming the important contribution of PC to this pathway. Activation of argininosuccinate shunt may also occur in the vascular wall of aged mice. It was demonstrated in this PhD thesis that proinflammatory stimulation with IL-1β significantly induced arginase activity and relative arginase activity to NOS activity in the aorta of young mice. This hypothesis is supported by an increase in +3 labelling of malate, fumarate and aspartate in the aorta of old mice during inflammation and accumulation of unlabelled malate and fumarate, indicating increased argininosuccinate shunt. Furthermore, increased proline synthesis with no changes in glutamate indicates that the source of proline is likely aspartate-derived ornithine. Argininosuccinate lyase (AL), producing L-arginine and fumarate, is abundantly expressed in vascular smooth muscle cells (Hattori et al., 1994). In turn, expression of argininosuccinate synthetase (AS), producing argininosuccinate from citrulline and aspartate and considered a rate-limiting enzyme for ureagenesis (Hecker et al., 1990) in vascular smooth muscle cells, was proven to be induced by inflammatory stimuli (Hattori et al., 1994).

Therefore, the mechanism described by Fu et al., including arginosuccinate shunt, is possibly also activated in the vascular wall of aged mice in PC-dependent matter during inflammation. The proposed mechanism is illustrated in **Figure 45** below.

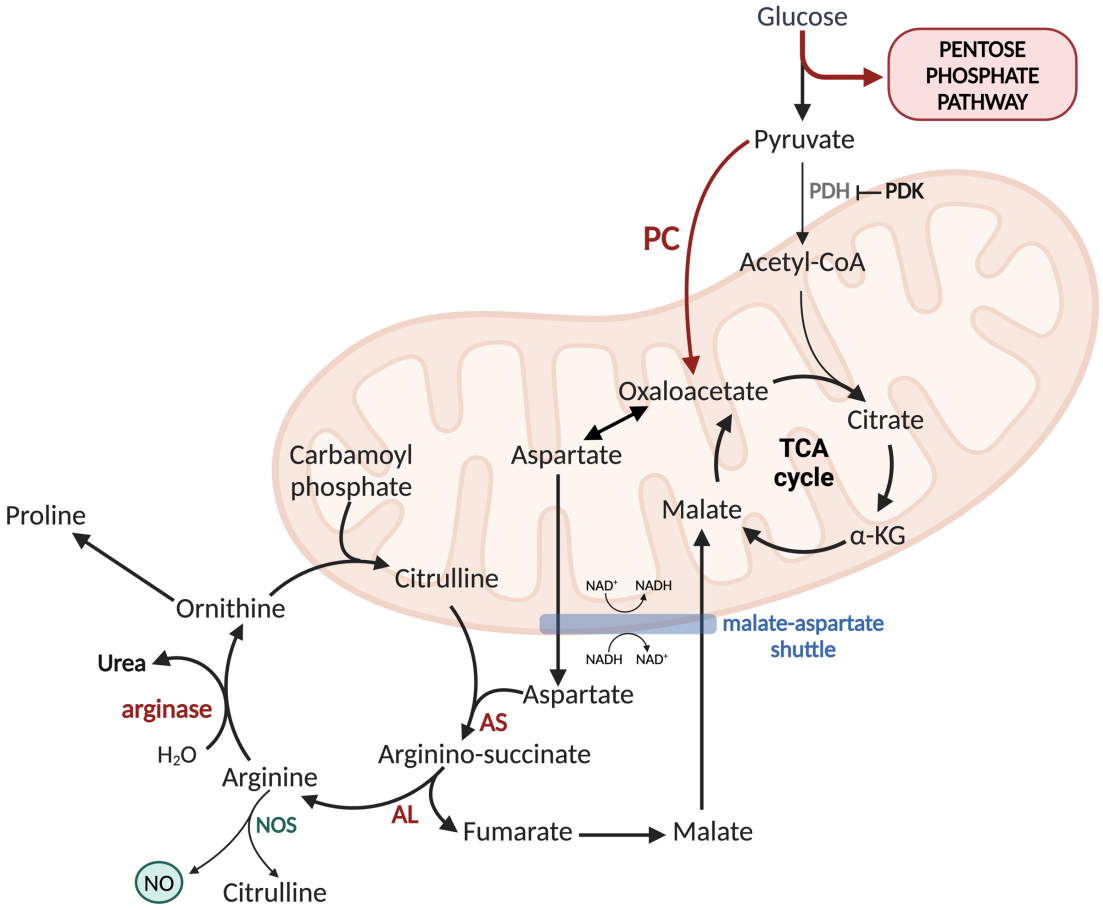

Figure 45. ***The hypothesised mechanism of PC and arginase-mediated reduction of NO synthesis in the aorta of old mice after stimulation with IL-1β.*** *Mechanism was proposed based on Fu et al., 2020. PC – pyruvate carboxylase; PDH – pyruvate dehydrogenase; PDK – pyruvate dehydrogenase kinase; AS –argininosuccinate synthetase; AL – argininosuccinate lyase; NOS – nitric oxide synthase.*

In old mice, basal activation of arginase was not observed as compared to young mice, but arginine utilisation by NOS was reduced. In the presence of inflammation, the potential arginase activity could cause a significant shift in arginine utilisation in the aorta of old mice due to the already impaired basal NOS activity in the aged aorta and further exacerbate endothelial dysfunction. In fact, previous research demonstrated that PC-deficient mice exhibited elevated levels of arginine in plasma (Cappel et al., 2019). Furthermore, inhibition of arginase restored NOS-dependent endothelial function in the aorta of aged rats (Kim et al., 2009). Taken together, PC-driven arginase activity could be another potential mechanism of metabolic contribution to IL-1β-induced severe deterioration of endothelial function in the ageing vessel wall. Testing the contribution of this pathway in further studies is warranted, for example by supplementing L-arginine.

10. The effect of inflammation on bioenergetic metabolism: alterations in glycolytic flux in the aorta of old mice

Except for functional impairment of baseline glycolysis and glycolytic capacity in the aorta of aged mice, the results of the fluxomic analysis suggest inefficient glycolytic flux in response to inflammation. In the aorta of young mice, there was an increase in the flux to lactate in response to inflammation without the accumulation of other glycolytic intermediates, reflecting efficient and accelerated glycolytic flux. In the aorta of old mice, inflammation caused only a minor increase in lactate, with an accumulation of DHAP, pyruvate, and alanine. DHAP accumulation may result from impaired conversion to G3P by triosephosphate isomerase. However, G3P was not detected in the analysis performed, and DHAP levels may also reflect the accumulation of both isomers and the impaired activity of GAPDH, which converts G3P to glycerate 1,3-bisphosphate. GAPDH is a NAD-dependent enzyme; therefore, NAD deficiency observed in old mice may contribute to decreased enzymatic activity and accumulation of upstream metabolites. Importantly, DHAP accumulation may reflect impaired glycolytic flux and metabolic deficiency, and DHAP was also shown to spontaneously form methylglyoxal (Kalapos, 2008). Methylglyoxal is a highly reactive and toxic compound, which was demonstrated to rapidly modify proteins forming advanced glycation end products (AGEs) (Ramasamy et al., 2006). The demonstrated consequences of methylglyoxal formation include impaired mitochondrial function (SinhaRoy et al., 2005), oxidative stress and inflammatory response (Ramasamy et al., 2005). Through protein glycation and oxidative damage, methylglyoxal can promote metabolic dysfunction (Lee et al., 2005; SinhaRoy et al., 2005; Wang et al., 2009a). Studies performed on different tissues (murine hippocampus) suggest an age-related decline in triosephosphate isomerase activity (Zhao et al., 2013), and reduced triosephosphate isomerase activity was identified as an underlying cause of increased methylglyoxal formation and protein glycation (Ahmed et al., 2003). Furthermore, previous studies have shown that methylglyoxal can induce mitochondrial dysfunction in rat aortic smooth muscle cells by inducing ROS production and reducing the activity of complex III of ETC (Wang et al., 2009b).

However, further studies are required to confirm whether inflammation-dependent overactivation of PPP in the aorta of old mice can drive methylglyoxal formation and whether it can further impair mitochondrial function.

11. The effect of inflammation on bioenergetic metabolism: purine metabolism

Another pathway significantly activated by IL-1β -induced vascular inflammation in the aorta of young and old mice was *de novo* purine synthesis. Notably, in the aorta of old mice, this effect was markedly more pronounced. Purines have been described as having signalling properties crucial in the inflammatory response (Linden et al., 2019), but these mechanisms have not been investigated in this study.

On the other hand, the increased purine degradation, reflected by an increase in hypoxanthine labelling, could support the hypothesis that purines could be a byproduct of excessive activation of PPP utilised for NADPH production rather than fulfilling a specific demand, but obviously, the vasoprotective role of adenosine needs to be taken into account (Kutryb-Zając et al., 2023).

Furthermore, an increase in serine and glycine synthesis suggests activation of one-carbon metabolism, which provides tetrahydrofolate for the purine synthesis pathway. Serine and glycine are intermediates of the folate cycle, which provides NADPH and tetrahydrofolate derivatives for purine synthesis (Zarou et al., 2021). Glycine is also a precursor of IMP. It is compelling to speculate that excessive activation of PPP and purine biosynthetic pathway could shift glycine and serine metabolism for folate intermediates and IMP production, indirectly reducing glutathione synthesis by depleting a pool of precursors and promoting oxidative stress.

Methotrexate is an inhibitor of dihydrofolate reductase, the enzyme responsible for the production of tetrahydrofolate; a cofactor required for *de novo* purine synthesis. It is noteworthy that methotrexate exhibited a protective effect on vascular function in old mice in the presence of IL-1β-induced vascular inflammation. However, this effect was more pronounced in phenylephrine-dependent contraction than in endothelium-dependent vasodilation. The observed effect of methotrexate was exclusively present in the aorta of old mice, which is consistent with the observed augmented activation of vascular purine synthesis in old mice. This observation may imply that purine metabolism, even if its upregulation is a consequence of upstream PPP upregulation, may also play a role in the development of vascular dysfunction. Inhibiting tetrahydrofolate production could provide more glycine and serine availability for glutathione synthesis and downregulate oxidative stress. Furthermore, enhanced purine metabolism can promote oxidative stress *via* NOX activation (Seifert et al., 1989), which could have a synergistic detrimental effect together with increased G6PD activity.

Moreover, increased purine degradation *via* xanthine oxidase activity was also demonstrated to generate ROS (Bortolotti et al., 2021; Savio et al., 2021). On the other hand, inhibition of the production of tetrahydrofolate may also result in a fall in tetrahydrobiopterin content, an essential cofactor of NOS activity.

However, methotrexate exhibits multiple off-target effects, and it remains unclear whether the beneficial influence on vascular contractility to phenylephrine can be attributed to inhibition of purine synthesis or other effects. For instance, methotrexate was demonstrated to inhibit the malic enzyme, 2-oxoglutarate and isocitrate dehydrogenases *in vitro* (Caetano et al., 1997), enzymes which also generate NADPH. Therefore, the effect of methotrexate could also be related to decreased NADPH production and consequent decrease of NOX activity. Recent studies also demonstrated inflammation-independent improvement of endothelial function by methotrexate in patients with chronic inflammatory diseases, suggesting other mechanisms related to endothelial cells (Cafaro et al., 2022; Deyab et al., 2017).

Given the complex picture of the possible underlying mechanisms of the protective effect of methotrexate for vascular function, the role of excessive purine synthesis in vascular inflammation and the reason for the difference of these effects in young and old mice requires further studies.

12. Summary of the metabolic reprogramming in vascular ageing

The results of this PhD thesis suggest that the overactivation of PPP, the lack of mitochondrial metabolic flexibility, impaired glycolytic efficiency, and reliance on pyruvate-dependent anaplerotic pathways could all contribute to vascular metabolomic reprogramming in ageing, and the aggravated endothelial dysfunction in response to proinflammatory stimuli in the aorta of aged mice.

In the aorta of young mice, activation of glycolysis and mitochondrial respiration in response to inflammation reflected the vascular metabolic flexibility. In the aorta of middle-aged mice and old mice, the mitochondrial respiratory response to inflammatory stimulation was impaired.

Accordingly, it could be concluded that reduced mitochondrial adaptability could be the early hallmark and contributing metabolic mechanisms to age-dependent vascular dysfunction and lesser resilience of old vasculature to adapt to proinflammatory stimuli.

Impairment of metabolic flexibility corresponded with arterial stiffness and endothelial dysfunction *in vivo* and severe IL-1β-induced endothelial and smooth muscle cell dysfunction, highlighting the critical role of vascular mitochondrial respiration resilience in vascular health.

The major metabolic shift toward PPP and impairment of pyruvate oxidation found in the aorta of old mice in response to inflammation have multiple bioenergetic and functional consequences for the vascular wall. Importantly, inhibition of PPP decreased the severity of endothelial dysfunction during inflammation in the aorta of old mice, which could be attributed not only directly to PPP overactivation but also to a redirection of more glucose-derived carbons to boost mitochondrial respiration. This hypothesis was supported by the observation that in the aorta of young mice exhibiting flexible and efficient vascular bioenergetic metabolism, IL-1β-induced endothelial dysfunction was less advanced and importantly, inhibition of PPP did not affect endothelial function.

This PhD thesis has revealed several unresolved issues that have the potential to affect the function of aged vessels but have not been studied in detail. In the context of inflammaging, impaired glycolytic flux and DHAP accumulation, activated one-carbon metabolism and purine synthesis, argininosuccinate shunt and arginase activity all have the capacity to regulate NO-dependent function. Furthermore, impairment of pyruvate oxidation due to increased PDK activity or decreased PDH activity, and enhanced TCA anaplerosis in response to inflammation appeared as major potential pharmacotherapeutic mechanisms of vascular metabolic reprogramming that require further studies. Targeting the above-mentioned metabolic mechanisms may prove a promising therapeutic strategy to improve endothelial function in inflammaging.

VI. CONCLUSIONS

1. Vascular mitochondrial metabolism was crucial for vascular NO production and maintaining healthy endothelium-dependent vasodilation in the murine aorta. NO-dependent relaxation of the isolated aorta depended more on bioenergetic processes related to oxidative phosphorylation than glycolysis

2. Vascular ageing was associated with impairment of vascular function, structural remodelling and stiffening. Changes in vascular phenotype were associated with the impairment of metabolic capacity and flexibility, likely linked to chronic metabolic reprogramming towards the overactivation of PPP and NAD pool depletion.

3. The IL-1β-induced vascular inflammation caused endothelial dysfunction and vascular smooth muscle cell dysfunction that was more severe in the aorta of old mice. The lack of vascular mitochondrial metabolic flexibility, impaired glycolytic efficiency, and a shift from pyruvate oxidation to anaplerotic pathways could all contribute to vascular metabolic reprogramming in ageing and the aggravated endothelial dysfunction in response to proinflammatory stimuli in the aorta of aged mice.

4. Inhibition of PPP with dehydroepiandrosterone markedly improved endothelial function in old mice in the presence of inflammation, but this effect was not observed in the aorta of young mice, highlighting the key role of ageing-dependent maladaptive overactivation of PPP in vascular dysfunction in response to inflammation. Beneficial vasoprotective effects of PPP inhibition could be attributed not only directly to PPP downregulation but also to a redirection of glucose-derived carbons to boost vascular mitochondrial respiration.

VII. BIBLIOGRAPHY

Ahmed, N., Battah, S., Karachalias, N., Babaei-Jadidi, R., Horányi, M., Baróti, K., Hollan, S., Thornalley, P.J., 2003. Increased formation of methylglyoxal and protein glycation, oxidation and nitrosation in triosephosphate isomerase deficiency. Biochimica et Biophysica Acta (BBA) - Molecular Basis of Disease 1639, 121–132. https://doi.org/10.1016/j.bbadis.2003.08.002

Aird, W.C., 2012. Endothelial Cell Heterogeneity. Cold Spring Harbor Perspectives in Medicine 2, a006429–a006429. https://doi.org/10.1101/cshperspect.a006429

Alonso, F., Boittin, F.-X., Bény, J.-L., Haefliger, J.-A., 2010. Loss of connexin40 is associated with decreased endothelium-dependent relaxations and eNOS levels in the mouse aorta. American Journal of Physiology-Heart and Circulatory Physiology 299, H1365–H1373. https://doi.org/10.1152/ajpheart.00029.2010

Aranda, J.F., Ramírez, C.M., Mittelbrunn, M., 2024. Inflammageing, a targetable pathway for preventing cardiovascular diseases. Cardiovascular Research cvae240. https://doi.org/10.1093/cvr/cvae240

Atkinson, D.E., Walton, G.M., 1967. Adenosine Triphosphate Conservation in Metabolic Regulation. Journal of Biological Chemistry 242, 3239–3241. https://doi.org/10.1016/S0021-9258(18)95956-9

Balboa, D., Barsby, T., Lithovius, V., Saarimäki-Vire, J., Omar-Hmeadi, M., Dyachok, O., Montaser, H., Lund, P.-E., Yang, M., Ibrahim, H., Näätänen, A., Chandra, V., Vihinen, H., Jokitalo, E., Kvist, J., Ustinov, J., Nieminen, A.I., Kuuluvainen, E., Hietakangas, V., Katajisto, P., Lau, J., Carlsson, P.-O., Barg, S., Tengholm, A., Otonkoski, T., 2022. Functional, metabolic and transcriptional maturation of human pancreatic islets derived from stem cells. Nat Biotechnol 40, 1042–1055. https://doi.org/10.1038/s41587-022-01219-z

Bar, A., Kieronska-Rudek, A., Proniewski, B., Suraj-Prażmowska, J., Czamara, K., Marczyk, B., Matyjaszczyk-Gwarda, K., Jasztal, A., Kuś, E., Majka, Z., Kaczor, A., Kurpińska, A., Walczak, M., Pieterman, E.J., Princen, H.M.G., Chlopicki, S., 2020. In Vivo Magnetic Resonance Imaging-Based Detection of Heterogeneous Endothelial Response in Thoracic and Abdominal Aorta to Short-Term High-Fat Diet Ascribed to Differences in Perivascular Adipose Tissue in Mice. Journal of the American Heart Association 9. https://doi.org/10.1161/JAHA.120.016929

Bar, A., Skorka, T., Jasinski, K., Chlopicki, S., 2015. MRI-based assessment of endothelial function in mice in vivo. Pharmacological Reports 67, 765–770. https://doi.org/10.1016/j.pharep.2015.05.007

Bar, A., Targosz-Korecka, M., Suraj, J., Proniewski, B., Jasztal, A., Marczyk, B., Sternak, M., Przybyło, M., Kurpińska, A., Walczak, M., Kostogrys, R.B., Szymonski, M., Chlopicki, S., 2019. Degradation of Glycocalyx and Multiple Manifestations of Endothelial Dysfunction Coincide in the Early Phase of Endothelial Dysfunction Before Atherosclerotic Plaque Development in Apolipoprotein E/Low-Density Lipoprotein Receptor-Deficient Mice. Journal of the American Heart Association 8. https://doi.org/10.1161/JAHA.118.011171

Bkaily, G., Abou Abdallah, N., Simon, Y., Jazzar, A., Jacques, D., 2021. Vascular smooth muscle remodeling in health and disease. Can. J. Physiol. Pharmacol. 99, 171–178. https://doi.org/10.1139/cjpp-2020-0399

Bornstein, M.R., Neinast, M.D., Zeng, X., Chu, Q., Axsom, J., Thorsheim, C., Li, K., Blair, M.C., Rabinowitz, J.D., Arany, Z., 2023. Comprehensive quantification of metabolic flux during acute cold stress in mice. Cell Metabolism 35, 2077-2092.e6. https://doi.org/10.1016/j.cmet.2023.09.002

Bortolotti, M., Polito, L., Battelli, M.G., Bolognesi, A., 2021. Xanthine oxidoreductase: One enzyme for multiple physiological tasks. Redox Biology 41, 101882. https://doi.org/10.1016/j.redox.2021.101882

Bowker-Kinley, M.M., Davis, I.W., Wu, P., Harris, A.R., Popov, M.K., 1998. Evidence for existence of tissue-specific regulation of the mammalian pyruvate dehydrogenase complex. Biochemical Journal 329, 191–196. https://doi.org/10.1042/bj3290191

Butler, T.M., Siegman, M.J., 1985. High-Energy Phosphate Metabolism in Vascular Smooth Muscle. Annu. Rev. Physiol. 47, 629–643. https://doi.org/10.1146/annurev.ph.47.030185.003213

Cabreiro, F., Ackerman, D., Doonan, R., Araiz, C., Back, P., Papp, D., Braeckman, B.P., Gems, D., 2011. Increased life span from overexpression of superoxide dismutase in Caenorhabditis elegans is not caused by decreased oxidative damage. Free Radical Biology and Medicine 51, 1575–1582. https://doi.org/10.1016/j.freeradbiomed.2011.07.020

Caetano, N.N., Campello, A.P., Carnieri, E.G.S., Kluppel, M.L.W., Oliveira, M.B.M., 1997. Effect of methotrexate (MTX) on NAD(P)+ dehydrogenases of HeLa cells: malic enzyme, 2-oxoglutarate and isocitrate dehydrogenases. Cell Biochem. Funct. 15, 259–264. https://doi.org/10.1002/(SICI)1099-0844(199712)15:4%3C259::AID-CBF749%3E3.0.CO;2-D

Cafaro, G., Petito, E., Bistoni, O., Falcinelli, E., Cipriani, S., Borghi, M.C., Bonifacio, A.F., Giglio, E., Alunno, A., Perricone, C., Gerli, R., Gresele, P., Bartoloni, E., 2022. Methotrexate improves endothelial function in early rheumatoid arthritis patients after 3 months of treatment. Arthritis Res Ther 24, 236. https://doi.org/10.1186/s13075-022-02930-7

Campisi, J., Kapahi, P., Lithgow, G.J., Melov, S., Newman, J.C., Verdin, E., 2019. From discoveries in ageing research to therapeutics for healthy ageing. Nature 571, 183–192. https://doi.org/10.1038/s41586-019-1365-2

Camporez, J.P.G., Akamine, E.H., Davel, A.P., Franci, C.R., Rossoni, L.V., De Oliveira Carvalho, C.R., 2011. Dehydroepiandrosterone protects against oxidative stress-induced endothelial dysfunction in ovariectomized rats. The Journal of Physiology 589, 2585–2596. https://doi.org/10.1113/jphysiol.2011.206078

Cantó, C., Houtkooper, R.H., Pirinen, E., Youn, D.Y., Oosterveer, M.H., Cen, Y., Fernandez-Marcos, P.J., Yamamoto, H., Andreux, P.A., Cettour-Rose, P., Gademann, K., Rinsch, C., Schoonjans, K., Sauve, A.A., Auwerx, J., 2012. The NAD+ Precursor Nicotinamide Riboside Enhances Oxidative Metabolism and Protects against High-Fat Diet-Induced Obesity. Cell Metabolism 15, 838–847. https://doi.org/10.1016/j.cmet.2012.04.022

Canugovi, C., Stevenson, M.D., Vendrov, A.E., Hayami, T., Robidoux, J., Xiao, H., Zhang, Y.-Y., Eitzman, D.T., Runge, M.S., Madamanchi, N.R., 2019. Increased mitochondrial NADPH oxidase 4 (NOX4) expression in aging is a causative factor in aortic stiffening. Redox Biology 26, 101288. https://doi.org/10.1016/j.redox.2019.101288

Cao, G., Xuan, X., Hu, J., Zhang, R., Jin, H., Dong, H., 2022. How vascular smooth muscle cell phenotype switching contributes to vascular disease. Cell Commun Signal 20, 180. https://doi.org/10.1186/s12964-022-00993-2

Cappel, D.A., Deja, S., Duarte, J.A.G., Kucejova, B., Iñigo, M., Fletcher, J.A., Fu, X., Berglund, E.D., Liu, T., Elmquist, J.K., Hammer, S., Mishra, P., Browning, J.D., Burgess, S.C., 2019. Pyruvate-Carboxylase-Mediated Anaplerosis Promotes Antioxidant Capacity by Sustaining TCA Cycle and Redox Metabolism in Liver. Cell Metabolism 29, 1291-1305.e8. https://doi.org/10.1016/j.cmet.2019.03.014

Cappelli-Bigazzi, M., Battaglia, C., Pannain, S., Chiariello, M., Ambrosio, G., 1997. Role of oxidative metabolism on endothelium-dependent vascular relaxation of isolated vessels. Journal of Molecular and Cellular Cardiology 29, 871–879. https://doi.org/10.1006/jmcc.1996.0286

Chen, J., Xu, L., Huang, C., 2014. DHEA inhibits vascular remodeling following arterial injury: a possible role in suppression of inflammation and oxidative stress derived from vascular smooth muscle cells. Mol Cell Biochem 388, 75–84. https://doi.org/10.1007/s11010-013-1900-7

Chen, T., Xie, Q., Tan, B., Yi, Q., Xiang, H., Wang, R., Zhou, Q., He, B., Tian, J., Zhu, J., Xu, H., 2024a. Inhibition of Pyruvate Dehydrogenase Kinase 4 Protects Cardiomyocytes from lipopolysaccharide-Induced Mitochondrial Damage by Reducing Lactate Accumulation. Inflammation 47, 1356–1370. https://doi.org/10.1007/s10753-024-01981-z

Chen, T., Ye, L., Zhu, J., Tan, B., Yi, Q., Sun, Y., Xie, Q., Xiang, H., Wang, R., Tian, J., Xu, H., 2024b. Inhibition of Pyruvate Dehydrogenase Kinase 4 Attenuates Myocardial and Mitochondrial Injury in Sepsis-Induced Cardiomyopathy. The Journal of Infectious Diseases 229, 1178–1188. https://doi.org/10.1093/infdis/jiad365

Chung, C.-M., Lin, Y.-S., Chang, S.-T., Cheng, H.-W., Yang, T.-Y., Hsiao, J.-F., Pan, K.-L., Hsu, J.-T., Chu, C.-M., 2012. Arterial Stiffness Is the Independent Factor of Left Ventricular Hypertrophy Determined by Electrocardiogram. The American Journal of the Medical Sciences 344, 190–193. https://doi.org/10.1097/MAJ.0b013e318242a354

Consitt, L.A., Saxena, G., Saneda, A., Houmard, J.A., 2016. Age-related impairments in skeletal muscle PDH phosphorylation and plasma lactate are indicative of metabolic inflexibility and the effects of exercise training. American Journal of Physiology-Endocrinology and Metabolism 311, E145–E156. https://doi.org/10.1152/ajpendo.00452.2015

Csiszar, A., Labinskyy, N., Jimenez, R., Pinto, J.T., Ballabh, P., Losonczy, G., Pearson, K.J., De Cabo, R., Ungvari, Z., 2009. Anti-oxidative and anti-inflammatory vasoprotective effects of caloric restriction in aging: Role of circulating factors and SIRT1. Mechanisms of Ageing and Development 130, 518–527. https://doi.org/10.1016/j.mad.2009.06.004

Csiszar, A., Tarantini, S., Yabluchanskiy, A., Balasubramanian, P., Kiss, T., Farkas, E., Baur, J.A., Ungvari, Z., 2019. Role of endothelial NAD $^{+}$ deficiency in age-related vascular dysfunction. American Journal of Physiology-Heart and Circulatory Physiology 316, H1253–H1266. https://doi.org/10.1152/ajpheart.00039.2019

Csonka, C., Páli, T., Bencsik, P., Görbe, A., Ferdinandy, P., Csont, T., 2015. Measurement of NO in biological samples. British J Pharmacology 172, 1620–1632. https://doi.org/10.1111/bph.12832

Culic, O., Gruwel, M.L., Schrader, J., 1997. Energy turnover of vascular endothelial cells. American Journal of Physiology-Cell Physiology 273, C205–C213. https://doi.org/10.1152/ajpcell.1997.273.1.C205

Dabertrand, F., Harraz, O.F., Koide, M., Longden, T.A., Rosehart, A.C., Hill-Eubanks, D.C., Joutel, A., Nelson, M.T., 2021. PIP $_2$ corrects cerebral blood flow deficits in small vessel disease by rescuing capillary Kir2.1 activity. Proc. Natl. Acad. Sci. U.S.A. 118, e2025998118. https://doi.org/10.1073/pnas.2025998118

Daiber, A., Chlopicki, S., 2020. Revisiting pharmacology of oxidative stress and endothelial dysfunction in cardiovascular disease: Evidence for redox-based therapies. Free Radical Biology and Medicine 157, 15–37. https://doi.org/10.1016/j.freeradbiomed.2020.02.026

De Bock, K., Georgiadou, M., Schoors, S., Kuchnio, A., Wong, B.W., Cantelmo, A.R., Quaegebeur, A., Ghesquière, B., Cauwenberghs, S., Eelen, G., Phng, L.-K., Betz, I., Tembuyser, B., Brepoels, K., Welti, J., Geudens, I., Segura, I., Cruys, B., Bifari, F., Decimo, I., Blanco, R., Wyns, S., Vangindertael, J., Rocha, S., Collins, R.T., Munck, S., Daelemans, D., Imamura, H., Devlieger, R., Rider, M., Van Veldhoven, P.P., Schuit, F., Bartrons, R., Hofkens, J., Fraisl, P., Telang, S., DeBerardinis, R.J., Schoonjans, L., Vinckier, S., Chesney, J., Gerhardt, H., Dewerchin, M., Carmeliet, P., 2013. Role of PFKFB3-Driven Glycolysis in Vessel Sprouting. Cell 154, 651–663. https://doi.org/10.1016/j.cell.2013.06.037

De Bock, K., Georgiadou, M., Carmeliet, P., 2013. Role of Endothelial Cell Metabolism in Vessel Sprouting. Cell Metabolism 18, 634–647. https://doi.org/10.1016/j.cmet.2013.08.001

Deyab, G., Hokstad, I., Whist, J.E., Smastuen, M.C., Agewall, S., Lyberg, T., Ronda, N., Mikkelsen, K., Hjeltnes, G., Hollan, I., 2017. Methotrexate and anti-tumor necrosis factor treatment improves endothelial function in patients with inflammatory arthritis. Arthritis Res Ther 19, 232. https://doi.org/10.1186/s13075-017-1439-1

Dobrina, A., Rossi, F., 1983. Metabolic properties of freshly isolated bovine endothelial cells. Biochimica et Biophysica Acta (BBA) - Molecular Cell Research 762, 295–301. https://doi.org/10.1016/0167-4889(83)90084-8

Donato, A.J., Eskurza, I., Silver, A.E., Levy, A.S., Pierce, G.L., Gates, P.E., Seals, D.R., 2007. Direct Evidence of Endothelial Oxidative Stress With Aging in Humans: Relation to Impaired Endothelium-Dependent Dilation and Upregulation of Nuclear Factor-κB. Circulation Research 100, 1659–1666. https://doi.org/10.1161/01.RES.0000269183.13937.e8

Donato, A.J., Gano, L.B., Eskurza, I., Silver, A.E., Gates, P.E., Jablonski, K., Seals, D.R., 2009. Vascular endothelial dysfunction with aging: endothelin-1 and endothelial nitric oxide

synthase. American Journal of Physiology-Heart and Circulatory Physiology 297, H425–H432. https://doi.org/10.1152/ajpheart.00689.2008

Doran, A.C., 2022. Inflammation Resolution: Implications for Atherosclerosis. Circulation Research 130, 130–148. https://doi.org/10.1161/CIRCRESAHA.121.319822

Eskurza, I., Monahan, K.D., Robinson, J.A., Seals, D.R., 2004. Effect of acute and chronic ascorbic acid on flow-mediated dilatation with sedentary and physically active human ageing. The Journal of Physiology 556, 315–324. https://doi.org/10.1113/jphysiol.2003.057042

Fabbri, E., An, Y., Zoli, M., Simonsick, E.M., Guralnik, J.M., Bandinelli, S., Boyd, C.M., Ferrucci, L., 2015. Aging and the Burden of Multimorbidity: Associations With Inflammatory and Anabolic Hormonal Biomarkers. The Journals of Gerontology: Series A 70, 63–70. https://doi.org/10.1093/gerona/glu127

Fan, T.W.M., Bruntz, R.C., Yang, Y., Song, H., Chernyavskaya, Y., Deng, P., Zhang, Y., Shah, P.P., Beverly, L.J., Qi, Z., Mahan, A.L., Higashi, R.M., Dang, C.V., Lane, A.N., 2019. De novo synthesis of serine and glycine fuels purine nucleotide biosynthesis in human lung cancer tissues. Journal of Biological Chemistry 294, 13464–13477. https://doi.org/10.1074/jbc.RA119.008743

Fink, B., Dikalov, S., Fink, N., 2006. ESR techniques for the detection of nitric oxide in vivo as an index of endothelial function. Pharmacological Reports.

Fleenor, B.S., 2012. Large Elastic Artery Stiffness with Aging: Novel Translational Mechanisms and Interventions. Aging Dis. 4, 76–83.

Fleenor, B.S., Seals, D.R., Zigler, M.L., Sindler, A.L., 2012. Superoxide-lowering therapy with TEMPOL reverses arterial dysfunction with aging in mice. Aging Cell 11, 269–276. https://doi.org/10.1111/j.1474-9726.2011.00783.x

Fontana, L., Kennedy, B.K., Longo, V.D., Seals, D., Melov, S., 2014. Medical research: Treat ageing. Nature 511, 405–407. https://doi.org/10.1038/511405a

Foote, K., Reinhold, J., Yu, E.P.K., Figg, N.L., Finigan, A., Murphy, M.P., Bennett, M.R., 2018. Restoring mitochondrial DNA copy number preserves mitochondrial function and delays vascular aging in mice. Aging Cell 17, e12773. https://doi.org/10.1111/acel.12773

Forteza, M.J., Berg, M., Edsfeldt, A., Sun, J., Baumgartner, R., Kareinen, I., Casagrande, F.B., Hedin, U., Zhang, S., Vuckovic, I., Dzeja, P.P., Polyzos, K.A., Gisterå, A., Trauelsen, M., Schwartz, T.W., Dib, L., Herrmann, J., Monaco, C., Matic, L., Gonçalves, I., Ketelhuth, D.F.J., 2023. Pyruvate dehydrogenase kinase regulates vascular inflammation in atherosclerosis and increases cardiovascular risk. Cardiovascular Research 119, 1524–1536. https://doi.org/10.1093/cvr/cvad038

Franceschi, C., Garagnani, P., Parini, P., Giuliani, C., Santoro, A., 2018. Inflammaging: a new immune–metabolic viewpoint for age-related diseases. Nat Rev Endocrinol 14, 576–590. https://doi.org/10.1038/s41574-018-0059-4

Fu, A., Alvarez-Perez, J.C., Avizonis, D., Kin, T., Ficarro, S.B., Choi, D.W., Karakose, E., Badur, M.G., Evans, L., Rosselot, C., Bridon, G., Bird, G.H., Seo, H.-S., Dhe-Paganon, S., Kamphorst, J.J., Stewart, A.F., James Shapiro, A.M., Marto, J.A., Walensky, L.D., Jones, R.G., Garcia-Ocana, A., Danial, N.N., 2020. Glucose-dependent partitioning of

arginine to the urea cycle protects β-cells from inflammation. Nat Metab 2, 432–446. https://doi.org/10.1038/s42255-020-0199-4

Fullerton, J.N., Gilroy, D.W., 2016. Resolution of inflammation: a new therapeutic frontier. Nat Rev Drug Discov 15, 551–567. https://doi.org/10.1038/nrd.2016.39

Furchgott, R.F., 1983. Role of endothelium in responses of vascular smooth muscle. Circulation Research 53, 557–573. https://doi.org/10.1161/01.RES.53.5.557

Furman, D., Campisi, J., Verdin, E., Carrera-Bastos, P., Targ, S., Franceschi, C., Ferrucci, L., Gilroy, D.W., Fasano, A., Miller, G.W., Miller, A.H., Mantovani, A., Weyand, C.M., Barzilai, N., Goronzy, J.J., Rando, T.A., Effros, R.B., Lucia, A., Kleinstreuer, N., Slavich, G.M., 2019. Chronic inflammation in the etiology of disease across the life span. Nat Med 25, 1822–1832. https://doi.org/10.1038/s41591-019-0675-0

Gioscia-Ryan, R.A., LaRocca, T.J., Sindler, A.L., Zigler, M.C., Murphy, M.P., Seals, D.R., 2014. Mitochondria-targeted antioxidant (MitoQ) ameliorates age-related arterial endothelial dysfunction in mice. Journal of Physiology 592, 2549–2561. https://doi.org/10.1113/jphysiol.2013.268680

Gomes, A.P., Price, N.L., Ling, A.J.Y., Moslehi, J.J., Montgomery, M.K., Rajman, L., White, J.P., Teodoro, J.S., Wrann, C.D., Hubbard, B.P., Mercken, E.M., Palmeira, C.M., de Cabo, R., Rolo, A.P., Turner, N., Bell, E.L., Sinclair, D.A., 2013a. Declining NAD+ Induces a Pseudohypoxic State Disrupting Nuclear-Mitochondrial Communication during Aging. Cell 155, 1624–1638. https://doi.org/10.1016/j.cell.2013.11.037

Gomes, A.P., Price, N.L., Ling, A.J.Y., Moslehi, J.J., Montgomery, M.K., Rajman, L., White, J.P., Teodoro, J.S., Wrann, C.D., Hubbard, B.P., Mercken, E.M., Palmeira, C.M., de Cabo, R., Rolo, A.P., Turner, N., Bell, E.L., Sinclair, D.A., 2013b. Declining NAD+ Induces a Pseudohypoxic State Disrupting Nuclear-Mitochondrial Communication during Aging. Cell 155, 1624–1638. https://doi.org/10.1016/j.cell.2013.11.037

Griffith, T.M., Edwards, D.H., Henderson, A.H., 1987. Unstimulated release of endothelium derived relaxing factor is independent of mitochondrial ATP generation. Cardiovascular Research 21, 565–568. https://doi.org/10.1093/cvr/21.8.565

Griffith, T.M., Edwards, D.H., Newby, A.C., Lewis, M.J., Henderson, A.H., 1986. Production of endothelium derived relaxant factor is dependent on oxidative phosphorylation and extracellular calcium. Cardiovascular Research 20, 7–12. https://doi.org/10.1093/cvr/20.1.7

Gryglewski, R.J., Bunting, S., Moncada, S., Flower, R.J., Vane, J.R., 1976. Arterial walls are protected against deposition of platelet thrombi by a substance (prostaglandin X) which they make from prostaglandin endoperoxides. Prostaglandins 12, 685–713. https://doi.org/10.1016/0090-6980(76)90047-2

Haas, R., Cucchi, D., Smith, J., Pucino, V., Macdougall, C.E., Mauro, C., 2016. Intermediates of Metabolism: From Bystanders to Signalling Molecules. Trends in Biochemical Sciences 41, 460–471. https://doi.org/10.1016/j.tibs.2016.02.003

Han, B., Zhang, YiXuan, Liu, C., Ji, P., Xing, Z., Geng, X., Chi, K., Gong, M., Li, Y., Zhang, Ying, Fu, Z., Hong, Q., Cai, G., Chen, X., Sun, X., 2024. Renal inflammation combined with renal function reserve reduction accelerate kidney aging via pentose phosphate pathway. iScience 27, 110045. https://doi.org/10.1016/j.isci.2024.110045

Harman, D., 1972. The Biologic Clock: The Mitochondria? J American Geriatrics Society 20, 145–147. https://doi.org/10.1111/j.1532-5415.1972.tb00787.x

Harman, D., 1956. Aging: A Theory Based on Free Radical and Radiation Chemistry. Journal of Gerontology 11, 298–300. https://doi.org/10.1093/geronj/11.3.298

Hattori, Y., Campbell, E.B., Gross, S.S., 1994. Argininosuccinate synthetase mRNA and activity are induced by immunostimulants in vascular smooth muscle. Role in the regeneration or arginine for nitric oxide synthesis. Journal of Biological Chemistry 269, 9405–9408. https://doi.org/10.1016/S0021-9258(17)36893-X

He, W., Ding, C., Lin, T., Wang, B., Wang, W., Deng, Z., Jin, T., Shang, Y., Zheng, D., Bai, T., Zhang, M., Li, R., Jin, J., He, Q., 2024. An enzyme-mimicking reactive oxygen species scavenger targeting oxidative stress-inflammation cycle ameliorates IR-AKI by inhibiting pyruvate dehydrogenase kinase 4. Theranostics 14, 7534–7553. https://doi.org/10.7150/thno.101229

Hecker, M., Sessa, W.C., Harris, H.J., Änggård, E.E., Vane, J.R., 1990. The Metabolism of L-Arginine and Its Significance for the Biosynthesis of Endothelium-Derived Relaxing Factor: Cultured Endothelial Cells Recycle L- Citrulline to L-Arginine. Proceedings of the National Academy of Sciences of the United States of America 87, 8612–8616.

Herzig, S., Shaw, R.J., 2018. AMPK: guardian of metabolism and mitochondrial homeostasis. Nat Rev Mol Cell Biol 19, 121–135. https://doi.org/10.1038/nrm.2017.95

Hogg, N., 2010. Detection of nitric oxide by electron paramagnetic resonance spectroscopy. Free Radical Biology and Medicine 49, 122–129. https://doi.org/10.1016/j.freeradbiomed.2010.03.009

Huerta-García, E., Ventura-Gallegos, J.L., Victoriano, Ma.E.C., Montiél-Dávalos, A., Tinoco-Jaramillo, G., López-Marure, R., 2012. Dehydroepiandrosterone inhibits the activation and dysfunction of endothelial cells induced by high glucose concentration. Steroids 77, 233–240. https://doi.org/10.1016/j.steroids.2011.11.010

Joannides, R., Haefeli, W.E., Linder, L., Richard, V., Bakkali, E.H., Thuillez, C., Lüscher, T.F., 1995. Nitric Oxide Is Responsible for Flow-Dependent Dilatation of Human Peripheral Conduit Arteries In Vivo. Circulation 91, 1314–1319. https://doi.org/10.1161/01.CIR.91.5.1314

Junaid, A., Schoeman, J., Yang, W., Stam, W., Mashaghi, A., van Zonneveld, A.J., Hankemeier, T., 2020. Metabolic response of blood vessels to TNFα. eLife 9, 1–28. https://doi.org/10.7554/eLife.54754

Kaczara, P., Czyzynska-Cichon, I., Kus, E., Kurpinska, A., Olkowicz, M., Wojnar-Lason, K., Pacia, M.Z., Lytvynenko, O., Baes, M., Chlopicki, S., 2024. Liver sinusoidal endothelial cells rely on oxidative phosphorylation but avoid processing long-chain fatty acids in their mitochondria. Cell Mol Biol Lett 29, 67. https://doi.org/10.1186/s11658-024-00584-8

Kalapos, M.P., 2008. The tandem of free radicals and methylglyoxal. Chemico-Biological Interactions 171, 251–271. https://doi.org/10.1016/j.cbi.2007.11.009

Kalucka, J., De Rooij, L.P.M.H., Goveia, J., Rohlenova, K., Dumas, S.J., Meta, E., Conchinha, N.V., Taverna, F., Teuwen, L.-A., Veys, K., García-Caballero, M., Khan, S., Geldhof, V., Sokol, L., Chen, R., Treps, L., Borri, M., De Zeeuw, P., Dubois, C., Karakach, T.K., Falkenberg, K.D., Parys, M., Yin, X., Vinckier, S., Du, Y., Fenton, R.A., Schoonjans,

L., Dewerchin, M., Eelen, G., Thienpont, B., Lin, L., Bolund, L., Li, X., Luo, Y., Carmeliet, P., 2020. Single-Cell Transcriptome Atlas of Murine Endothelial Cells. Cell 180, 764-779.e20. https://doi.org/10.1016/j.cell.2020.01.015

Kamper, A.M., Spilt, A., De Craen, A.J.M., Van Buchem, M.A., Westendorp, R.G.J., Blauw, G.J., 2004. Basal cerebral blood flow is dependent on the nitric oxide pathway in elderly but not in young healthy men. Experimental Gerontology 39, 1245–1248. https://doi.org/10.1016/j.exger.2004.04.001

Karaś, A., Bar, A., Pandian, K., Jasztal, A., Kuryłowicz, Z., Kutryb-Zając, B., Buczek, E., Rocchetti, S., Mohaissen, T., Jędrzejewska, A., Harms, A.C., Kaczara, P., Chłopicki, S., 2024. Functional deterioration of vascular mitochondrial and glycolytic capacity in the aortic rings of aged mice. GeroScience 46, 3831–3844. https://doi.org/10.1007/s11357-024-01091-6

Khang, A.R., Kim, D.H., Kim, M.-J., Oh, C.J., Jeon, J.-H., Choi, S.H., Lee, I.-K., 2024. Reducing Oxidative Stress and Inflammation by Pyruvate Dehydrogenase Kinase 4 Inhibition Is Important in Prevention of Renal Ischemia-Reperfusion Injury in Diabetic Mice. Diabetes Metab J 48, 405–417. https://doi.org/10.4093/dmj.2023.0196

Khoo, J.P., Alp, N.J., Bendall, J.K., Kawashima, S., Yokoyama, M., Zhang, Y.-H., Casadei, B., Channon, K.M., 2004. EPR quantification of vascular nitric oxide production in genetically modified mouse models. Nitric Oxide 10, 156–161. https://doi.org/10.1016/j.niox.2004.04.003

Kim, J.H., Bugaj, L.J., Oh, Y.J., Bivalacqua, T.J., Ryoo, S., Soucy, K.G., Santhanam, L., Webb, A., Camara, A., Sikka, G., Nyhan, D., Shoukas, A.A., Ilies, M., Christianson, D.W., Champion, H.C., Berkowitz, D.E., 2009. Arginase inhibition restores NOS coupling and reverses endothelial dysfunction and vascular stiffness in old rats. Journal of Applied Physiology 107, 1249–1257. https://doi.org/10.1152/japplphysiol.91393.2008

Kiss, T., Giles, C.B., Tarantini, S., Yabluchanskiy, A., Balasubramanian, P., Gautam, T., Csipo, T., Nyúl-Tóth, Á., Lipecz, A., Szabo, C., Farkas, E., Wren, J.D., Csiszar, A., Ungvari, Z., 2019. Nicotinamide mononucleotide (NMN) supplementation promotes anti-aging miRNA expression profile in the aorta of aged mice, predicting epigenetic rejuvenation and anti-atherogenic effects. GeroScience 41, 419–439. https://doi.org/10.1007/s11357-019-00095-x

Krüger-Genge, A., Blocki, A., Franke, R.-P., Jung, F., 2019. Vascular Endothelial Cell Biology: An Update. IJMS 20, 4411. https://doi.org/10.3390/ijms20184411

Kutryb-Zając, B., Kawecka, A., Nasadiuk, K., Braczko, A., Stawarska, K., Caiazzo, E., Koszałka, P., Cicala, C., 2023. Drugs targeting adenosine signaling pathways: A current view. Biomedicine & Pharmacotherapy 165, 115184. https://doi.org/10.1016/j.biopha.2023.115184

Lacorre, D.-A., Baekkevold, E.S., Garrido, I., Brandtzaeg, P., Haraldsen, G., Amalric, F., Girard, J.-P., 2004. Plasticity of endothelial cells: rapid dedifferentiation of freshly isolated high endothelial venule endothelial cells outside the lymphoid tissue microenvironment. Blood 103, 4164–4172. https://doi.org/10.1182/blood-2003-10-3537

Lakatta, E.G., Levy, D., 2003. Arterial and Cardiac Aging: Major Shareholders in Cardiovascular Disease Enterprises: Part I: Aging Arteries: A “Set Up” for Vascular

Disease. Circulation 107, 139–146. https://doi.org/10.1161/01.CIR.0000048892.83521.58

LaRocca, T.J., Hearon, C.M., Henson, G.D., Seals, D.R., 2014a. Mitochondrial quality control and age-associated arterial stiffening. Experimental Gerontology 58, 78–82. https://doi.org/10.1016/j.exger.2014.07.008

LaRocca, T.J., Hearon, C.M., Henson, G.D., Seals, D.R., 2014b. Mitochondrial quality control and age-associated arterial stiffening. Experimental Gerontology 58, 78–82. https://doi.org/10.1016/j.exger.2014.07.008

Larocca, T.J., Henson, G.D., Thorburn, A., Sindler, A.L., Pierce, G.L., Seals, D.R., 2012. Translational evidence that impaired autophagy contributes to arterial ageing. Journal of Physiology 590, 3305–3316. https://doi.org/10.1113/jphysiol.2012.229690

Lee, H.J., Howell, S.K., Sanford, R.J., Beisswenger, P.J., 2005. Methylglyoxal Can Modify GAPDH Activity and Structure. Annals of the New York Academy of Sciences 1043, 135–145. https://doi.org/10.1196/annals.1333.017

Lee, S.J., Jeong, J.Y., Oh, C.J., Park, S., Kim, J.-Y., Kim, H.-J., Doo Kim, N., Choi, Y.-K., Do, J.-Y., Go, Y., Ha, C.-M., Choi, J.-Y., Huh, S., Ho Jeoung, N., Lee, K.-U., Choi, H.-S., Wang, Y., Park, K.-G., Harris, R.A., Lee, I.-K., 2015. Pyruvate Dehydrogenase Kinase 4 Promotes Vascular Calcification via SMAD1/5/8 Phosphorylation. Sci Rep 5, 16577. https://doi.org/10.1038/srep16577

Leopold, J.A., Zhang, Y.-Y., Scribner, A.W., Stanton, R.C., Loscalzo, J., 2003. Glucose-6-Phosphate Dehydrogenase Overexpression Decreases Endothelial Cell Oxidant Stress and Increases Bioavailable Nitric Oxide. ATVB 23, 411–417. https://doi.org/10.1161/01.ATV.0000056744.26901.BA

Li, W., Mital, S., Ojaimi, C., Csiszar, A., Kaley, G., Hintze, T.H., 2004. Premature death and age-related cardiac dysfunction in male eNOS-knockout mice. Journal of Molecular and Cellular Cardiology 37, 671–680. https://doi.org/10.1016/j.yjmcc.2004.05.005

Li, X., Sun, X., Carmeliet, P., 2019. Hallmarks of Endothelial Cell Metabolism in Health and Disease. Cell Metabolism 30, 414–433. https://doi.org/10.1016/j.cmet.2019.08.011

Libby, P., 2017. Interleukin-1 Beta as a Target for Atherosclerosis Therapy: Biological Basis of CANTOS and Beyond. Journal of the American College of Cardiology 70, 2278–2289. https://doi.org/10.1016/j.jacc.2017.09.028

Linden, J., Koch-Nolte, F., Dahl, G., 2019. Purine Release, Metabolism, and Signaling in the Inflammatory Response. Annu. Rev. Immunol. 37, 325–347. https://doi.org/10.1146/annurev-immunol-051116-052406

Lohman, A.W., Billaud, M., Isakson, B.E., 2012. Mechanisms of ATP release and signalling in the blood vessel wall. Cardiovascular Research 95, 269–280. https://doi.org/10.1093/cvr/cvs187

López-Otín, C., Blasco, M.A., Partridge, L., Serrano, M., Kroemer, G., 2023. Hallmarks of aging: An expanding universe. Cell 186, 243–278. https://doi.org/10.1016/j.cell.2022.11.001

Marin-Valencia, I., Roe, C.R., Pascual, J.M., 2010. Pyruvate carboxylase deficiency: Mechanisms, mimics and anaplerosis. Molecular Genetics and Metabolism 101, 9–17. https://doi.org/10.1016/j.ymgme.2010.05.004

Martin, S.S., Aday, A.W., Almarzooq, Z.I., Anderson, C.A.M., Arora, P., Avery, C.L., Baker-Smith, C.M., Barone Gibbs, B., Beaton, A.Z., Boehme, A.K., Commodore-Mensah, Y., Currie, M.E., Elkind, M.S.V., Evenson, K.R., Generoso, G., Heard, D.G., Hiremath, S., Johansen, M.C., Kalani, R., Kazi, D.S., Ko, D., Liu, J., Magnani, J.W., Michos, E.D., Mussolino, M.E., Navaneethan, S.D., Parikh, N.I., Perman, S.M., Poudel, R., Rezk-Hanna, M., Roth, G.A., Shah, N.S., St-Onge, M.-P., Thacker, E.L., Tsao, C.W., Urbut, S.M., Van Spall, H.G.C., Voeks, J.H., Wang, N.-Y., Wong, N.D., Wong, S.S., Yaffe, K., Palaniappan, L.P., on behalf of the American Heart Association Council on Epidemiology and Prevention Statistics Committee and Stroke Statistics Subcommittee, 2024. 2024 Heart Disease and Stroke Statistics: A Report of US and Global Data From the American Heart Association. Circulation 149. https://doi.org/10.1161/CIR.0000000000001209

Massudi, H., Grant, R., Braidy, N., Guest, J., Farnsworth, B., Guillemin, G.J., 2012. Age-Associated Changes In Oxidative Stress and NAD+ Metabolism In Human Tissue. PLoS ONE 7, e42357. https://doi.org/10.1371/journal.pone.0042357

Mateuszuk, Ł., Campagna, R., Kutryb-zając, B., Kuś, K., Słominska, E.M., Smolenski, R.T., Chlopicki, S., Centre, J., Jcet, T., 2020. Reversal of endothelial dysfunction by nicotinamide mononucleotide via extracellular conversion to nicotinamide riboside. Biochemical Pharmacology 178, 114019. https://doi.org/10.1016/j.bcp.2020.114019

Matsui, R., Xu, S., Maitland, K.A., Hayes, A., Leopold, J.A., Handy, D.E., Loscalzo, J., Cohen, R.A., 2005. Glucose-6 Phosphate Dehydrogenase Deficiency Decreases the Vascular Response to Angiotensin II. Circulation 112, 257–263. https://doi.org/10.1161/CIRCULATIONAHA.104.499095

Mitchell, G.F., 2008. Effects of central arterial aging on the structure and function of the peripheral vasculature: implications for end-organ damage. Journal of Applied Physiology 105, 1652–1660. https://doi.org/10.1152/japplphysiol.90549.2008

Mitchell, G.F., Hwang, S.-J., Vasan, R.S., Larson, M.G., Pencina, M.J., Hamburg, N.M., Vita, J.A., Levy, D., Benjamin, E.J., 2010. Arterial Stiffness and Cardiovascular Events: The Framingham Heart Study. Circulation 121, 505–511. https://doi.org/10.1161/CIRCULATIONAHA.109.886655

Moncada, S., Gryglewski, R., Bunting, S., Vane, J.R., 1976. An enzyme isolated from arteries transforms prostaglandin endoperoxides to an unstable substance that inhibits platelet aggregation. Nature 263, 663–665. https://doi.org/10.1038/263663a0

Morita, M., Gravel, S.-P., Hulea, L., Larsson, O., Pollak, M., St-Pierre, J., Topisirovic, I., 2015. mTOR coordinates protein synthesis, mitochondrial activity and proliferation. Cell Cycle 14, 473–480. https://doi.org/10.4161/15384101.2014.991572

Mouchiroud, L., Houtkooper, R.H., Moullan, N., Katsyuba, E., Ryu, D., Cantó, C., Mottis, A., Jo, Y.-S., Viswanathan, M., Schoonjans, K., Guarente, L., Auwerx, J., 2013. The NAD+/Sirtuin Pathway Modulates Longevity through Activation of Mitochondrial UPR and FOXO Signaling. Cell 154, 430–441. https://doi.org/10.1016/j.cell.2013.06.016

Murad, F., 1994. The Nitric Oxide–Cyclic GMP Signal Transduction System for Intracellular and Intercellular Communication, in: Proceedings of the 1992 Laurentian Hormone

Conference. Elsevier, pp. 239–248. https://doi.org/10.1016/B978-0-12-571149-4.50016-7

Nakai, N., Sato, Y., Oshida, Y., Yoshimura, A., Fujitsuka, N., Sugiyama, S., Shimomura, Y., 1997. Effects of aging on the activities of pyruvate dehydrogenase complex and its kinase in rat heart. Life Sciences 60, 2309–2314. https://doi.org/10.1016/S0024-3205(97)00286-5

Netea, M.G., Domínguez-Andrés, J., Barreiro, L.B., Chavakis, T., Divangahi, M., Fuchs, E., Joosten, L.A.B., Van Der Meer, J.W.M., Mhlanga, M.M., Mulder, W.J.M., Riksen, N.P., Schlitzer, A., Schultze, J.L., Stabell Benn, C., Sun, J.C., Xavier, R.J., Latz, E., 2020. Defining trained immunity and its role in health and disease. Nat Rev Immunol 20, 375–388. https://doi.org/10.1038/s41577-020-0285-6

Niccoli, T., Partridge, L., 2012. Ageing as a Risk Factor for Disease. Current Biology 22, R741–R752. https://doi.org/10.1016/j.cub.2012.07.024

Olkowicz, M., Karas, A., Berkowicz, P., Kaczara, P., Jasztal, A., Kurylowicz, Z., Fedak, F., Rosales-Solano, H., Roy, K.S., Kij, A., Buczek, E., Pawliszyn, J., Chlopicki, S., 2024. Upregulation of ALOX12−12-HETE pathway impairs AMPK-dependent modulation of vascular metabolism in ApoE/LDLR−/− mice. Pharmacological Research 210, 107478. https://doi.org/10.1016/j.phrs.2024.107478

Palmer, R.M.J., Ferrige, A.G., Moncada, S., 1987. Nitric oxide release accounts for the biological activity of endothelium-derived relaxing factor. Nature 327, 524–526. https://doi.org/10.1038/327524a0

Pan, H., Xue, C., Auerbach, B.J., Fan, J., Bashore, A.C., Cui, J., Yang, D.Y., Trignano, S.B., Liu, W., Shi, J., Ihuegbu, C.O., Bush, E.C., Worley, J., Vlahos, L., Laise, P., Solomon, R.A., Connolly, E.S., Califano, A., Sims, P.A., Zhang, H., Li, M., Reilly, M.P., 2020. Single-Cell Genomics Reveals a Novel Cell State During Smooth Muscle Cell Phenotypic Switching and Potential Therapeutic Targets for Atherosclerosis in Mouse and Human. Circulation 142, 2060–2075. https://doi.org/10.1161/CIRCULATIONAHA.120.048378

Panagaki, T., Pecze, L., Randi, E.B., Nieminen, A.I., Szabo, C., 2022. Role of the cystathionine β-synthase / H2S pathway in the development of cellular metabolic dysfunction and pseudohypoxia in down syndrome. Redox Biology 55, 102416. https://doi.org/10.1016/j.redox.2022.102416

Pandian, K., Huang, L., Junaid, A., Harms, A.C., Van Zonneveld, A.J., Hankemeier, T., 2023. Tracer-based metabolomics for profiling nitric oxide metabolites in a 3D microvessel-on-a-chip model (preprint). Cell Biology. https://doi.org/10.1101/2023.12.03.569402

Pedraza, A., Sicilia, M.D., Rubio, S., Pérez-Bendito, D., 2006. Pharmaceutical quality control of acid and neutral drugs based on competitive self-assembly in amphiphilic systems. Analyst 131, 81–89. https://doi.org/10.1039/B509978A

Peiró, C., Romacho, T., Azcutia, V., Villalobos, L., Fernández, E., Bolaños, J.P., Moncada, S., Sánchez-Ferrer, C.F., 2016. Inflammation, glucose, and vascular cell damage: the role of the pentose phosphate pathway. Cardiovasc Diabetol 15, 82. https://doi.org/10.1186/s12933-016-0397-2

Pérez, V.I., Bokov, A., Remmen, H.V., Mele, J., Ran, Q., Ikeno, Y., Richardson, A., 2009. Is the oxidative stress theory of aging dead? Biochimica et Biophysica Acta (BBA) - General Subjects 1790, 1005–1014. https://doi.org/10.1016/j.bbagen.2009.06.003

Picciotto, N.E., Gano, L.B., Johnson, L.C., Martens, C.R., Sindler, A.L., Mills, K.F., Imai, S., Seals, D.R., 2016. Nicotinamide mononucleotide supplementation reverses vascular dysfunction and oxidative stress with aging in mice. Aging Cell 15, 522–530. https://doi.org/10.1111/acel.12461

Przyborowski, K., Proniewski, B., Czarny, J., Smeda, M., Sitek, B., Zakrzewska, A., Zoladz, J.A., Chlopicki, S., 2018. Vascular Nitric Oxide–Superoxide Balance and Thrombus Formation after Acute Exercise. Medicine & Science in Sports & Exercise 50, 1405–1412. https://doi.org/10.1249/MSS.0000000000001589

Qiu, H., Zhu, Y., Sun, Z., Trzeciakowski, J.P., Gansner, M., Depre, C., Resuello, R.R.G., Natividad, F.F., Hunter, W.C., Genin, G.M., Elson, E.L., Vatner, D.E., Meininger, G.A., Vatner, S.F., 2010. Short Communication: Vascular Smooth Muscle Cell Stiffness As a Mechanism for Increased Aortic Stiffness With Aging. Circulation Research 107, 615–619. https://doi.org/10.1161/CIRCRESAHA.110.221846

Radi, R., 2013. Peroxynitrite, a Stealthy Biological Oxidant. Journal of Biological Chemistry 288, 26464–26472. https://doi.org/10.1074/jbc.R113.472936

Rajendran, P., Rengarajan, T., Thangavel, J., Nishigaki, Y., Sakthisekaran, D., Sethi, G., Nishigaki, I., 2013. The Vascular Endothelium and Human Diseases. Int. J. Biol. Sci. 9, 1057–1069. https://doi.org/10.7150/ijbs.7502

Ramasamy, R., Vannucci, S.J., Yan, S.S.D., Herold, K., Yan, S.F., Schmidt, A.M., 2005. Advanced glycation end products and RAGE: a common thread in aging, diabetes, neurodegeneration, and inflammation. Glycobiology 15, 16R-28R. https://doi.org/10.1093/glycob/cwi053

Ramasamy, R., Yan, S.F., Schmidt, A.M., 2006. Methylglyoxal Comes of AGE. Cell 124, 258–260. https://doi.org/10.1016/j.cell.2006.01.002

Ray, A., Ch. Maharana, K., Meenakshi, S., Singh, S., 2023. Endothelial dysfunction and its relation in different disorders: Recent update. Health Sciences Review 7, 100084. https://doi.org/10.1016/j.hsr.2023.100084

Ridker, P.M., Cushman, M., Stampfer, M.J., Tracy, R.P., Hennekens, C.H., 1997. Inflammation, Aspirin, and the Risk of Cardiovascular Disease in Apparently Healthy Men. N Engl J Med 336, 973–979. https://doi.org/10.1056/NEJM199704033361401

Ridker, P.M., Thuren, T., Zalewski, A., Libby, P., 2011. Interleukin-1β inhibition and the prevention of recurrent cardiovascular events: Rationale and Design of the Canakinumab Anti-inflammatory Thrombosis Outcomes Study (CANTOS). American Heart Journal 162, 597–605. https://doi.org/10.1016/j.ahj.2011.06.012

Riksen, N.P., Netea, M.G., 2021. Immunometabolic control of trained immunity. Molecular Aspects of Medicine 77, 100897. https://doi.org/10.1016/j.mam.2020.100897

Rodman, D.M., Mallet, J., McMurtry, I.F., 1991. Difference in effect of inhibitors of energy metabolism on endothelium-dependent relaxation of rat pulmonary artery and aorta. American journal of respiratory cell and molecular biology 4, 237–242. https://doi.org/10.1165/ajrcmb/4.3.237

Rom, O., Liu, Y., Finney, A.C., Ghrayeb, A., Zhao, Y., Shukha, Y., Wang, L., Rajanayake, K.K., Das, S., Rashdan, N.A., Weissman, N., Delgadillo, L., Wen, B., Garcia-Barrio, M.T., Aviram, M., Kevil, C.G., Yurdagul, A., Pattillo, C.B., Zhang, J., Sun, D., Hayek, T., Gottlieb, E., Mor, I., Chen, Y.E., 2022. Induction of glutathione biosynthesis by glycine-based treatment mitigates atherosclerosis. Redox Biology 52, 102313. https://doi.org/10.1016/j.redox.2022.102313

Rossman, M.J., LaRocca, T.J., Martens, C.R., Seals, D.R., 2018. Healthy lifestyle-based approaches for successful vascular aging. Journal of Applied Physiology 125, 1888–1900. https://doi.org/10.1152/japplphysiol.00521.2018

Saarti, M., Almukhtar, H., Smith, P.A., Roberts, R.E., 2021. Effect of mitochondrial complex III inhibitors on the regulation of vascular tone in porcine coronary artery. European Journal of Pharmacology 896, 173917. https://doi.org/10.1016/j.ejphar.2021.173917

Savio, L.E.B., Leite-Aguiar, R., Alves, V.S., Coutinho-Silva, R., Wyse, A.T.S., 2021. Purinergic signaling in the modulation of redox biology. Redox Biology 47, 102137. https://doi.org/10.1016/j.redox.2021.102137

Schmidt, K., Windler, R., De Wit, C., 2016. Communication Through Gap Junctions in the Endothelium, in: Advances in Pharmacology. Elsevier, pp. 209–240. https://doi.org/10.1016/bs.apha.2016.04.004

Schnitzler, J.G., Hoogeveen, R.M., Ali, L., Prange, K.H.M., Waissi, F., van Weeghel, M., Bachmann, J.C., Versloot, M., Borrelli, M.J., Yeang, C., De Kleijn, D.P.V., Houtkooper, R.H., Koschinsky, M.L., de Winther, M.P.J., Groen, A.K., Witztum, J.L., Tsimikas, S., Stroes, E.S.G., Kroon, J., 2020. Atherogenic Lipoprotein(a) Increases Vascular Glycolysis, Thereby Facilitating Inflammation and Leukocyte Extravasation. Circulation Research 126, 1346–1359. https://doi.org/10.1161/CIRCRESAHA.119.316206

Segal, J., Ingbar, S.H., 1982. A postulated mechanism for the coordinate effects of ionophore A23187 on calcium uptake and cell viability in rat thymocytes. Biochimica et Biophysica Acta (BBA) - Biomembranes 684, 7–11. https://doi.org/10.1016/0005-2736(82)90042-6

Seifert, R., Burde, R., Schultz, G., 1989. Activation of NADPH oxidase by purine and pyrimidine nucleotides involves G proteins and is potentiated by chemotactic peptides. Biochemical Journal 259, 813–819. https://doi.org/10.1042/bj2590813

Sekhar, R.V., McKay, S.V., Patel, S.G., Guthikonda, A.P., Reddy, V.T., Balasubramanyam, A., Jahoor, F., 2011. Glutathione Synthesis Is Diminished in Patients With Uncontrolled Diabetes and Restored by Dietary Supplementation With Cysteine and Glycine. Diabetes Care 34, 162–167. https://doi.org/10.2337/dc10-1006

Selen, E.S., Rodriguez, S., Cavagnini, K.S., Kim, H.-B., Na, C.H., Wolfgang, M.J., 2022. Requirement of hepatic pyruvate carboxylase during fasting, high fat, and ketogenic diet. Journal of Biological Chemistry 298, 102648. https://doi.org/10.1016/j.jbc.2022.102648

Sendama, W., 2020. The effect of ageing on the resolution of inflammation. Ageing Research Reviews 57, 101000. https://doi.org/10.1016/j.arr.2019.101000

Shi, J., Yang, Y., Cheng, A., Xu, G., He, F., 2020. Metabolism of vascular smooth muscle cells in vascular diseases. American Journal of Physiology-Heart and Circulatory Physiology 319, H613–H631. https://doi.org/10.1152/ajpheart.00220.2020

Shiva, S., Gladwin, M.T., 2007. Cross-Talk between the Red Blood Cell and the Endothelium: Nitric Oxide as a Paracrine and Endocrine Regulator of Vascular Tone, in: Aird, W.C. (Ed.), Endothelial Biomedicine. Cambridge University Press, pp. 562–575. https://doi.org/10.1017/CBO9780511546198.063

SinhaRoy, S., Banerjee, S., Ray, M., Ray, S., 2005. Possible involvement of glutamic and/or aspartic acid residue(s) and requirement of mitochondrial integrity for the protective effect of creatine against inhibition of cardiac mitochondrial respiration by methylglyoxal. Mol Cell Biochem 271, 167–176. https://doi.org/10.1007/s11010-005-6277-9

Slade, L., Chalker, J., Kuksal, N., Young, A., Gardiner, D., Mailloux, R.J., 2017. Examination of the superoxide/hydrogen peroxide forming and quenching potential of mouse liver mitochondria. Biochimica et Biophysica Acta (BBA) - General Subjects 1861, 1960–1969. https://doi.org/10.1016/j.bbagen.2017.05.010

Spier, S.A., Delp, M.D., Meininger, C.J., Donato, A.J., Ramsey, M.W., Muller-Delp, J.M., 2004. Effects of ageing and exercise training on endothelium-dependent vasodilatation and structure of rat skeletal muscle arterioles. The Journal of Physiology 556, 947–958. https://doi.org/10.1113/jphysiol.2003.060301

Spolarics, Z., Wu, J.-X., 1997. Tumor necrosis factor alpha augments the expression of glucose-6-phosphate dehydrogenase in rat hepatic endothelial and Kupffer cells. Life Sciences 60, 565–571. https://doi.org/10.1016/S0024-3205(96)00641-8

Sprague, A.H., Khalil, R.A., 2009. Inflammatory cytokines in vascular dysfunction and vascular disease. Biochemical Pharmacology 78, 539–552. https://doi.org/10.1016/j.bcp.2009.04.029

Stamm, P., Oelze, M., Steven, S., Kröller-Schön, S., Kvandova, M., Kalinovic, S., Jasztal, A., Kij, A., Kuntic, M., Bayo Jimenez, M.T., Proniewski, B., Li, H., Schulz, E., Chlopicki, S., Daiber, A., Münzel, T., 2021. Direct comparison of inorganic nitrite and nitrate on vascular dysfunction and oxidative damage in experimental arterial hypertension. Nitric Oxide 113–114, 57–69. https://doi.org/10.1016/j.niox.2021.06.001

Sternak, M., Bar, A., Adamski, M.G., Mohaissen, T., Marczyk, B., Kieronska, A., Stojak, M., Kus, K., Tarjus, A., Jaisser, F., Chlopicki, S., 2018. The deletion of endothelial sodium channel a (αENaC) impairs endothelium-dependent vasodilation and endothelial barrier integrity in endotoxemia in Vivo. Frontiers in Pharmacology 9, 1–11. https://doi.org/10.3389/fphar.2018.00178

Taddei, S., Virdis, A., Mattei, P., Ghiadoni, L., Gennari, A., Fasolo, C.B., Sudano, I., Salvetti, A., 1995. Aging and Endothelial Function in Normotensive Subjects and Patients With Essential Hypertension. Circulation 91, 1981–1987. https://doi.org/10.1161/01.CIR.91.7.1981

Tang, E.H.C., Vanhoutte, P.M., 2008. Gap Junction Inhibitors Reduce Endothelium-Dependent Contractions in the Aorta of Spontaneously Hypertensive Rats. J Pharmacol Exp Ther 327, 148–153. https://doi.org/10.1124/jpet.108.140046

Toda, N., 2012. Age-related changes in endothelial function and blood flow regulation. Pharmacology & Therapeutics 133, 159–176. https://doi.org/10.1016/j.pharmthera.2011.10.004

Tyrrell, D.J., Blin, M.G., Song, J., Wood, S.C., Goldstein, D.R., 2020a. Aging impairs mitochondrial function and mitophagy and elevates interleukin 6 within the cerebral vasculature. Journal of the American Heart Association 9. https://doi.org/10.1161/JAHA.120.017820

Tyrrell, D.J., Blin, M.G., Song, J., Wood, S.C., Zhang, M., Beard, D.A., Goldstein, D.R., 2020b. Age-Associated Mitochondrial Dysfunction Accelerates Atherogenesis. Circulation Research 126, 298–314. https://doi.org/10.1161/CIRCRESAHA.119.315644

Ungvari, Z., Tarantini, S., Donato, A.J., Galvan, V., Csiszar, A., 2018. Mechanisms of vascular aging. Circulation Research 123, 849–867. https://doi.org/10.1161/CIRCRESAHA.118.311378

Ungvari, Z., Tarantini, S., Sorond, F., Merkely, B., Csiszar, A., 2020. Mechanisms of Vascular Aging, A Geroscience Perspective. Journal of the American College of Cardiology 75, 931–941. https://doi.org/10.1016/j.jacc.2019.11.061

Vaitkevicius, P.V., Fleg, J.L., Engel, J.H., O'Connor, F.C., Wright, J.G., Lakatta, L.E., Yin, F.C., Lakatta, E.G., 1993. Effects of age and aerobic capacity on arterial stiffness in healthy adults. Circulation 88, 1456–1462. https://doi.org/10.1161/01.CIR.88.4.1456

Vallejo, S., Palacios, E., Romacho, T., Villalobos, L., Peiró, C., Sánchez-Ferrer, C.F., 2014. The interleukin-1 receptor antagonist anakinra improves endothelial dysfunction in streptozotocin-induced diabetic rats. Cardiovasc Diabetol 13, 158. https://doi.org/10.1186/s12933-014-0158-z

Van Der Loo, B., Labugger, R., Skepper, J.N., Bachschmid, M., Kilo, J., Powell, J.M., Palacios-Callender, M., Erusalimsky, J.D., Quaschning, T., Malinski, T., Gygi, D., Ullrich, V., Lüscher, T.F., 2000. Enhanced Peroxynitrite Formation Is Associated with Vascular Aging. The Journal of Experimental Medicine 192, 1731–1744. https://doi.org/10.1084/jem.192.12.1731

Walford, R.L., Harris, S.B., Weindruch, R., 1987. Dietary Restriction and Aging: Historical Phases, Mechanisms and Current Directions. The Journal of Nutrition 117, 1650–1654. https://doi.org/10.1093/jn/117.10.1650

Walker, K.A., Basisty, N., Wilson, D.M., Ferrucci, L., 2022. Connecting aging biology and inflammation in the omics era. Journal of Clinical Investigation 132, e158448. https://doi.org/10.1172/JCI158448

Wang, D., Wang, Q., Yan, G., Qiao, Y., Sun, L., Zhu, B., Tang, C., Gu, Y., 2015. High glucose and interleukin 1β-induced apoptosis in human umbilical vein endothelial cells involves in down-regulation of monocarboxylate transporter 4. Biochemical and Biophysical Research Communications 466, 607–614. https://doi.org/10.1016/j.bbrc.2015.09.016

Wang, H., Liu, J., Wu, L., 2009a. Methylglyoxal-induced mitochondrial dysfunction in vascular smooth muscle cells. Biochemical Pharmacology 77, 1709–1716. https://doi.org/10.1016/j.bcp.2009.02.024

Wang, H., Liu, J., Wu, L., 2009b. Methylglyoxal-induced mitochondrial dysfunction in vascular smooth muscle cells. Biochemical Pharmacology 77, 1709–1716. https://doi.org/10.1016/j.bcp.2009.02.024

Wang, L., Duan, Q., Wang, T., Ahmed, M., Zhang, N., Li, Y., Li, L., Yao, X., 2015. Mitochondrial Respiratory Chain Inhibitors Involved in ROS Production Induced by Acute High Concentrations of Iodide and the Effects of SOD as a Protective Factor. Oxidative Medicine and Cellular Longevity 2015, 1–14. https://doi.org/10.1155/2015/217670

Weir, C.J., Gibson, I.F., Martin, W., 1991. Effects of metabolic inhibitors on endothelium-dependent and endothelium-independent vasodilatation of rat and rabbit aorta. British Journal of Pharmacology 102, 162–166. https://doi.org/10.1111/j.1476-5381.1991.tb12147.x

Wilson, C., Lee, M.D., Buckley, C., Zhang, X., McCarron, J.G., 2023. Mitochondrial ATP Production is Required for Endothelial Cell Control of Vascular Tone. Function 4, zqac063. https://doi.org/10.1093/function/zqac063

Xiao, W., Oldham, W.M., Priolo, C., Pandey, A.K., Loscalzo, J., 2021. Immunometabolic Endothelial Phenotypes: Integrating Inflammation and Glucose Metabolism. Circulation Research 129, 9–29. https://doi.org/10.1161/CIRCRESAHA.120.318805

Xie, N., Zhang, L., Gao, W., Huang, C., Huber, P.E., Zhou, X., Li, C., Shen, G., Zou, B., 2020. NAD+ metabolism: pathophysiologic mechanisms and therapeutic potential. Sig Transduct Target Ther 5, 227. https://doi.org/10.1038/s41392-020-00311-7

Xue, D., Xu, J., McGuire, S.O., Devitre, D., Sun, G.Y., 1999. Studies on the cytosolic phospholipase A2 in immortalized astrocytes (DITNC) revealed new properties of the calcium ionophore, A23187. Neurochemical Research 24, 1285–1291. https://doi.org/10.1023/A:1020981224876

Yaniv, Y., Juhaszova, M., Sollott, S.J., 2013. Age-related changes of myocardial ATP supply and demand mechanisms. Trends in Endocrinology & Metabolism 24, 495–505. https://doi.org/10.1016/j.tem.2013.06.001

Zarou, M.M., Vazquez, A., Vignir Helgason, G., 2021. Folate metabolism: a re-emerging therapeutic target in haematological cancers. Leukemia 35, 1539–1551. https://doi.org/10.1038/s41375-021-01189-2

Zeng, Y., Zhang, X.F., Fu, B.M., Tarbell, J.M., 2018. The Role of Endothelial Surface Glycocalyx in Mechanosensing and Transduction, in: Fu, B.M., Wright, N.T. (Eds.), Molecular, Cellular, and Tissue Engineering of the Vascular System, Advances in Experimental Medicine and Biology. Springer International Publishing, Cham, pp. 1–27. https://doi.org/10.1007/978-3-319-96445-4_1

Zhang, P., Chang, Z., Yang, J., Feng, J., Yu, Y., Pei, Y., Wang, J., Zhao, F., Zhou, R., 2019. Vasorelaxation effect of 18β-glycyrrhetinic acid on the thoracic aorta of rats: proposed mechanism.

Zhang, S., Hulver, M.W., McMillan, R.P., Cline, M.A., Gilbert, E.R., 2014. The pivotal role of pyruvate dehydrogenase kinases in metabolic flexibility. Nutr Metab (Lond) 11, 10. https://doi.org/10.1186/1743-7075-11-10

Zhang, X., Zheng, B., Zhao, L., Shen, J., Yang, Z., Zhang, Y., Fan, R., Zhang, M., Ma, D., Zheng, L., Zhao, M., Liu, H., Wen, J., 2022. KLF4-PFKFB3-driven glycolysis is essential for phenotypic switching of vascular smooth muscle cells. Commun Biol 5, 1332. https://doi.org/10.1038/s42003-022-04302-y

Zhao, L., Jia, Y., Yan, D., Zhou, C., Han, J., Yu, J., 2013. Aging-related changes of triose phosphate isomerase in hippocampus of senescence accelerated mouse and the intervention of acupuncture. Neuroscience Letters 542, 59–64. https://doi.org/10.1016/j.neulet.2013.03.002

Zhou, X., Zhang, Y., He, L., Wan, D., Liu, G., Wu, X., Yin, Y., 2017. Serine prevents LPS-induced intestinal inflammation and barrier damage via p53-dependent glutathione synthesis and AMPK activation. Journal of Functional Foods 39, 225–232. https://doi.org/10.1016/j.jff.2017.10.026

Zuhra, K., Szabo, C., 2022. The two faces of cyanide: an environmental toxin and a potential novel mammalian gasotransmitter. The FEBS Journal 289, 2481–2515. https://doi.org/10.1111/febs.16135

Acknowledgement:

Figures 1, 2, 3, 28, 44, and 45 were created with Biorender.com.

VIII. LIST OF PHD CANDIDATE'S PUBLICATIONS

Publications related to this doctoral thesis:

1) **Karaś, A.,** Bar, A., Pandian, K., Jasztal, A., Kuryłowicz, Z., Kutryb-Zając, B., Buczek, E., Rocchetti, S., Mohaissen, T., Jędrzejewska, A., Harms, A.C., Kaczara, P., Chłopicki, S., 2024. Functional deterioration of vascular mitochondrial and glycolytic capacity in the aortic rings of aged mice. GeroScience 46, 3831–3844. https://doi.org/10.1007/s11357-024-01091-6

Publications not related to this doctoral thesis:

1) Czarnek, M., Sarad, K., **Karaś, A.,** Kochan, J., Bereta, J., 2021. Non-targeting control for MISSION shRNA library silences SNRPD3 leading to cell death or permanent growth arrest. Molecular Therapy - Nucleic Acids 26, 711–731. https://doi.org/10.1016/j.omtn.2021.09.004
2) Mohaissen, T., Kij, A., Bar, A., Marczyk, B., Wojnar-Lason, K., Buczek, E., **Karas, A.**, Garcia-Redondo, A.B., Briones, A.M., Chlopicki, S., 2024. Chymase-independent vascular Ang-(1–12)/Ang II pathway and TXA2 generation are involved in endothelial dysfunction in the murine model of heart failure. European Journal of Pharmacology 966, 176296. https://doi.org/10.1016/j.ejphar.2023.176296
3) Olkowicz, M., **Karas, A.**, Berkowicz, P., Kaczara, P., Jasztal, A., Kurylowicz, Z., Fedak, F., Rosales-Solano, H., Roy, K.S., Kij, A., Buczek, E., Pawliszyn, J., Chlopicki, S., 2024. Upregulation of ALOX12−12-HETE pathway impairs AMPK-dependent modulation of vascular metabolism in ApoE/LDLR−/− mice. Pharmacological Research 210, 107478. https://doi.org/10.1016/j.phrs.2024.107478
4) Pośpiech, E., Bar, A., Pisarek-Pacek, A., **Karaś, A**., Branicki, W., Chlopicki, S., 2024. Epigenetic clock in the aorta and age-related endothelial dysfunction in mice. GeroScience 46, 3993–4002. https://doi.org/10.1007/s11357-024-01086-3